NOAA Technical Report NESDIS 144

doi:10.7289/V5RB72KG

Regional Surface Climate Conditions in CMIP3 and CMIP5 for the United States: Differences, Similarities, and Implications for the U.S. National Climate Assessment

Washington, D.C.
July 2015

U.S. DEPARTMENT OF COMMERCE
National Oceanic and Atmospheric Administration
National Environmental Satellite, Data, and Information Service

NOAA TECHNICAL REPORTS

National Environmental Satellite, Data, and Information Service

The National Environmental Satellite, Data, and Information Service (NESDIS) manages the Nation's civil Earth-observing satellite systems, as well as global national data bases for meteorology, oceanography, geophysics, and solar-terrestrial sciences. From these sources, it develops and disseminates environmental data and information products critical to the protection of life and property, national defense, the national economy, energy development and distribution, global food supplies, and the development of natural resources.

Publication in the NOAA Technical Report series does not preclude later publication in scientific journals in expanded or modified form. The NESDIS series of NOAA Technical Reports is a continuation of the former NESS and EDIS series of NOAA Technical Reports and the NESC and EDS series of Environmental Science Services Administration (ESSA) Technical Reports.

Copies of earlier reports may be available by contacting NESDIS Chief of Staff, NOAA/ NESDIS, 1335 East-West Highway, SSMC1, Silver Spring, MD 20910, (301) 713-3578.

NOAA Technical Report NESDIS 144

doi:10.7289/V5RB72KG

Regional Surface Climate Conditions in CMIP3 and CMIP5 for the United States: Differences, Similarities, and Implications for the U.S. National Climate Assessment

Liqiang Sun, Kenneth E. Kunkel, Laura E. Stevens, and Andrew Buddenberg
Cooperative Institute for Climate and Satellites – North Carolina
North Carolina State University and NOAA National Centers for Environmental Information
Asheville, NC

J. Greg Dobson
National Environmental Modeling and Analysis Center
University of North Carolina at Asheville
Asheville, NC

David R. Easterling
NOAA National Centers for Environmental Information
Asheville, NC

U.S. DEPARTMENT OF COMMERCE
Penny Pritzker, Secretary of Commerce

National Oceanic and Atmospheric Administration
Dr. Kathryn Sullivan, Under Secretary of Commerce for Oceans and Atmosphere and NOAA Administrator

National Environmental Satellite, Data, and Information Service
Stephen Volz, Assistant Administrator

PREFACE

"Regional Climate Trends and Scenarios for the U.S. National Climate Assessment", published as NOAA Technical Report NESDIS 142 (TR142), consisted of a series of regional climate descriptions designed to provide input for use in the development of the Third National Climate Assessment (NCA3). In TR142 and NCA3, the Coupled-Model Intercomparison Project (CMIP) Phase 3 (CMIP3) climate model simulations were used as the primary basis for climate scenarios. As part of a sustained assessment approach, it was intended that TR142 would be updated as new and well-vetted model results became available. Since then, the CMIP Phase 5 (CMIP5) model simulations have become available and analyzed in depth. The purpose of this report is to compare the CMIP3 results in TR142 with CMIP5 projections and to report on implications for the findings presented in NCA3.

Recommended Citation:

Sun, L., K.E. Kunkel, L.E. Stevens, A. Buddenberg, J.G. Dobson, and D.R. Easterling, 2015: Regional Surface Climate Conditions in CMIP3 and CMIP5 for the United States: Differences, Similarities, and Implications for the U.S. National Climate Assessment, *NOAA Technical Report NESDIS 144,* 111 pp. doi:10.7289/V5RB72KG

1. INTRODUCTION

The Global Change Research Act of 1990[1] mandated that national assessments of climate change be prepared not less frequently than every four years. The Third National Climate Assessment (NCA3) was published in 2014 (Melillo et al. 2014). To support the development of the NCA3, a technical report entitled "Regional Climate Trends and Scenarios for the U.S. National Climate Assessment," published as NOAA Technical Report NESDIS 142, parts 1 through 9 (Kunkel et al. 2013a,b,c,d,e,f,g; Stewart et al. 2013; Keener et al. 2013) was developed to provide basic physical climate information for the NCA3 authors. The National Climate Assessment and Development Advisory Committee (NCADAC), a federal advisory committee established in the spring of 2011, produced the NCA3 and established the guidelines for input information. Of central interest to this report, the NCADAC directed the "use of simulations forced by the A2 emissions scenario as the primary basis for the high climate future and by the B1 emissions scenario as the primary basis for the low climate future for the 2013 report" for climate scenarios. These scenarios were generated by the Intergovernmental Panel on Climate Change (IPCC) and are described in the IPCC Special Report on Emissions Scenarios (SRES; IPCC 2000). The climate simulations consisted of fifteen coupled Atmosphere-Ocean General Circulation Models (AOGCMs) from the World Climate Research Programme (WCRP) Coupled Model Intercomparison Project Phase 3 (CMIP3) multi-model dataset (PCMDI 2014).

As the NCA3 was being produced, new climate model simulations were being developed for the IPCC Fifth Assessment Report (AR5; IPCC 2013) in a new project called CMIP Phase 5 (CMIP5). The NCADAC made the decision to use CMIP3 model simulations primarily for NCA3 because the full suite of CMIP5 simulations were not yet available at the time of the initiation of the NCA3 and because the CMIP3 simulations had been intensively vetted by the scientific community. However, the CMIP5 simulations became available before the report was completed and thus some graphics of CMIP5 data were included in the NCA3. Another data set that became available in the latter stages of development of the NCA3 was a statistically downscaled data set using a modern methodology (Hayhoe 2014). A number of graphics in the NCA3 were based on this data set.

With the release of the NCA3, the question arises whether the CMIP5 simulations produce projections that are sufficiently different from CMIP3 to affect the key findings of NCA3. The purpose of this report is to document the similarities and differences between CMIP3 and CMIP5 simulations for surface climate conditions focused on the United States.

All available data, metadata, and high-resolution figures from this report are available for download at: https://www.cicsnc.org/about/tsu/tr144-data.

1.1. Findings from NOAA Technical Report NESDIS 142

NOAA Technical Report NESDIS 142: "Regional Climate Trends and Scenarios for the U.S. National Climate Assessment" (TR142) consisted of nine parts. Eight of them covered one of the eight regions defined in the NCA3 (Kunkel et al. 2013a,b,c,d,e,f; Stewart et al. 2013; Keener et al. 2013). The ninth summarized conditions for the contiguous United States (Kunkel et al. 2013g).

[1] http://hdl.loc.gov/loc.uscongress/legislation.101s169

Each document contains two major sections. One section summarizes historical conditions. The description of the historical climate focused primarily on trends in temperature and precipitation metrics that are important in that region. The second section summarizes climate model simulations for the A2 and B1 scenarios of the future path of greenhouse gas emissions. These simulations incorporate analyses from multiple sources, the core source being CMIP3 simulations. Additionally, simulations from the North American Regional Climate Change Assessment Program (NARCCAP) were used. Analyses of the simulated future climate are provided for the periods of 2021–2050, 2041–2070, and 2070–2099, with changes calculated with respect to an historical climate reference period (1971–1999, 1971–2000, or 1980–2000).

The information on historical climate variations and trends was produced in order to provide a regional context for historical experience and future projections. No formal attribution of trends was performed and no implicit attribution was intended. For variables and locations where a historical trend is similar in direction to future projections, it can provide insights into potential future impacts by comparison with past impacts. Some of the key characteristics of the historical climate included in these documents are:

- Climatic phenomena that have major impacts on the U.S. include: heavy rainfall and floods, drought, extreme heat and cold, winter storms (in northern regions), severe thunderstorms and tornadoes, and tropical cyclones.
- The U.S. as a whole has experienced statistically significant warming since 1895 in all seasons. This warming has not been uniform in space. Warming has been greatest in the west and north. By contrast, the southeast has not experienced any overall century-scale warming, one of the few regions globally not to exhibit an overall warming trend in surface temperature over the 20th century (IPCC 2007). This "warming hole" also includes parts of the Great Plains and Midwest regions in the summer.
- Temperatures increased rapidly in the early part of the 20th century, then decreased slightly during the middle of the 20th century. Since about 1980, temperatures have been increasing.
- The number of extreme hot spells averaged over the continental United States has tended to increase since a minimum in the 1960s, such that over the continental United States the 2000s experienced the second highest number of any decade. The decade with highest number over the continental United States remains the 1930s; this is principally due to very high numbers over the Great Plains region, the center of the "Dust Bowl." Recent increases in hot spells are greatest in the western and northeastern regions. The number of extreme cold spells has decreased since a peak in the 1980s. The 2000s had the smallest number of any decade since 1895, the beginning year of our analysis.
- There have been statistically significant upward trends in annual and fall precipitation. Trends in other seasons are not statistically significant.
- A national upward trend in the number of extreme precipitation events is highly statistically significant. The 2000s experienced the greatest number of such extremes. Regionally, this upward trend is prominent in the eastern regions, while far western regions have not experienced an overall trend.
- The length of the freeze-free season has increased by about two weeks since 1900. The increase has been greater in the western U.S. than in the eastern United States.
- Lakes with long-term ice cover records show sizeable decreases in ice cover area and duration.

The climate characteristics simulated by climate models for the B1 and A2 scenarios have the following key features:

- Both the CMIP3 and NARCCAP simulations indicate that spatial variations in ensemble-average temperature increase are relatively small, with the greatest temperature increases simulated in the interior and the least in coastal regions. The CMIP3 models indicate that temperature increases across the entire contiguous U.S. are statistically significant (for all three future time periods and both scenarios).
- For the near future, temperature increases are simulated to be similar in magnitude for the high and low scenarios, whereas late in the 21st century the high emissions scenario indicates approximately double the amount of warming.
- The range of model-simulated temperature changes is substantial, indicating substantial uncertainty in the magnitude of warming associated with each scenario. However, in each model simulation, the warming is unequivocal and large compared to historical variations. This is also true for all of the derived temperature variables described below. It should be noted that the model range is not a complete measure of total projection uncertainty.
- NARCCAP model simulations for the middle of the 21st century indicate increases in the number of days with a maximum temperature of more than 95°F, with the increases ranging from more than 35 days in the southeast and southwest to less than 5 in the far north. The number of consecutive warm days is simulated to increase the most in the south-central and southwest areas (for the A2 scenario at mid-century).
- The number of days with minimum temperatures below 10°F is simulated to decrease across the U.S. by mid-century in the A2 scenario. The largest decreases of more than 20 days are simulated in the far north and mountain regions. The area of near-zero days below 10°F expands considerably. The number of days below 32°F is simulated to decrease by more than 20 days across much of the central and northern United States.
- Increases in the length of the freeze-free season are in the range of 20 to 30 days across most of the United States, with larger increases of up to 50 days in portions of the far west (for the A2 scenario at mid-century).
- Cooling degree days increase by more than 800 in the southeast and southwest, with smaller increases to the north; the increases everywhere represent large percentage changes. Correspondingly, heating degree days are simulated to decrease by less than 500 in the south to more than 1,300 in the far north and western mountains (for the A2 scenario at mid-century).
- Precipitation is simulated by both the CMIP3 and NARCCAP models to generally increase in the north and decrease in the southwest. Under the A2 scenario, the changes are statistically significant in the far north and southwest by the end of the 21st century. In the central part of the country, these changes are either not statistically significant or the models are not in agreement on the sign of the changes. The range of model-simulated precipitation changes is considerably larger than the multi-model mean change.
- Changes in the number of days with precipitation greater than one inch are not statistically significant over most of the country (for the A2 scenario at mid-century).
- The number of consecutive days with precipitation less than 0.1 inches shows statistically significant increases for the southwest. In most other areas, the changes are not statistically significant (for the A2 scenario at mid-century).

- Many models do not indicate a statistically significant change in temperature (with respect to 2001–2010) for the near future, reflecting natural variability. However, as the time period progresses, a greater number of models simulate statistically significant temperature changes, with all being significant at the 95% confidence level by 2035 (for the high emissions scenario) and 2055 (for the low emissions scenario), reflecting that the human-induced component of change is large compared to natural variations.
- Many of the modeled values of decadal precipitation change are not statistically significant, with respect to 2001–2010, out to 2091–2099, reflecting that the human-induced component of change is small compared to natural variations.

A comparison of model simulations of the 20th century with observations indicates the following:

- The observed changes in temperature are generally within the envelope of modeled changes on an annual basis. For the summer season, the observed increase in temperature from the 1920s to the Dust Bowl era of the 1930s and the subsequent decrease from the 1930s to the 1940s are not simulated by any model. However, the extreme temperatures of that era were likely exacerbated by human-caused land degradation (Cook et al. 2009), an aspect that is not incorporated into model simulations; thus there is no expectation that models would simulate those extreme temperatures at the specific time and place of their actual occurrence because this event was most likely a result of internal climate system variability. Most other seasonal changes are within the envelope of model simulations.
- The variability in observed precipitation change tends to be somewhat higher than that of the models, although decadal values are generally within the envelope of the model simulations.

1.2. CMIP3 and CMIP5 Community Modeling Efforts

The Coupled Model Intercomparison Project (CMIP) is a project of the World Climate Research Programme (WCRP) Working Group on Coupled Modeling (WGCM). This project provides a standard experimental protocol for studying Global Climate Models (GCMs). In CMIP Phase 3 (CMIP3), 17 different modeling groups produced simulations that were used in the IPCC Fourth Assessment Report (AR4; IPCC 2007). Altogether, there were 25 different model representations.[2] In CMIP Phase 5 (CMIP5), an even larger number of groups produced simulations for the IPCC Fifth Assessment Report (AR5; IPCC 2013), with over 60 representations from 28 different models.[3]

As well as a greater number of simulations, CMIP5 includes models with higher spatial resolutions and a more developed representation of physical processes than for CMIP3. The spatial resolution of the great majority of CMIP3 model simulations is 2°–3° (a grid point spacing of approximately 100–200 miles), with a few slightly greater or smaller. For CMIP5, the spatial resolution of most models is in the 1°–2° range, or about 60–130 miles.

[2] For a complete list of CMIP3 models, see: http://www-pcmdi.llnl.gov/ipcc/model_documentation/ipcc_model_documentation.php
[3] For a complete list of CMIP5 models, see: http://cmip-pcmdi.llnl.gov/cmip5/availability.html

Both CMIP3 and CMIP5 include the following experiments, which were used in this report:

a) Simulations of the 20th century using best estimates of the temporal variations in external forcing factors (such as greenhouse gas concentrations, solar output, volcanic aerosol concentrations); and

b) Simulations of the 21st century assuming changing greenhouse gas concentrations following various scenarios. Herein, we show results for CMIP3 simulations under the SRES B1, A1B, and A2 scenarios, and CMIP5 simulations under the RCP2.6, RCP4.5, RCP6.0, and RCP8.5 scenarios. See Section 1.3 for a description of these scenarios.

In order to facilitate comparisons across the various scenarios, a subset of all available models was chosen. The requirement for inclusion of a model was that it had simulations for the SRES A2, A1B, and B1 scenarios for CMIP3 or the RCP2.6, 4.5, 6.0, and 8.5 scenarios for CMIP5 (see scenarios discussion in Section 1.3). This requirement reduced the number of models used in this report to 14 for CMIP3 and 16 for CMIP5. These models, and their spatial resolutions, are listed in Tables 1 and 2.

1.3. Scenarios

The A2, A1B, and B1 scenarios used in the CMIP3 simulations represent different narrative storylines about possible future social, economic, technological, and demographic developments. These SRES scenarios have internally consistent relationships that were used to describe future pathways of greenhouse gas emissions. The A2 scenario "describes a very heterogeneous world. The underlying theme is self-reliance and preservation of local identities. Fertility patterns across regions converge very slowly, which results in continuously increasing global population. Economic development is primarily regionally oriented and per capita economic growth and technological change are more fragmented and slower than in the other storylines" (IPCC 2000). The A1B scenario describes "a future world of very rapid economic growth, low population growth and rapid introduction of new and more efficient technology. Major underlying themes are economic and cultural convergence and capacity building, with a substantial reduction in regional differences in per capita income" (IPCC 2000) The B1 scenario describes "a convergent world with…global population that peaks in mid-century and declines thereafter…but with rapid changes in economic structures toward a service and information economy, with reductions in material intensity, and the introduction of clean and resource-efficient technologies. The emphasis is on global solutions to economic, social, and environmental sustainability, including improved equity, but without additional climate initiatives" (IPCC 2000). At the end of the 21st century, carbon dioxide (CO_2), one of the main emission driving forces, reaches 850 ppm and continues rising in the A2 scenario, stabilizes at 550 ppm for the B1 scenario, and stabilizes at 720 ppm for the A1B scenario, as shown in Fig. 1a.

The CMIP5 simulations use a new set of scenarios called Representative Concentration Pathways (RCPs). These are based on radiative forcing trajectories, rather than socioeconomic "storylines." They are named according to the radiative forcing level at 2100 (Moss et al. 2010). There are four RCPs: 2.6, 4.5, 6.0, and 8.5, with the numbers representing the 2100 radiative forcing increase relative to pre-industrial levels in W m^{-2}. They span a wider range of forcings than was used in CMIP3. The carbon dioxide (CO_2) concentrations (Fig. 1a, right panel) for RCP4.5 and RCP6.0 cross over at around 2060; before then the radiative forcing is larger for RCP4.5. The concentration

for RCP2.6 is also slightly higher than RCP6.0 early in the 21st century. Comparing the SRES (Fig. 1a, left panel) with the RCP (Fig. 1a, right panel) scenarios, the RCP4.5 and RCP6.0 scenarios are similar to B1 and A1B, respectively. The A2 scenario is intermediate between RCP6.0 and RCP8.5. The RCP2.6 scenario is lower than any SRES scenario.

Aerosol emissions in CMIP5 RCPs are significantly reduced in the 21st century compared with those in CMIP3 SRES. All RCPs include the assumption that aerosol control becomes more stringent over time as a result of rising income levels. Globally, this would cause aerosol emissions to decrease over time—although trends can be different for specific regions or at particular moments in time. A second factor that influences the results across the RCPs is climate policy (van Vuuren et al. 2011). Projections of global mean aerosol effective radiative forcing (ERF) in all RCPs show a large positive value at 2100 relative to 2000, nearly returning to its 1850 levels, as is expected given the RCP emissions. The projections of drastic reductions in aerosol emissions may be overly optimistic, as they assume virtually all nations in the world become wealthy and that emissions reductions are directly dependent on wealth (IPCC 2013).

Anthropogenic aerosols have exerted a cooling influence on the Earth since pre-industrial times, which has masked some of the global mean warming from greenhouse gases that would have occurred in their absence. Therefore, the projected decrease in emissions of anthropogenic aerosols in the future would eventually unmask this warming, and the impact of aerosols on climate change becomes small under these RCPs (IPCC 2013).

The range of simulated global temperature changes in CMIP3 and CMIP5 is shown in Fig. 1b. The multi-model mean temperature increase at 2099, with respect to a base period of 1901–1960, is 3.9°F, 5.6°F, and 7.0°F for the CMIP3 SRES scenarios of B1, A1B, and A2, respectively (left panel). For CMIP5 (right panel), the temperature increases are 2.8°F, 4.2°F, 5.2°F, and 8.3°F for RCPs 2.6, 4.5, 6.0, and 8.5, respectively. Although the wider range in the CMIP5 simulations could be due in part to a newer generation of models, the primary cause is most likely the wider range of emissions in the RCPs. The 2100 atmospheric concentration of greenhouse gases (CO_2-equivalent) ranges from 421 ppm for RCP2.6, 650 ppm for RCP4.5, 850 ppm for RCP6.0, to 1370 ppm for RCP8.5 (van Vuuren et al. 2011). Note that RCP8.5 assumes radiative forcing levels continue rising after year 2100, RCP6.0 and RCP4.5 assume radiative forcing levels have stabilized in 2100, and RCP2.6 assumes the radiative forcing level peaks before 2100 and then declines. It should be noted that the SRES A1Fi scenario represented a 2100 concentration of 970 ppm. However, relatively few CMIP3 models performed simulations for this scenario.

Table 1. *The 14 CMIP3 models and their climate modeling groups/institutions used in these analyses. A single ensemble member was used for each model simulation. The number of global grid points and the spatial resolutions of each model are also listed.*

Model	Climate Modeling Group/Institution(s)	Country	# of Global Grid Points (Lon x Lat)	Longitude Resolution (°)	Latitude Resolution (°)
CCSM3	National Center for Atmospheric Research	USA	256 x 128	1.40625	1.40625
CGCM3.1(T47)	Canadian Centre for Climate Modelling & Analysis	Canada	96 x 48	3.75000	3.70900
CNRM-CM3	Centre National de Recherches Météorologiques, Météo-France	France	128 x 64	2.81250	2.81250
CSIRO-Mk3.0	Commonwealth Scientific and Industrial Research Organisation	Australia	192 x 96	1.87500	1.87500
ECHO-G	Meteorological Institute of the University of Bonn/Institute of KMA/Model and Data group	Germany/Korea	96 x 48	3.75000	3.75000
ECHAM5/MPI-OM	Max Planck Institute for Meteorology	Germany	192 x 96	1.87500	1.87500
GFDL-CM2.0	NOAA Geophysical Fluid Dynamics Laboratory	USA	144 x 90	2.50000	2.00000
GFDL-CM2.1	NOAA Geophysical Fluid Dynamics Laboratory	USA	144 x 90	2.50000	2.00000
INM-CM3.0	Institute of Numerical Mathematics, Russian Academy of Science	Russia	72 x 45	5.00000	4.00000
IPSL-CM4	Institut Pierre-Simon Laplace	France	96 x 72	3.75000	2.50000
MIROC3.2(medres)	Center for Climate System Research, The University of Tokyo/National Institute for Environmental Studies/Frontier Research Center for Global Change, Japan Agency for Marine-Earth Science and Technology	Japan	128 x 64	2.81250	2.81250
MRI-CGCM2.3.2	Meteorological Research Institute, Japan Meteorological Agency	Japan	128 x 64	2.81250	2.81250
PCM	National Center for Atmospheric Research	USA	128 x 64	2.81250	2.81250
UKMO-HadCM3	Hadley Centre for Climate Prediction and Research, Met Office	UK	128 x 64	2.81250	2.81250

Table 2. *The 16 CMIP5 models and their climate modeling groups/institutions used in these analyses. Multiple ensemble members were used for some model simulations. The number of global grid points and the spatial resolutions of each model are also listed.*

Model	Climate Modeling Group/Institution(s)	Country	# of Ensemble Members	# of Global Grid Points (Lon x Lat)	Longitude Resolution (°)	Latitude Resolution (°)
BCC-CSM1.1	Beijing Climate Center, China Meteorological Administration	China	1	128 x 64	2.81250	2.81250
CCSM4	National Center for Atmospheric Research	USA	6	288 x 192	1.25000	0.94241
CSIRO-Mk3.6.0	Commonwealth Scientific and Industrial Research Organisation in collaboration with the Queensland Climate Change Centre of Excellence	Australia	10	192 x 96	1.87500	1.86468
FIO-ESM	The First Institute of Oceanography, SOA	China	3	128 x 64	2.81250	2.81250
GFDL-CM3	NOAA Geophysical Fluid Dynamics Laboratory	USA	1	144 x 90	2.50000	2.00000
GFDL-ESM2G	NOAA Geophysical Fluid Dynamics Laboratory	USA	1	144 x 90	2.50000	2.00000
GFDL-ESM2M	NOAA Geophysical Fluid Dynamics Laboratory	USA	1	144 x 90	2.50000	2.00000
GISS-E2-R	NASA Goddard Institute for Space Studies	USA	3	144 x 90	2.50000	2.00000
HadGEM2-AO	Hadley Centre for Climate Prediction and Research, Met Office	UK	1	192 x 145	1.87500	1.25000
HadGEM2-ES	Hadley Centre for Climate Prediction and Research, Met Office[4]	UK	4	192 x 145	1.87500	1.25000
IPSL-CM5A-LR	Institut Pierre-Simon Laplace	France	1	96 x 96	3.75000	1.89473
IPSL-CM5A-MR	Institut Pierre-Simon Laplace	France	1	144 x 143	2.50000	1.26761
MIROC5	Atmosphere and Ocean Research Institute, The University of Tokyo/National Institute for Environmental Studies/Japan Agency for Marine-Earth Science and Technology	Japan	1	256 x 128	1.40625	1.40044
MIROC-ESM	Japan Agency for Marine-Earth Science and Technology/Atmosphere and Ocean Research Institute, The University of Tokyo/National Institute for Environmental Studies	Japan	1	128 x 64	2.81250	2.81250
MIROC-ESM-CHEM	Japan Agency for Marine-Earth Science and Technology/Atmosphere and Ocean Research Institute, The University of Tokyo/National Institute for Environmental Studies	Japan	1	128 x 64	2.81250	2.81250
MRI-CGCM3	Meteorological Research Institute, Japan Meteorological Agency	Japan	1	320 x 160	1.12500	1.12128

[4] Additional HadGEM2-ES realizations contributed by Instituto Nacional de Pesquisas Espaciais, Brazil

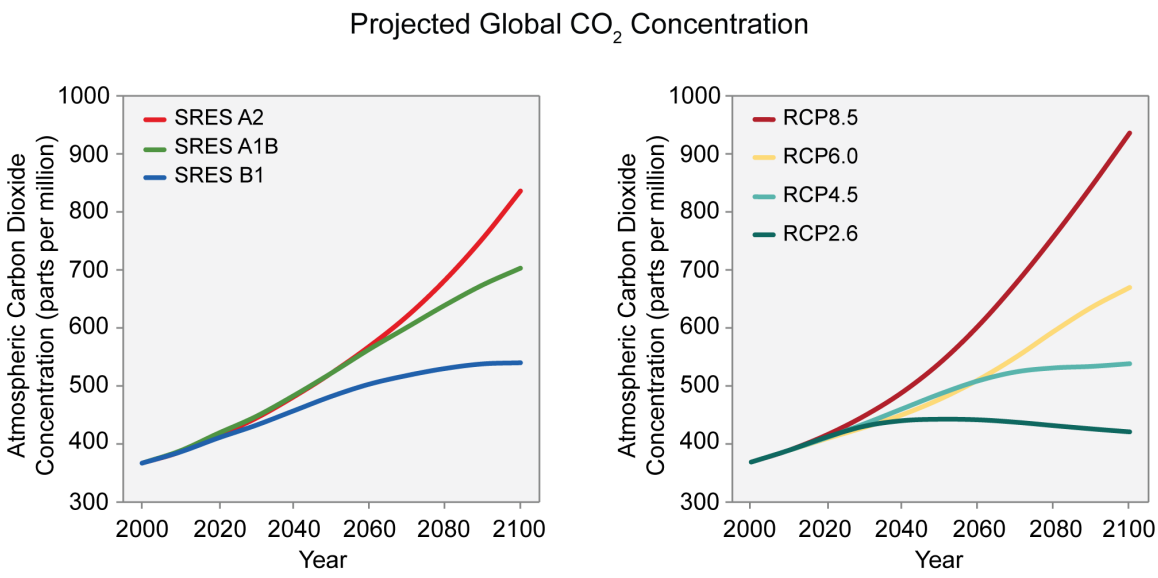

Figure 1a. *Time series of global average atmospheric carbon dioxide concentration for specific emissions pathways. The left panel shows the CMIP3 simulations for the SRES A2, A1B and B1 scenarios. The right panel shows the CMIP5 simulations for the RCP8.5, 6.0, 4.5, and 2.6 scenarios. Figure source: Adapted from Melillo et al. (2014).*

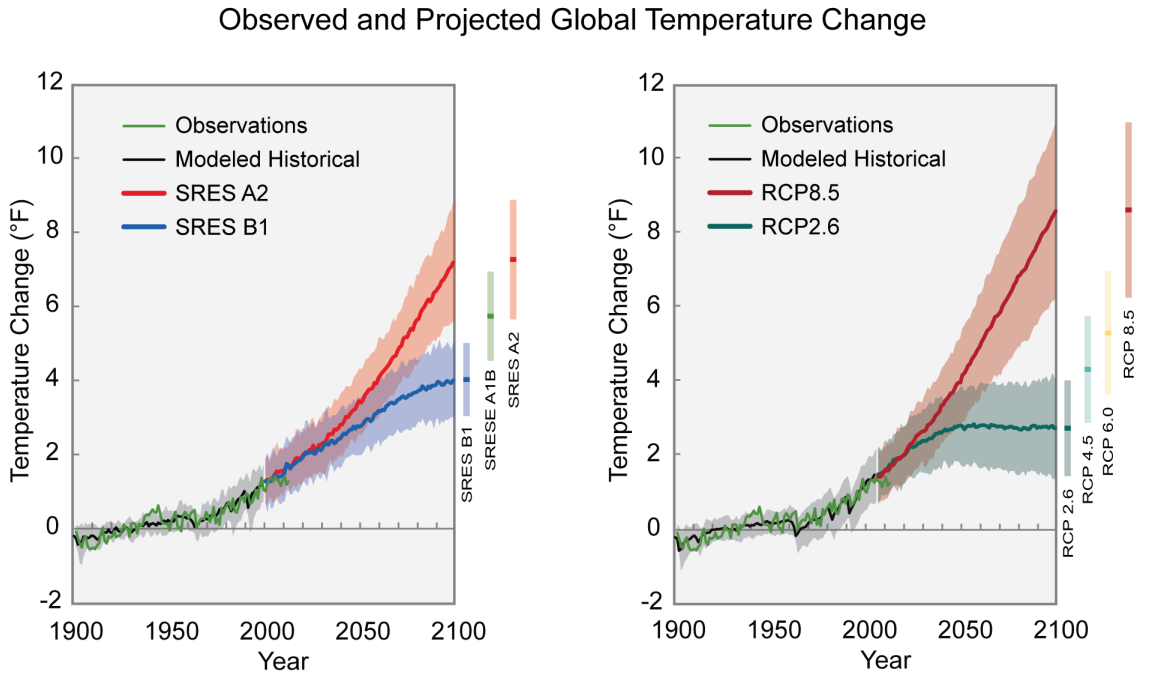

Figure 1b. *Time series of global average temperature changes (relative to the 1901–1960 average) for specific emissions pathways. Shading indicates the range (5th to 95th percentile) of results from a suite of climate models. Projections in 2099 for additional emissions pathways are indicated by the bars to the right of each panel. The left panel shows the CMIP3 simulations for the SRES A2 and B1 scenarios. The right panel shows the CMIP5 simulations for the RCP8.5 and 2.6 scenarios. The thick solid lines show the multi-model mean values. The thin green line shows the observed global temperature. Figure source: Adapted from Melillo et al. (2014).*

Table 3. *The 10 CLIMDEX CMIP3 models and their climate modeling groups/institutions used in these analyses.*

Model	Climate Modeling Group/Institution(s)	Country
CGCM3.1(T47)	Canadian Centre for Climate Modelling & Analysis	Canada
CGCM3.1(T63)	Canadian Centre for Climate Modelling & Analysis	Canada
CNRM-CM3	Centre National de Recherches Météorologiques, Météo-France	France
GFDL-CM2.0	NOAA Geophysical Fluid Dynamics Laboratory	USA
GISS-ER	NASA Goddard Institute for Space Studies	USA
IPSL-CM4	Institut Pierre-Simon Laplace	France
MIROC3.2(medres)	Center for Climate System Research (The University of Tokyo), National Institute for Environmental Studies, and Frontier Research Center for Global Change (JAMSTEC)	Japan
ECHO-G	Meteorological Institute of the University of Bonn/Institute of KMA/Model and Data group	Germany/Korea
ECHAM5/MPI-OM	Max Planck Institute for Meteorology	Germany
MRI-CGCM2.3.2	Meteorological Research Institute, Japan Meteorological Agency	Japan

Table 4. *The 14 CLIMDEX CMIP5 models and their climate modeling groups/institutions used in these analyses.*

Model	Climate Modeling Group/Institution(s)	Country
BCC-CSM1.1	Beijing Climate Center, China Meteorological Administration	China
BCC-CSM1.1(m)	Beijing Climate Center, China Meteorological Administration	China
CCSM4	National Center for Atmospheric Research	USA
CSIRO-Mk3.6.0	Commonwealth Scientific and Industrial Research Organisation in collaboration with the Queensland Climate Change Centre of Excellence	Australia
FGOALS-s2	LASG, Institute of Atmospheric Physics, Chinese Academy of Sciences	China
GFDL-ESM2G	NOAA Geophysical Fluid Dynamics Laboratory	USA
GFDL-ESM2M	NOAA Geophysical Fluid Dynamics Laboratory	USA
HadGEM2-ES	Hadley Centre for Climate Prediction and Research, Met Office[5]	UK
IPSL-CM5A-LR	Institut Pierre-Simon Laplace	France
MIROC5	Atmosphere and Ocean Research Institute, The University of Tokyo/National Institute for Environmental Studies/Japan Agency for Marine-Earth Science and Technology	Japan
MIROC-ESM-CHEM	Atmosphere and Ocean Research Institute, The University of Tokyo/National Institute for Environmental Studies/Japan Agency for Marine-Earth Science and Technology	Japan
MIROC-ESM	Atmosphere and Ocean Research Institute, The University of Tokyo/National Institute for Environmental Studies/Japan Agency for Marine-Earth Science and Technology	Japan
MRI-CGCM3	Meteorological Research Institute, Japan Meteorological Agency	Japan
NorESM1-M	Norwegian Climate Centre	Norway

[5] Additional HadGEM2-ES realizations contributed by Instituto Nacional de Pesquisas Espaciais, Brazil

Table 5. *Definitions of the 13 CLIMDEX extremes indices used in this report. More detailed descriptions can be found at http://www.climdex.org/indices.html.*

Index	Description
Number of frost days (T_{min} < 0°C)	Annual count of days when daily minimum temperature <0°C
Number of tropical nights (T_{min} > 20°C)	Annual count of days when daily minimum temperature >20°C
Growing season length (GSL)	Annual count between first span of at least 6 days with daily mean temperature >5°C and first span after July 1st of 6 days <5°C
Monthly maximum value of daily maximum temperature (TXx)	Monthly maximum value of daily maximum temperature
Monthly maximum value of daily minimum temperature (TXn)	Monthly maximum value of daily minimum temperature
Monthly Minimum value of daily minimum temperature (TNn)	Monthly minimum value of daily minimum temperature
Warm spell duration index (WSDI)	Annual count of days with at least 6 consecutive days when daily maximum temperature >90th percentile
Cold spell duration index (CSDI)	Annual count of days with at least 6 consecutive days when daily maximum temperature <10th percentile
Monthly maximum 1-day precipitation (Rx1day)	Monthly maximum amount of precipitation in one day
Monthly maximum 5-day precipitation (Rx5day)	Monthly maximum amount of precipitation for a consecutive 5-day period
Maximum length of dry spell (CDD)	Count of the largest number of consecutive days with precipitation <1 mm
Maximum length of wet spell (CWD)	Count of the largest number of consecutive days with precipitation ≥1 mm
Total precipitation on the wettest of days (R99pTOT)	Annual total of precipitation on days when precipitation >99th percentile

2. DATA

The majority of analyses in this report use the direct data from the CMIP3 and CMIP5 models in order to assess the similarities and differences in future temperature and precipitation projections between the two.

For examination of future extreme conditions, a set of climate indices was analyzed. This set, a product of the CLIMDEX project, was computed for a number of climate models participating in both CMIP3 and CMIP5 (Sillmann et al. 2013a,b), listed in Tables 3 and 4, respectively. For this report, the data for several representative indices for both CMIP3 and CMIP5 were downloaded from the Canadian Centre for Climate Modelling and Analysis (CCCMA 2014). These indices are described in Table 5.

Analyses of historical temperature and precipitation use data from the nClimDiv dataset (Vose et al. 2014), obtained from NOAA's National Centers for Environmental Information (NCEI, formerly the National Climatic Data Center). These data are derived from bias-corrected monthly National Weather Service Cooperative Observer Network (COOP) observations and are gridded at a 5 x 5 km resolution for the time period of 1895–2013.

3. METHODS

Analyses are provided for the period of 2001–2100. The periods of 2021–2050, 2041–2070, and 2070–2099 are used to represent the early, middle, and later portions of the 21st century, respectively. These future periods will sometimes be denoted in the text by their midpoints of 2035, 2055, and 2085, respectively.

Climate changes are calculated with respect to an historical climate reference period (either 1971–2000, 1981–2000, or 2001–2010). Although a uniform reference period would be ideal, there were variations in data availability and in the needs of the author teams in NCA3 and thus several were used in TR142. The 1971–2000 period was used as the reference for CMIP mean temperature and precipitation maps. The 1981–2000 period was used as the historical reference for the CLIMDEX maps due to the data availability. The 2001–2010 period was used as reference period for analysis of decadal variability.

Four different types of analyses are represented, described as follows:

- **Multi-model mean maps** – Model simulations of future climate conditions typically exhibit considerable model-to-model variability. Some of this variability is due to true model differences in representing the physics of the climate system. However, since only one model realization is available in many cases, a portion of the variability is due to natural variability in the climate system unrelated to model physics differences. In most cases, the future climate scenario information is presented as multi-model mean maps. To produce these, each model's data is first re-gridded to common grids of approximately 2.8° latitude by 2.8° longitude (CMIP3), and 1.5° latitude by 1.5° longitude (CMIP5), respectively. Then, each grid point value is calculated as the mean of a common set of 14 CMIP3 models and a common set of 16 CMIP5 models at that grid point. Finally, the mean grid point values are mapped. This type of analysis weights all models equally. Although an equal weighting does not incorporate known differences among models in their fidelity in reproducing various climatic conditions, a number of research studies have found that the multi-model mean with equal weighting is superior to any single model in reproducing the present-day climate (Overland et al. 2011). In most cases, the multi-model mean maps include information about the variability of the model simulations. In addition, there are several graphs that show the variability of individual model results. These should be examined to gain an awareness of the magnitude of the uncertainties in each scenario's future values.
- **Spatially averaged products** – There are nine regions in total, one each for eight regions defined by the NCA, and one for the contiguous United States. The eight NCA regions are the Northeast, Southeast, Midwest, Great Plains, Northwest, Southwest, Alaska, and Hawai‘i/Pacific Islands. To produce spatially averaged data, all the grid point values within the region boundaries are averaged and represented as a single value. Note that some regions include a few grid boxes that are a combination of coastal and adjacent ocean areas, but these represent a small proportion of the total regional area. This is useful for general comparisons of different models, periods, and data sources. Because of the spatial aggregation, this product may not be suitable for many types of impacts analyses.

- **Probability density functions (PDFs)** – These are used here to illustrate the differences among models. To produce these, spatially averaged values are calculated for each model simulation. Then, the distribution of these spatially averaged values is displayed. This product provides an estimate of the uncertainty of future changes in a tabular form. As noted above, this information should be used as a complement to the multi-model mean maps.

- **Uncertainty statistics** – A variety of methods have been used to quantify statistical uncertainty of model projections, however, there is no consensus on the most suitable method to communicate the uncertainty. Five of these methods are described in the Appendix (and depicted in Fig. A1), some of which were used in different chapters of AR5 (IPCC 2013). The various methods emphasize different aspects of the uncertainty characteristics. Four of the five methods described in the Appendix produce quite similar results. The fifth uses a much different approach that distinguishes areas where there is high confidence in changes much smaller than natural variations from other areas of larger changes. NCA used Method #2, whereas TR142 used a variant of Method #4.

  For consistency, the method used in this report is the same as used in TR142, a variant of Method #4 which is described in Tebaldi et al. (2011). The statistical significance regarding the change in temperature and precipitation between each future time period and the model reference period was determined using a 2-sample *t*-test assuming unequal variances for those two samples. For each period (present and future climate), the mean and standard deviation were calculated using the 30 annual values. These were then used to calculate *t*. In order to assess the agreement between models, the following three categories were determined for each grid point, similar to that described in Tebaldi et al. (2011):

  - *Category 1*: If less than 50% of the models indicate a statistically significant change then the multi-model mean is shown in color. This means that model results are in general agreement that simulated changes are within historical variations;

  - *Category 2*: If more than 50% of the models indicate a statistically significant change but less than 67% of the significant models agree on the sign of the change, then the grid points are masked out, indicating that the models are in disagreement about the direction of change;

  - *Category 3*: If more than 50% of the models indicate a statistically significant change and more than 67% of the significant models agree on the sign of the change, then the multi-model mean is shown in color with hatching. Model results are in agreement that simulated changes are statistically significant and in a particular direction.

4. TEMPERATURE

4.1. Historical Simulations

Temperature analyses are provided for the period of 1901–2000, with changes calculated with respect to an historical reference period (1901–1960). As described in Section 2, observational data are from NCEI's nClimDiv dataset.

Figure 2 shows observed and simulated annual mean temperature for the contiguous United States. Observations are overlaid with annual multi-model mean temperatures from the 16 CMIP5 simulations listed in Table 2, using both full forcings (black line) and natural forcings only (gray line). The shaded regions indicate the 5th to 95th percentile range of individual annual model values. Observed annual temperatures were relatively cool at the start of the century, gradually increasing to reach a peak during Dust Bowl era of the 1920s and 30s. After a cooler period, a gradual increase in temperature has been seen from the early 1970s on, with 1998 being the warmest during this range of years. The trend in multi-model mean temperature from the full forcing CMIP5 simulations closely follows that of the observations, with less than 10 years having a recorded temperature that lies outside the 5th to 95th percentile range of the 16 models (red shading). The natural forcing-only simulations are also well aligned with the observations until the 1970s, after which the values begin to diverge. These natural forcing-only simulations do not reflect the recent increase in temperatures. This suggests that human factors have contributed to the warming.

Observed and simulated annual mean temperature for the six NCA regions in the contiguous United States, for 1901–2000, can be seen in Fig. 3 (Alaska and Hawai‘i are omitted due to a lack of sufficient observational data). Three time series are shown for each region: nClimDiv observations (black line), CMIP3 simulations (blue line), and CMIP5 simulations (red line). The shaded regions indicate the 5th to 95th percentile range of individual annual model values. Both the observations and CMIP simulations are smoothed with a 10-year moving boxcar filter. Temperatures in most regions follow a trend similar to that of the U.S. as a whole (see Fig. 2), rising to a peak in the 1920s/30s, cooling slightly until the 1970s, then rising again to the end of century and beyond. In western parts of the United States, the 1990s saw more consistently warm temperatures than any other period, although a few individual years in the 1920s and 1930s were as high or higher. In the Midwest and Great Plains regions, temperatures in the 1990s were on par with those from the Dust Bowl era. The Northeast region did not see a peak in temperatures during this time, with the annual average temperature in 1998 being 1.5°F higher than for any year during the 1920s and 30s. In the Southeast, temperatures in the 1920s and 1930s were generally warmer than in the 1990s.

The CMIP data are once again multi-model means, resulting in much less year-to-year variance in temperatures than the observed values because the timing of natural variations are not, and would not expected to be, synchronous among the CMIP simulations. This difference in variability between model and observed curves is just a consequence of the multi-model averaging. The simulations mostly follow the observed temperature trend, with CMIP5 values generally being slightly cooler than CMIP3 over the last 50 years. Both simulations align well with the observations during the early part of the record, with CMIP5 matching slightly more closely in recent years for the majority of regions. In the Southeast region, however, the observed cooling during the 1960s and 70s is not simulated by CMIP3 or CMIP5. This lack of warming is known as the "warming hole",

and is generally not simulated by climate models (Kunkel et al. 2006; Kumar et al. 2013; Pan et al. 2013). The research community is actively studying this feature to better understand the causes.

4.2. Projections

As noted above, this report is based on climate model simulations of the future using CMIP3 SRES and CMIP5 RCP scenarios. The resulting climate conditions are to be viewed as scenarios and there are no explicit or implicit assumptions about the probability of occurrence of any particular scenario.

CMIP analyses are provided for the periods of 2021–2050, 2041–2070, and 2070–2099, with changes calculated with respect to an historical climate reference period (1971–2000). These future periods will sometimes be denoted in the text by their midpoints of 2035, 2055, and 2085, respectively. Seasonal calculations use the following three-month periods: winter (December-January-February), spring (March-April-May), summer (June-July-August), and fall (September-October-November).

4.2.1. Mean Temperature

The surface air temperature is directly affected by increased downward infrared radiation from increased greenhouse gas concentrations. Figure 4 shows annual mean temperature time series for the contiguous United States. The upper panel shows nClimDiv observations (orange line) and historical CMIP3 simulations (black line) for 1901–2000, as well as simulated annual mean temperature for each CMIP3 scenario (colored lines) for 2001–2100. The lower panel shows nClimDiv observations (orange line) and historical CMIP5 simulations (black line) for 1901–2005, as well as simulated annual mean temperature for each CMIP5 scenario (colored lines) for 2006–2100. The shaded regions indicate the 5th to 95th percentile range of individual annual model values. Both the observations and CMIP simulations are smoothed with a 10-year moving boxcar filter. For the 20th century, both CMIP3 and CMIP5 historical simulations indicate an increase of about 2.0°F, which is slightly higher than the observed increase of 1.6°F (Kunkel et al. 2013g). The simulated temperature rises in CMIP3 and CMIP5 have not been constant, instead, they are marked by three distinct periods of change: warming from the 1900s to the 1930s, cooling from the 1940s to the 1960s, and warming from the 1970s to 2000. These three periods of change are observed as well, and the CMIP5 simulations are in better agreement with observations. The 5th to 95th percentile range of both CMIP3 and CMIP5 simulations are near constant during the 20th century, and the CMIP5 range is slightly larger. During the 21st century, both CMIP3 and CMIP5 simulations show similarly large temperature increases by 2100 compared to year 2000, with increases of 3.8°F, 6.2°F and 8.3°F for CMIP3 B1, A1B and A2 scenarios, respectively; and increases of 2.2°F, 4.4°F, 7.7°F, and 10.0°F for CMIP5 RCP2.6, 4.5, 6.0, and 8.5, respectively. The range of temperature increase in CMIP5 simulations is higher than that of CMIP3 simulations, reflecting the larger range of radiative forcing. The 5th to 95th percentile ranges of both CMIP3 and CMIP5 simulations are, in general, increasing as the temperature increases. A notable feature is the increased sensitivity of temperature changes to the radiative forcing with time. For the CMIP3 simulations, the temperature increase for the A1B scenario is higher than that for the A2 scenario prior to 2060, but lower than A2 after 2060. For CMIP5 simulations, temperatures for RCP2.6 increase by 2.5°F by the year 2040 and then decrease slightly. The temperature increase for RCP4.5 is higher than that for RCP6.0 prior to 2075. These features can be seen in Fig. 1a, which shows the projected global carbon dioxide concentration for the 21st century.

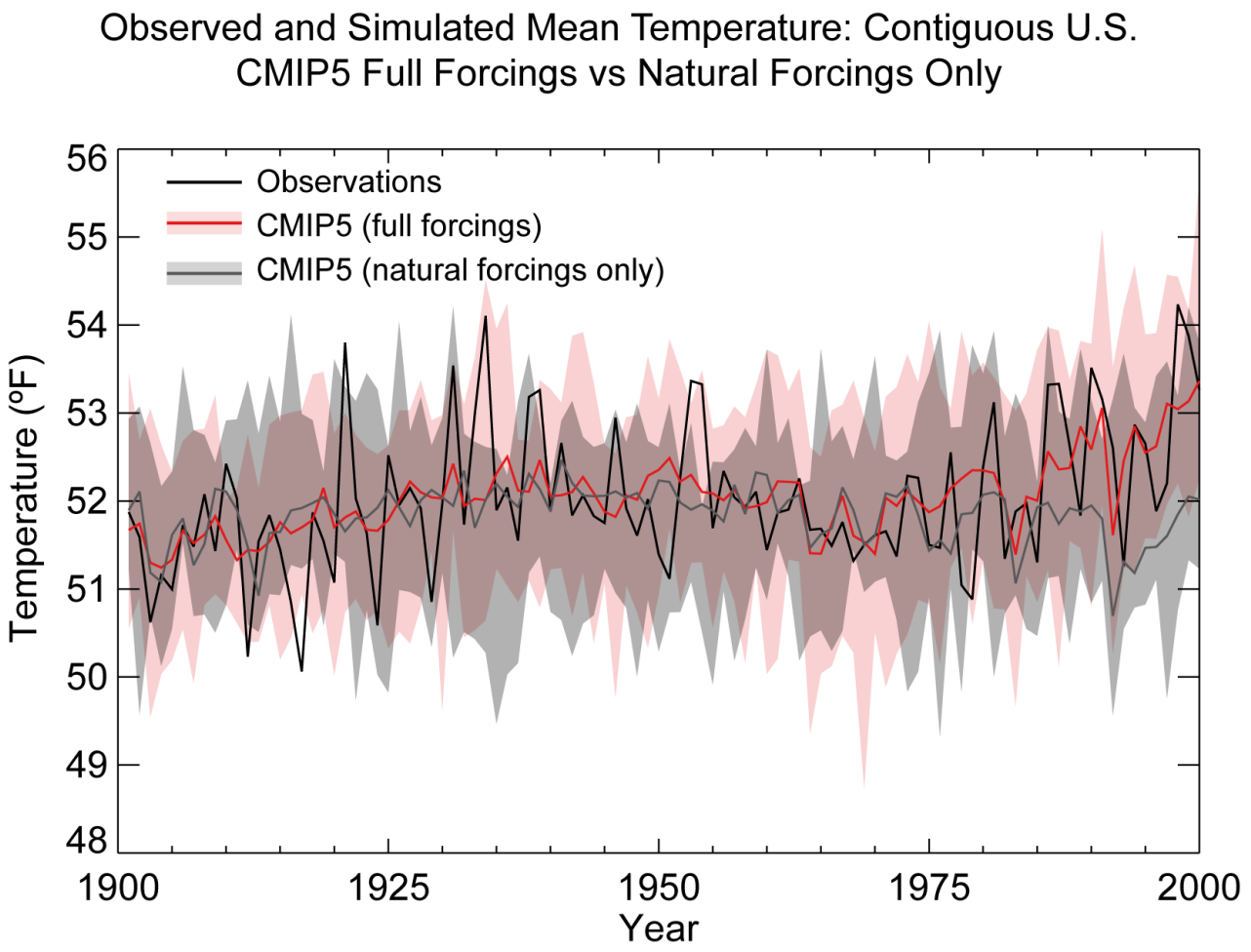

Figure 2. *Observed and simulated annual mean temperature (°F) for the contiguous U.S. for 1901–2000. Observational data are from NCEI's Climate Divisional Dataset (nClimDiv, black); simulations are CMIP5 multi-model means using full forcings (red) and natural forcings only (gray). Shaded areas represent the 5th–95th percentile range of the model simulations.*

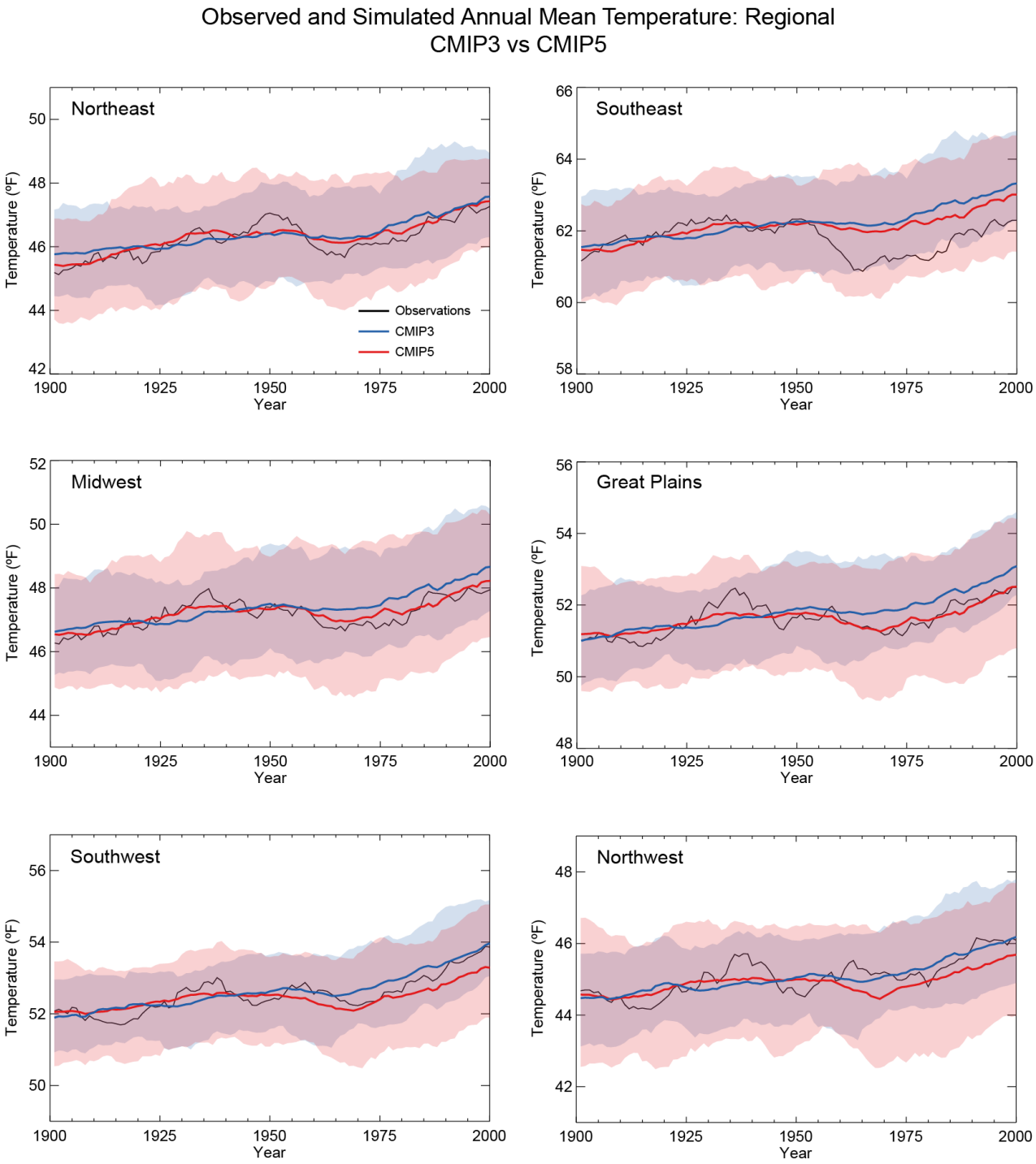

Figure 3. *Observed and simulated annual mean temperature (°F) for the six contiguous U.S. NCA regions for 1901–2000. Observational data are from NCEI's Climate Divisional Dataset (nClimDiv, black); simulations are multi-model means from CMIP3 (blue) and CMIP5 (red). Shaded areas represent the smoothed range of 5th–95th percentile range of the model simulations. Data are smoothed with a 10-year moving boxcar average. Note: these time series are on unique scales for each region.*

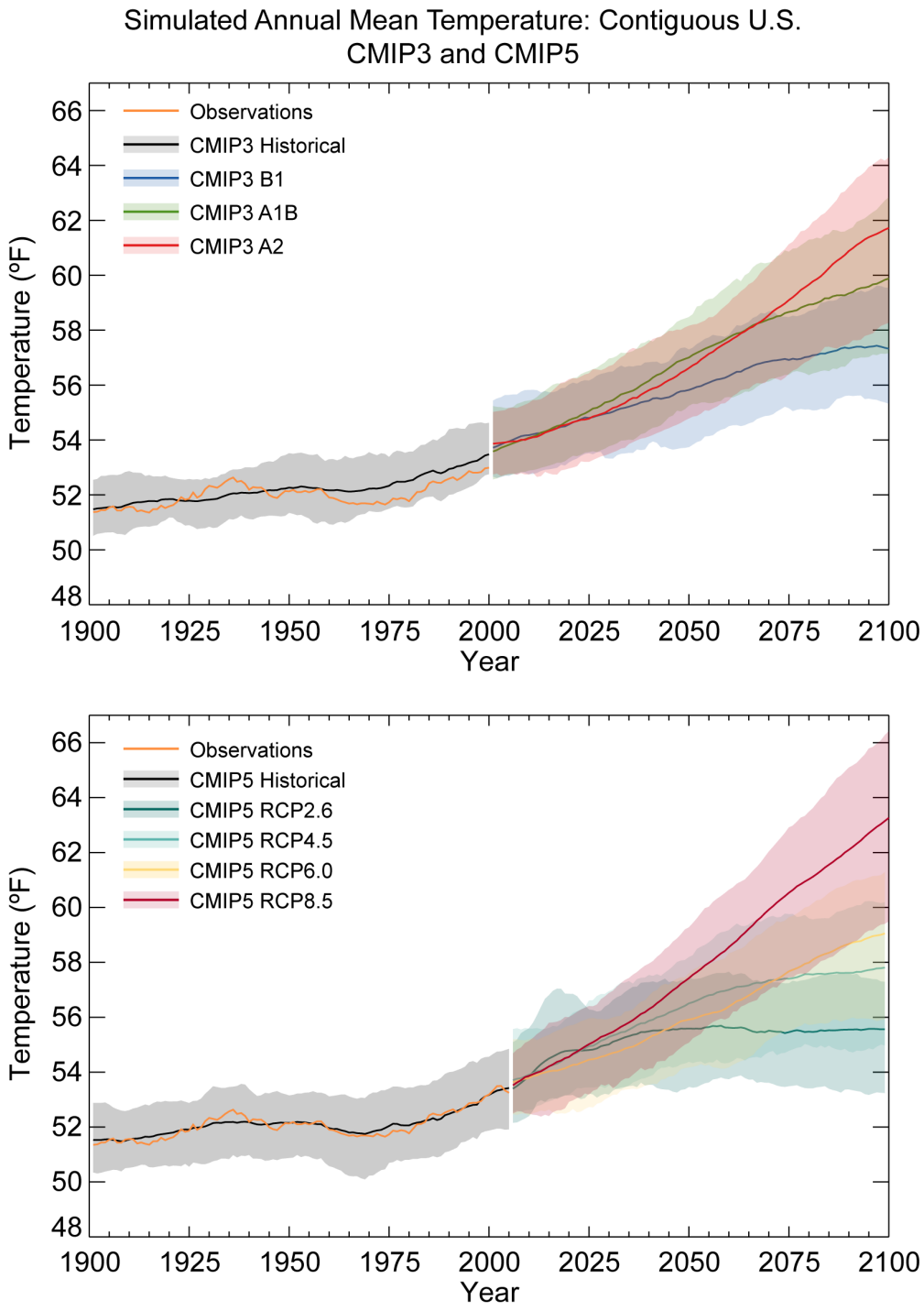

Figure 4. *Simulated annual mean temperature (°F) for the contiguous U.S. for 1900–2100. The upper panel shows observations from NCEI's Climate Divisional Dataset (nClimDiv, orange), multi-model mean simulations from CMIP3 for the historical period (black), and under the SRES B1 (blue), A1B (green), and A2 (red) scenarios. The lower panel shows observations from NCEI's Climate Divisional Dataset (nClimDiv, orange), multi-model mean simulations from CMIP5 for the historical period (black), and under the RCP2.6 (dark teal), 4.5 (light teal), 6.0 (yellow), and 8.5 (dark red) scenarios. Shaded areas represent the smoothed range of 5th–95th percentile range of the model simulations. Data are smoothed with a 10-year moving boxcar average.*

Figures 5a and 5b show the spatial distribution of multi-model mean simulated differences in average annual temperature for the future time period of 2021–2050 relative to the model reference period of 1971–2000. Both CMIP3 and CMIP5 simulations indicate an increase in temperature across the United States, compared to the reference period of 1971–2000, which is a continuation of the climatological upward trend of the last 30 years. Spatial variations are generally small across the contiguous U.S. and Hawai‘i, with a greater range of temperatures seen for Alaska under the CMIP5 scenario. Both CMIP3 and CMIP5 simulations also agree on the sign of change, with all grid points satisfying category 3 (see Section 3), i.e., the models are in agreement with regard to temperature increases throughout the country. For CMIP3 simulations, the temperature increases for the B1 scenario are less than 3°F everywhere throughout the contiguous U.S and up to 4°F in Alaska. For both the A1B and A2 scenarios, the temperature increases range from 2°F to 3°F along coastal areas of the contiguous U.S. to 3°F to 4°F over areas inland, with A1B being warmer for several states. For Alaska, A1B and A2 simulations range from increases of 2°F in the south to 5°F in the north. For CMIP5 simulations, the amount of warming by scenario generally ranges from high to low as follows: RCP8.5, RCP4.5, RCP2.6, and RCP6.0. The west coast and areas of the southeast exhibit less warming than other areas of the contiguous United States, with more pronounced warming in the Great Lakes and the Rocky Mountains regions. Again, there is a south-north gradient in temperature increases for Alaska, with increases of up to 8°F indicated under the RCP8.5 scenario. The range of changes among the four RCPs is higher than for the three CMIP3 scenarios, reflecting the larger range of radiative forcing. An exception, however, is Hawai‘i, where simulated temperature increases are less than 2°F for all but the RCP8.5 scenario. Temperature changes for RCP6.0 are less than for RCP2.6 and RCP4.5, reflecting the fact that greenhouse gas concentrations are actually less in RCP6.0 than the other two scenarios in this early 21st century period.

Figures 6a and 6b are the same as Figs. 5a and 5b, but for the period of 2041–2070. A continuation of warming is simulated in all scenarios, with the models agreeing on temperature increases across the United States (all grid points satisfying category 3). Among CMIP3 simulations, the B1 scenario simulates the least amount of warming, ranging from less than 2°F in Hawai‘i to 6°F in northern Alaska. The A1B and A2 scenarios simulate maximum increases of 3°F for Hawai‘i, 6°F for the contiguous United States, and 7°F for Alaska. Among CMIP5 simulations, RCP8.5 again simulates the most warming, with maxima of 6°F in the northern parts of the contiguous U.S. and the Rocky Mountains and more than 10°F in Alaska. Unlike for 2021–2050 (Fig. 5a), however, RCP6.0 is warmer than RCP2.6 for this period. The range of changes among the four RCPs is higher than for the three CMIP3 scenarios, and the overall range of temperature differences is larger than for 2021–2050. Temperature changes for RCP6.0 are less than for RCP4.5, reflecting the fact that greenhouse gas concentrations are actually less in RCP6.0 than in RCP4.5 in this mid-21st century period.

Figures 7a and 7b are the same as Figs. 5a and 5b, but for the period of 2070–2099. A continuation of warming is again simulated in all scenarios, with all grid points satisfying category 3. Among CMIP3 simulations, the B1 scenario simulates the least amount of warming, ranging from 2°F in southern Florida to 7°F in northern Alaska. The warming becomes larger in the A2 scenario than in the A1B scenario, with a maximum increase of 9°F in inland parts of the contiguous U.S. and more than 10°F in Alaska. Among CMIP5 simulations, RCP8.5 again simulates the most warming, with more than 10°F in the northern parts of the lower 48 and the majority of Alaska. RCP6.0 becomes warmer than RCP4.5, with increases of up to 7°F in the Great Lakes and more than 10°F in northern Alaska. RCP2.6 simulates the least amount of warming, ranging from less than 2°F in Hawai‘i and along the contiguous U.S. coast to 7°F in Alaska. The range of temperature changes between CMIP5 and CMIP3 is the largest compared to the periods of 2021–2050 and 2041–2070.

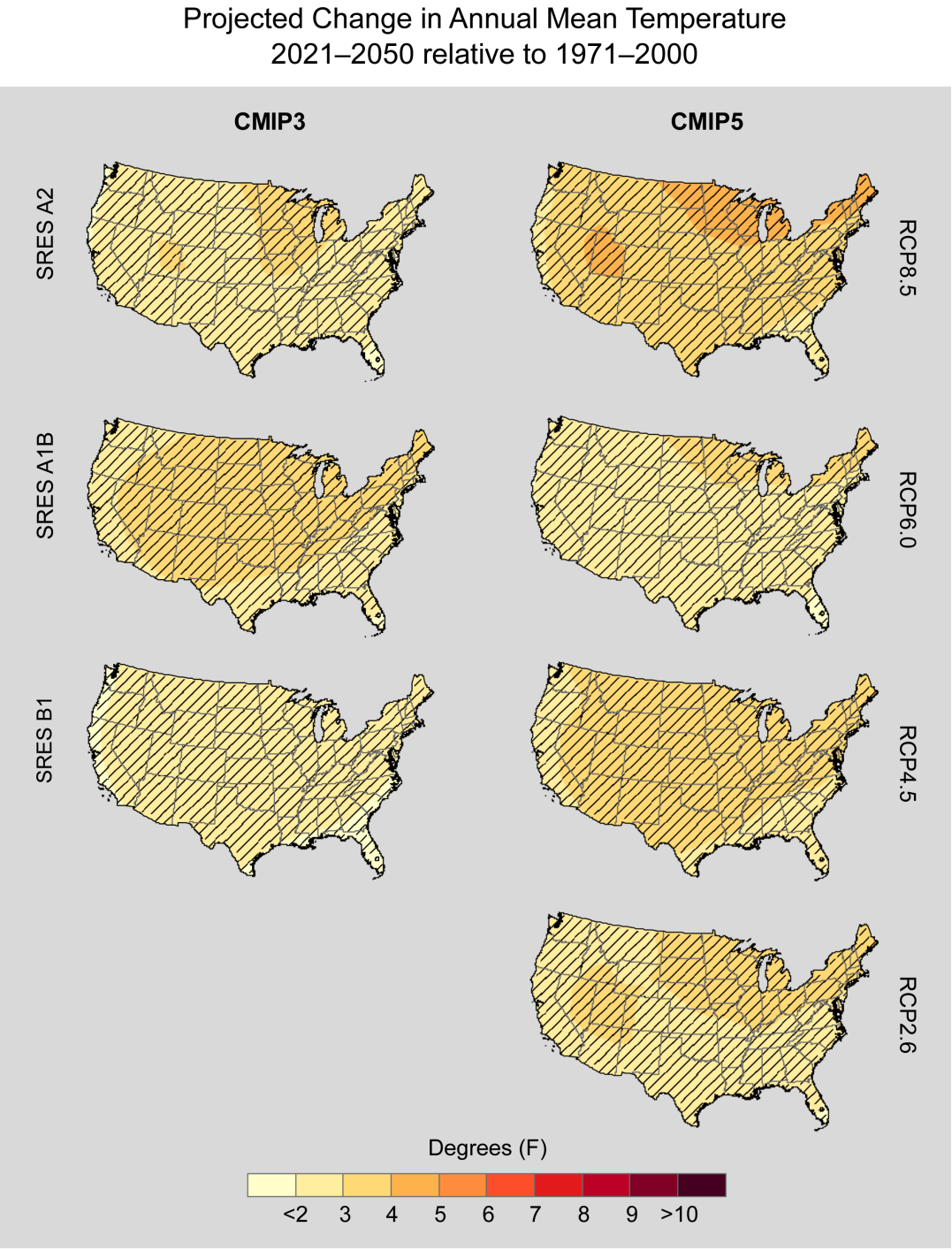

Figure 5a. *Projected change in annual mean temperature (°F) for the contiguous United States, for 2021–2050 with respect to the reference period of 1971–2000. These are multi-model means using CMIP3 SRES A2, A1B, and B1 scenarios (left column), and CMIP5 RCP8.5, 6.0, 4.5, and 2.6 scenarios (right column). Color with hatching (category 3) indicates that more than 50% of the models show a statistically significant change, and more than 67% agree on the sign of the change (see Section 3).*

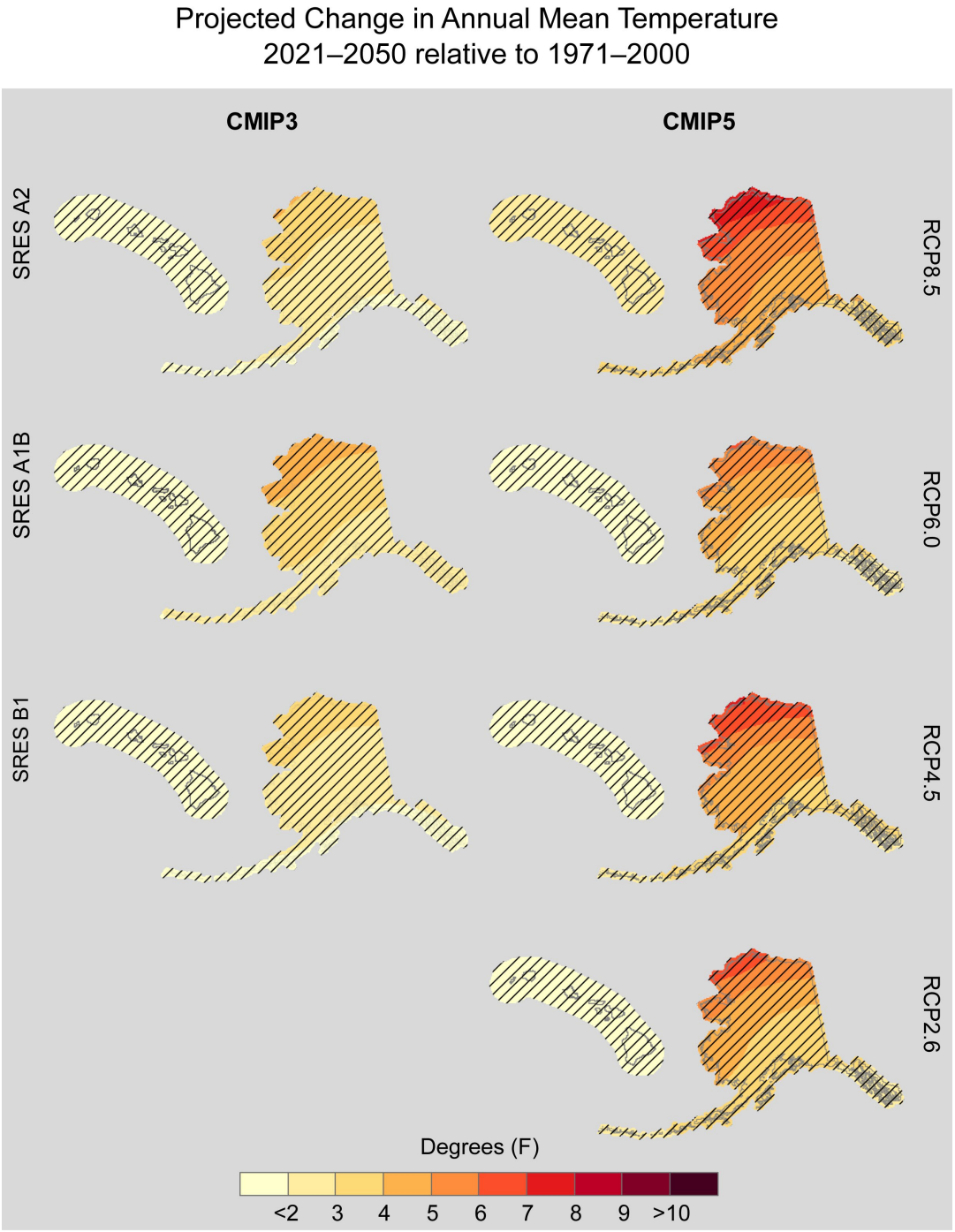

Figure 5b. *Projected change in annual mean temperature (°F) for Alaska and Hawai'i, for 2021–2050 with respect to the reference period of 1971–2000. These are multi-model means using CMIP3 SRES A2, A1B, and B1 scenarios (left column), and CMIP5 RCP8.5, 6.0, 4.5, and 2.6 scenarios (right column). Color with hatching (category 3) indicates that more than 50% of the models show a statistically significant change, and more than 67% agree on the sign of the change (see Section 3).*

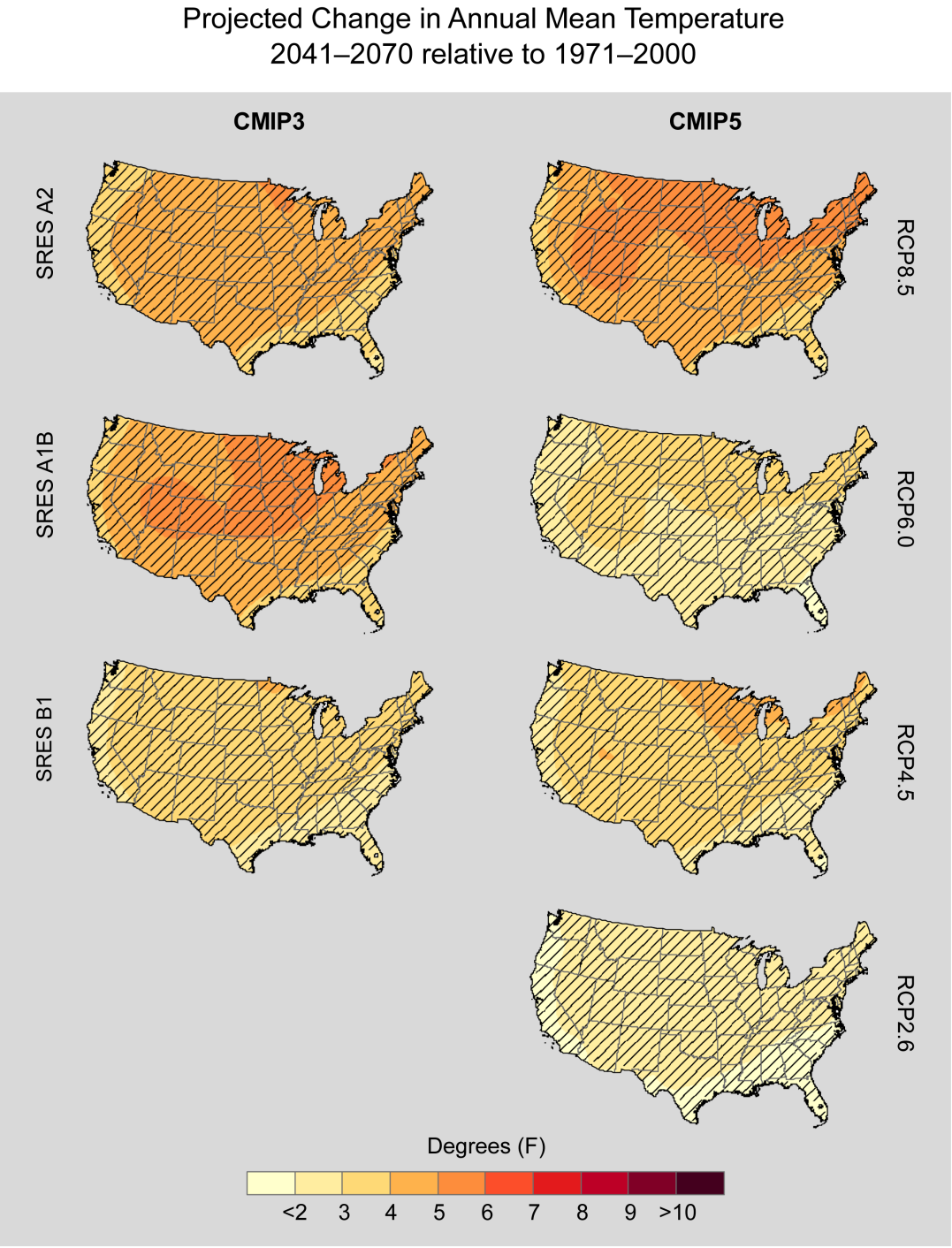

Figure 6a. *Projected change in annual mean temperature (°F) for the contiguous United States, for 2041–2070 with respect to the reference period of 1971–2000. These are multi-model means using CMIP3 SRES A2, A1B, and B1 scenarios (left column), and CMIP5 RCP8.5, 6.0, 4.5, and 2.6 scenarios (right column). Color with hatching (category 3) indicates that more than 50% of the models show a statistically significant change, and more than 67% agree on the sign of the change (see Section 3).*

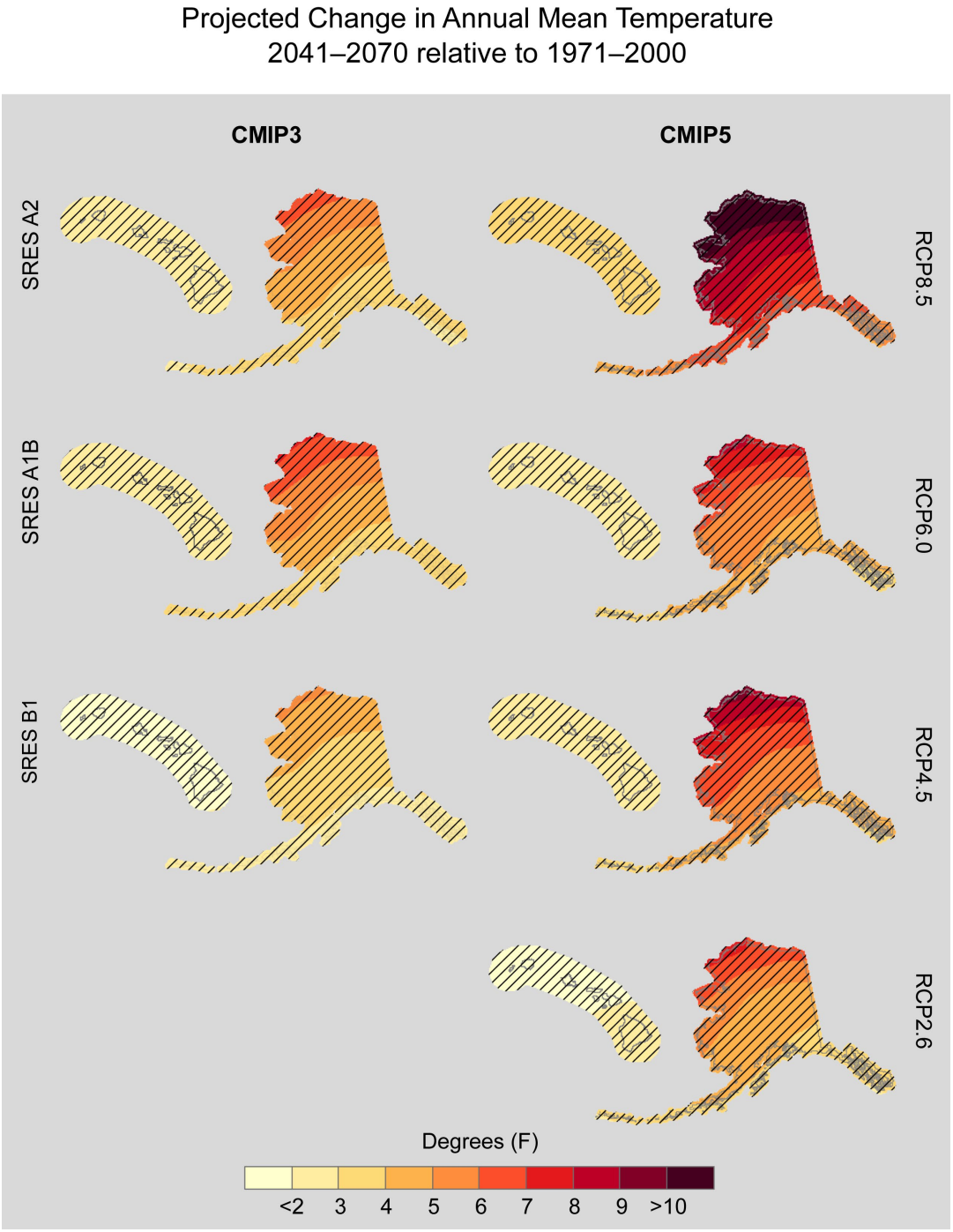

Figure 6b. *Projected change in annual mean temperature (°F) for Alaska and Hawai'i, for 2041–2070 with respect to the reference period of 1971–2000. These are multi-model means using CMIP3 SRES A2, A1B, and B1 scenarios (left column), and CMIP5 RCP8.5, 6.0, 4.5, and 2.6 scenarios (right column). Color with hatching (category 3) indicates that more than 50% of the models show a statistically significant change, and more than 67% agree on the sign of the change (see Section 3).*

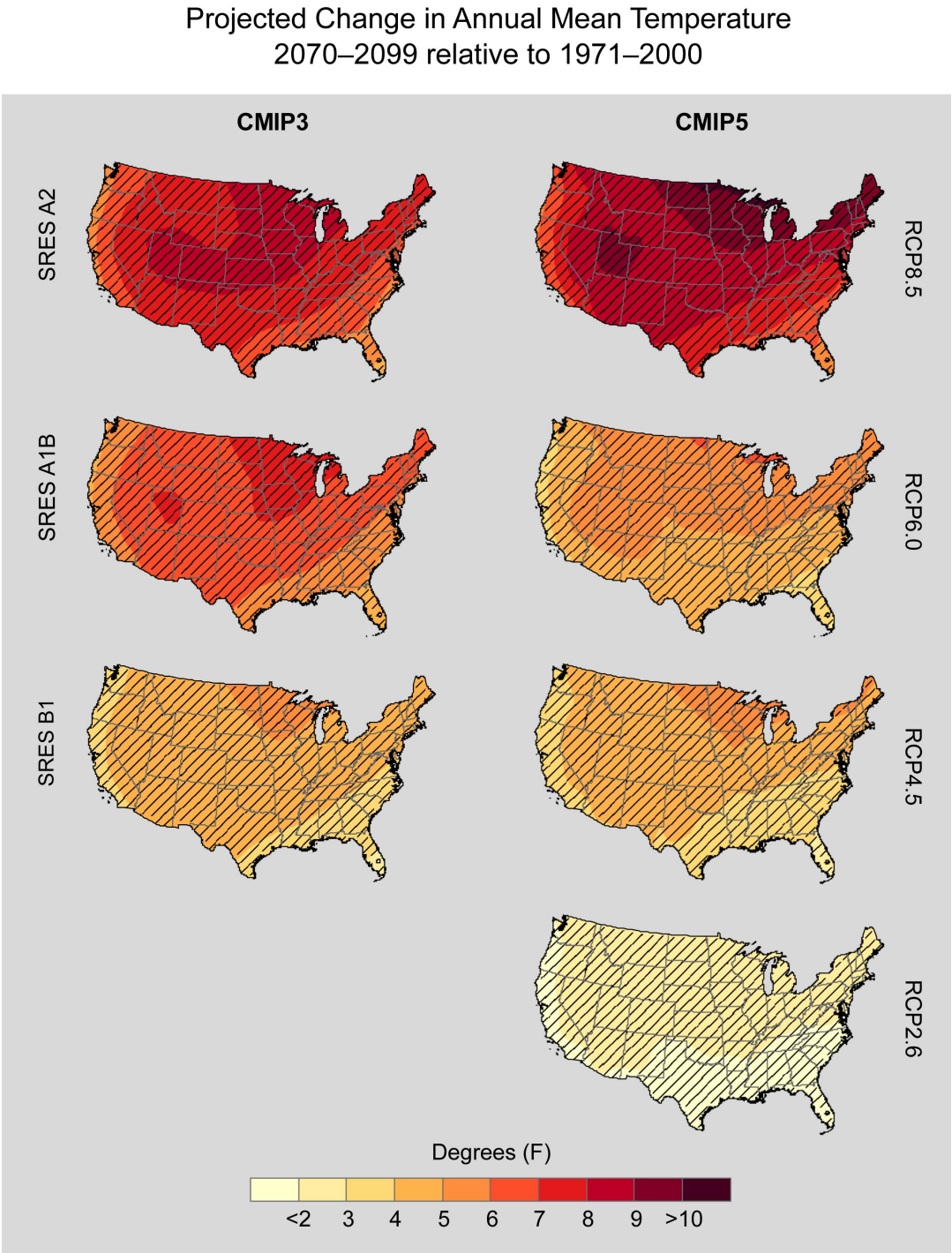

Figure 7a. *Projected change in annual mean temperature (°F) for the contiguous United States, for 2070–2099 with respect to the reference period of 1971–2000. These are multi-model means using CMIP3 SRES A2, A1B, and B1 scenarios (left column), and CMIP5 RCP8.5, 6.0, 4.5, and 2.6 scenarios (right column). Color with hatching (category 3) indicates that more than 50% of the models show a statistically significant change, and more than 67% agree on the sign of the change (see Section 3).*

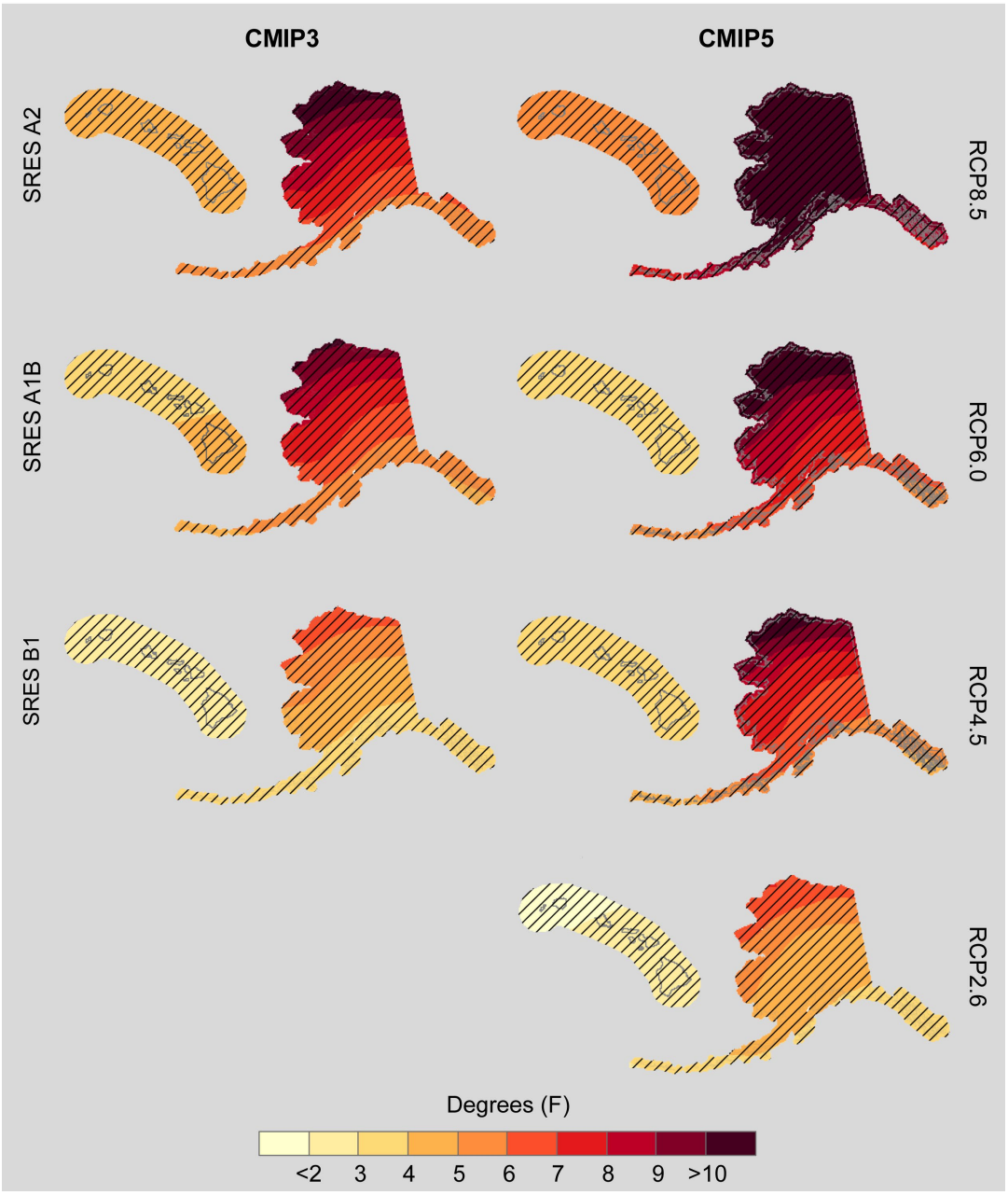

Figure 7b. *Projected change in annual mean temperature (°F) for Alaska and Hawai'i, for 2070–2099 with respect to the reference period of 1971–2000. These are multi-model means using CMIP3 SRES A2, A1B, and B1 scenarios (left column), and CMIP5 RCP8.5, 6.0, 4.5, and 2.6 scenarios (right column). Color with hatching (category 3) indicates that more than 50% of the models show a statistically significant change, and more than 67% agree on the sign of the change (see Section 3).*

Figure 8a shows the multi-model mean simulated seasonal temperature changes between 2041–2070 and 1971–2000 for the high scenarios of CMIP3 A2 and CMIP5 RCP8.5. The magnitude and the spatial pattern of simulated temperature changes vary with seasons, but once again all grid points satisfy category 3. Both scenarios simulate similar spatial patterns for the same season, with RCP8.5 being warmer. The winter season shows a general south-to-north gradient in simulated temperature changes for the contiguous United States, with the greatest warming (up to 6°F for A2 and 8°F for RCP8.5) occurring in the northern reaches of the country, and the least (less than 2°F for A2 and 2°–3°F for RCP8.5) occurring in the southeast. A southeast-to-northwest gradient can be seen for Alaska (Fig. 8b), with increases of over 10°F across the majority of the state for RCP8.5. Spring shows the least warming in most areas, with values of 3°–4°F (A2) and 4°–6°F (RCP8.5) over the central contiguous U.S. and 2°–3°F (A2) and 3°–4°F (RCP8.5) in the southeastern part of the country and the west coast. Simulated temperature increases for Alaska are higher, ranging up to 10°F for RCP8.5. The greatest amount of warming across the lower 48 can be seen for summer, and is characterized by enhanced warming in the Rocky Mountains, up to 6°F for A2 and 7°F for RCP8.5. By contrast, summer shows the least amount of warming of any season for Alaska, with values of 2°–4°F for A2 and 5°–7°F for RCP 8.5. Fall shows the least spatial variability for the contiguous United States, with values ranging from 2°–3°F (A2) and 3°–4°F (RCP8.5) in coastal areas to up to 6°F over the center of the country for RCP8.5. In Alaska, however, values range from 2°F in the southeast under the A2 scenario to greater than 10°F in the north under the RCP8.5 scenario. For Hawai‘i temperature changes are spatially uniform and the same for all seasons, with values of 2°–3°F under the A2 scenario and 3°–4°F under the RCP8.5 scenario.

Figure 9 shows the simulated change in annual mean temperature for three future time periods with respect to 1971–2000, averaged over the entire continental United States. For CMIP3, the A2, A1B, and B1 scenarios are shown. For CMIP5, all four RCP scenarios are shown. Both the multi-model mean and individual model values are displayed. For the high scenarios, the A2 (RCP8.5) models simulate average increases of 2.9(3.5)°F by 2035, 4.6(5.8)°F by 2055, and nearly 8(9.5)°F by 2085. The increases for the low A2 (RCP2.6) scenarios are similar in 2035 at around 2.5(3.0)°F, but by 2085 the increase of 4.8(3.2)°F is much smaller. The range of temperature changes among the different scenarios is considerably larger in the CMIP5 models by the end of the 21st century. The multi-model mean difference between B1 and A2 is about 3°F, but is around 6°F between RCP2.6 and RCP8.5. This is a direct result of the larger range of scenarios in the CMIP5 experiment than in the CMIP3 experiment. Temperature changes for RCP6.0 are less than for RCP2.6 in the early 21st century and less than for RCP4.5 in the early and mid-21st century periods, reflecting the fact that the relative greenhouse gas concentrations for these three scenarios actually cross over during the 21st century.

The distribution of simulated regional changes in annual mean temperature for 2041–2070 with respect to 1971–1999 is compared between the low and high scenarios for CMIP3 and CMIP5 in Table 6. At the middle of the 21st century, the median temperature changes are very similar between B1 and RCP2.6 in all regions, but the range is larger for RCP2.6. The similarity in median changes reflects the similarity of the two scenarios out to the middle of the 21st century—they diverge more toward the end of the century. The median changes and range of changes are larger for RCP8.5 than for A2 in all regions.

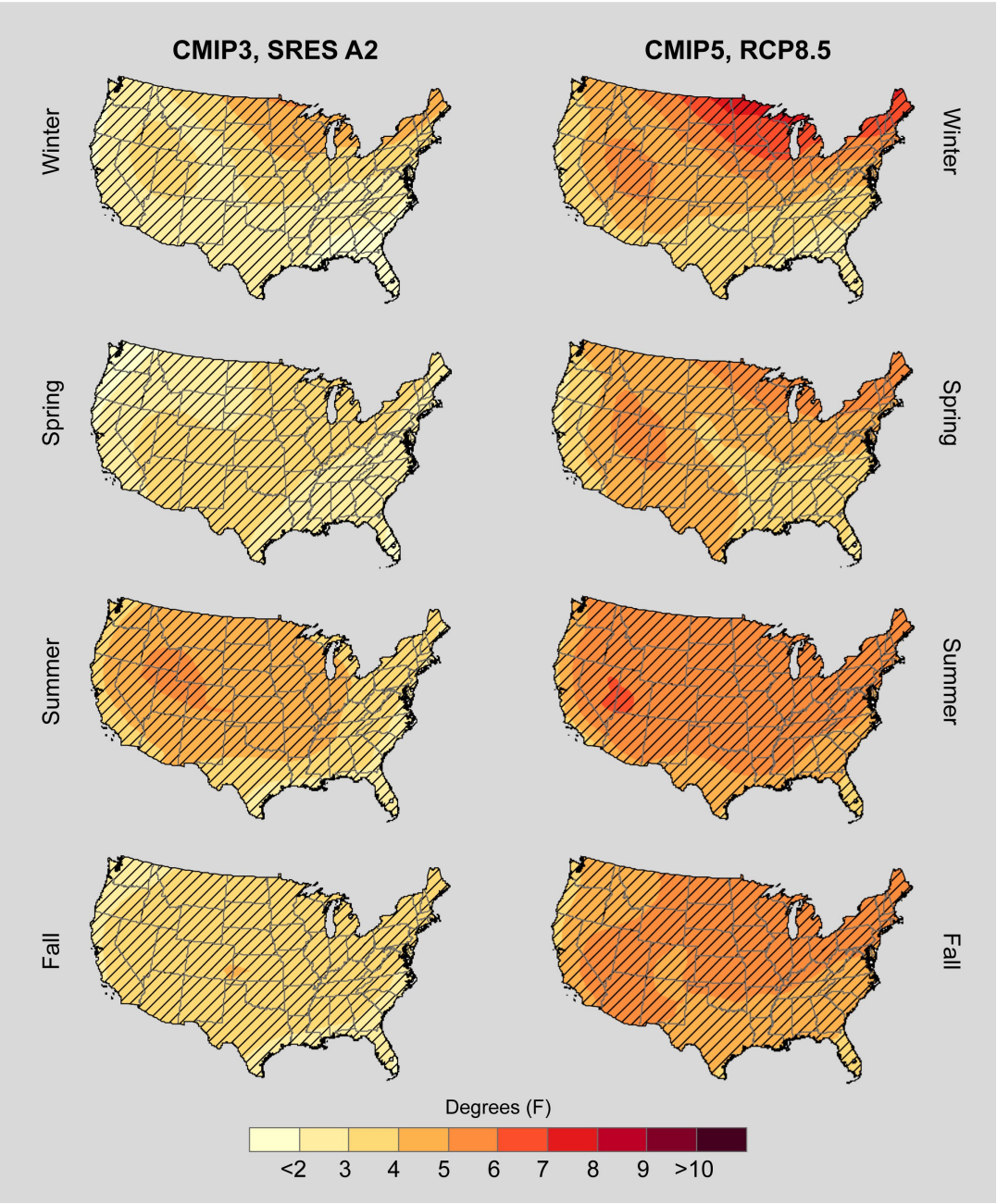

Figure 8a. *Projected change in seasonal mean temperature (°F) for the contiguous United States, for 2041–2070 with respect to the reference period of 1971–2000. These are multi-model means using CMIP3 SRES A2 (left column), and CMIP5 RCP8.5 (right column). Color with hatching (category 3) indicates that more than 50% of the models show a statistically significant change, and more than 67% agree on the sign of the change (see Section 3).*

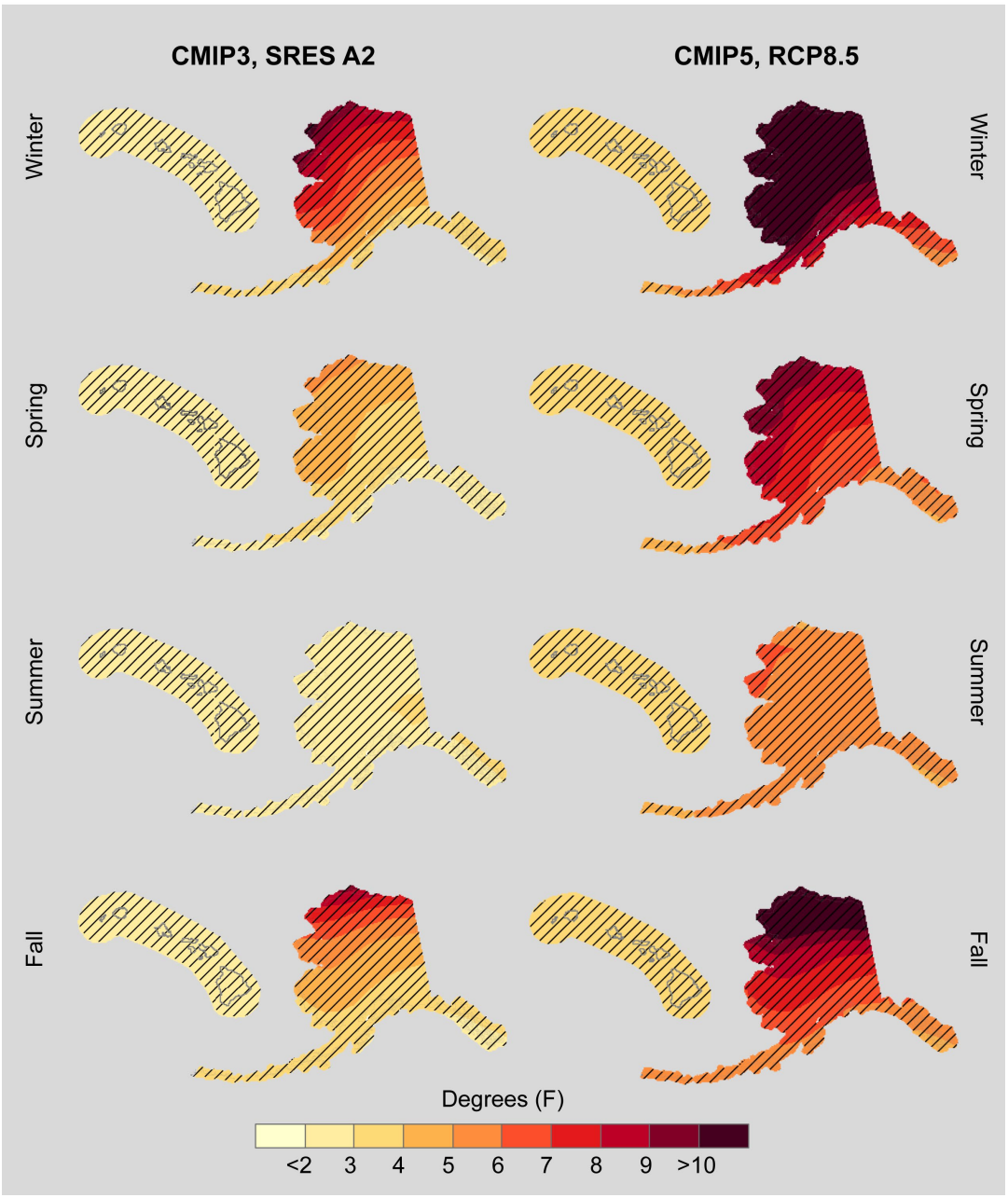

Figure 8b. *Projected change in seasonal mean temperature (°F) for Alaska and Hawai'i, for 2041–2070 with respect to the reference period of 1971–2000. These are multi-model means using CMIP3 SRES A2 (left column), and CMIP5 RCP8.5 (right column). Color with hatching (category 3) indicates that more than 50% of the models show a statistically significant change, and more than 67% agree on the sign of the change (see Section 3).*

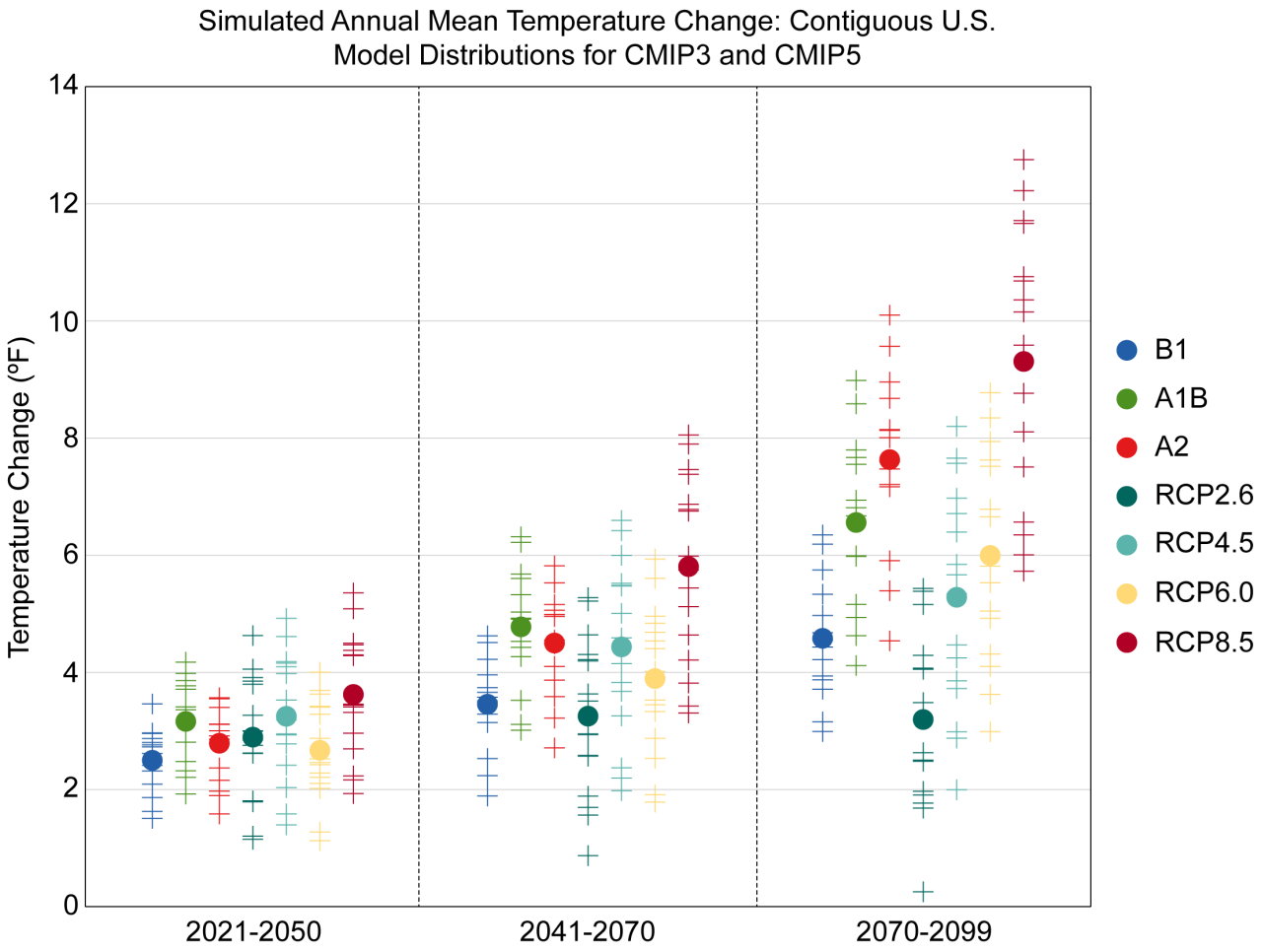

Figure 9. *Model distributions of simulated annual mean temperature change (°F) for the contiguous United States, for each future time period (2021–2050, 2041–2070, and 2070–2099) with respect to the reference period of 1971–2000 for each CMIP3 and CMIP5 scenario. The small plus signs (+) indicate each individual model and the circles depict the multi-model means.*

Table 6. *Distribution of the simulated change in annual mean temperature (°F) amongst models using the CMIP3 SRES B1 and A2 scenarios and the CMIP5 RCP2.6 and 8.5 scenarios, for each U.S. region. The lowest, 25th percentile, median, 75th percentile, and highest values are given for 2041–2070, with respect to the reference period of 1971–2000.*

Region	Scenario	Lowest	25th Percentile	Median	75th Percentile	Highest
Northeast	SRES B1	2.1	3.2	3.6	4.1	4.6
	RCP2.6	0.9	2.1	3.5	4.0	6.2
	SRES A2	2.9	4.1	4.8	5.3	5.7
	RCP8.5	3.9	4.9	6.1	8.0	9.1
Southeast	SRES B1	1.6	2.6	3.0	3.4	3.8
	RCP2.6	0.9	2.3	3.0	3.9	4.4
	SRES A2	2.3	3.3	4.3	4.5	5.4
	RCP8.5	2.9	4.0	5.1	6.4	6.8
Midwest	SRES B1	2.1	3.2	4.0	4.3	5.0
	RCP2.6	1.0	1.9	3.6	4.9	6.4
	SRES A2	2.9	4.1	5.1	5.6	6.3
	RCP8.5	3.6	4.6	6.2	8.1	9.6
Great Plains	SRES B1	1.9	2.9	3.5	4.3	4.7
	RCP2.6	0.9	1.7	3.3	4.5	5.2
	SRES A2	2.6	3.8	4.7	5.0	5.9
	RCP8.5	3.2	4.2	6.1	7.5	8.0
Southwest	SRES B1	1.8	2.6	3.6	4.1	4.8
	RCP2.6	0.7	1.9	3.3	4.1	5.3
	SRES A2	2.7	3.6	4.8	5.3	5.9
	RCP8.5	3.1	4.3	6.1	7.1	8.1
Northwest	SRES B1	1.9	2.3	3.2	4.0	4.4
	RCP2.6	0.8	1.7	3.1	4.2	5.6
	SRES A2	2.4	3.1	4.0	4.7	4.9
	RCP8.5	3.1	3.5	5.6	7.2	8.5
Alaska	SRES B1	2.6	3.1	4.0	4.6	5.5
	RCP2.6	1.5	3.8	4.7	6.5	10.1
	SRES A2	3.4	4.0	4.7	5.0	7.6
	RCP8.5	5.3	6.4	8.1	11.0	14.2
Hawai‘i	SRES B1	1.0	1.8	1.9	2.4	2.5
	RCP2.6	0.9	1.2	2.0	2.7	3.1
	SRES A2	1.7	2.4	2.7	2.8	3.0
	RCP8.5	2.0	3.0	3.3	4.5	4.9
Contiguous U.S.	SRES B1	1.9	2.8	3.5	4.1	4.6
	RCP2.6	0.9	1.9	3.2	4.3	5.3
	SRES A2	2.7	3.7	4.8	5.1	5.8
	RCP8.5	3.3	4.2	5.9	7.4	8.1

On decadal time scales, climate variations arising from natural factors can be comparable to or larger than changes arising from anthropogenic forcing. An analysis of change on such time scales was performed by examining the decadal changes simulated by the CMIP3 and CMIP5 models with respect to the most recent historical decade of 2001–2010. Figure 10 shows the simulated change in decadal mean values of annual temperature for each future decadal time period with respect to 2001–2010, averaged over the continental United States. For CMIP3, the A2, A1B, and B1 scenarios are shown. For CMIP5, all four RCP scenarios are shown. For the 2011–2020 decade, the temperature increases are not statistically significant relative to the 2001–2010 decade for many of the models. As the time period increases, more of the individual models simulate statistically significant temperature changes, with all being significant at the 95% confidence level by 2025 for RCP8.5, 2035 for the A2, A1B, and RCP4.5 scenarios, 2045 for RCP6.0, and 2055 for the B1 scenario. By these points in time, almost all of the model decadal mean values lie outside the 10th to 90th percentile range of the historical annual temperature anomalies. For RCP2.6, the temperature changes are not statistically significant for some models all the way out to 2095, and the changes for some models are within the 10th to 90th percentile range of the historical annual temperature anomalies, indicating the moderate temperature change under this very low scenario. As also shown in Fig. 10, the model simulations generally show increased variability over time.

The differences between the CMIP3 and CMIP5 results are relatively minor, and these small differences probably reflect the larger range of scenarios in CMIP5. For example, the very low RCP2.6 scenario includes some model simulations with temperature changes at the end of the 21st century being smaller than the 10th to 90th percentile range of the historical annual temperature anomalies—something not seen in any of the CMIP3 simulations.

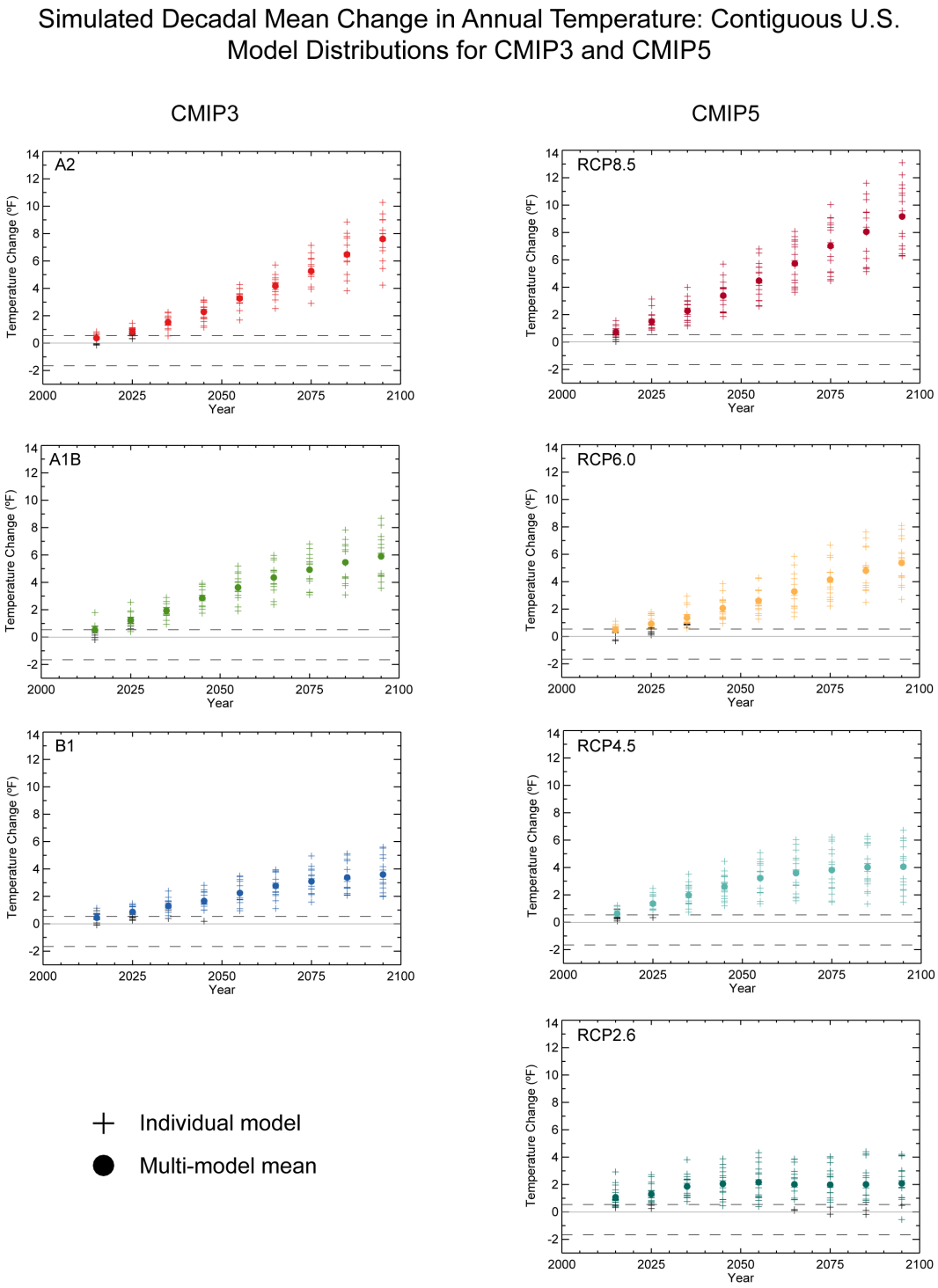

Figure 10. *Model distributions of simulated decadal mean change in annual temperature (°F) for the contiguous United States, for each future decadal time period (represented by their approximate midpoints, e.g., 2015 = 2011–2020), with respect to the reference period of 2001–2010. The left panels show values for the CMIP3 SRES B1 (blue), A1B (green), and A2 (red) scenarios. The right panels show values for the CMIP5 RCP2.6 (light teal), 4.5 (dark teal), 6.0 (yellow), and 8.5 (dark red) scenarios. Each individual model is represented by a plus sign (+), with circles depicting the multi-model means. These symbols are shown in color if the value is statistically significant at the 95% confidence level. Dashed lines indicate the 10th and 90th percentiles of observed temperature anomaly values from 1981–2010.*

4.2.2. Extreme Temperature

CLIMDEX extremes indices, as described in Section 2, were analyzed across two common periods for which data were available for both CMIP3 and CMIP5 models. These were identified as 1981–2000 and 2046–2065. The multi-model mean difference was also computed. In addition, average values for the NCA regions were computed for each model. Finally, multi-model mean and the 25th and 75th percentile values were computed for each region.

For RCP8.5, simulations (Fig. 11a) indicate about 10 to 20 fewer nights below freezing in 2046–2065 for much of the southern United States, with even larger changes—at least 30 fewer nights—across the north and intermountain west. This represents a decrease of about 25% or more over most of the contiguous United States. The decreases are statistically significant, i.e., these grid points satisfy category 3 (see Section 3), except over Florida where present-day values are already very small or zero. For Hawai‘i (Fig. 11b), changes are small (less than 5 fewer nights) and are not statistically significant for most models (category 1). Alaska (Fig. 11b) shows relatively large changes in the number of nights below freezing, with decreases ranging from 20 nights in southern portions of the state, to greater than 45 nights in coastal areas. These changes also satisfy category 1. The dependence of regional changes on scenario (Fig. 12) roughly follows that of the temperature changes. For CMIP3 (Fig. 12, top panel), the decreases are smallest for the B1 scenario. Decreases are similar for the A1B and A2 scenarios, although slightly larger for A1B. Although A2 is a higher emissions scenario out to 2100 with larger temperature increases compared to A1B, A1B is actually slightly higher at the middle of the 21st century and this is reflected in the slightly larger decreases in the number of freezing nights. The interquartile range of decreases of about 5 to 15 nights is substantial but smaller than the multi-model mean changes of 10 to 30 nights. The changes for Hawai‘i are zero because present-day values are zero.

For CMIP5 (Fig. 12, bottom panel), the range of changes among the four RCPs is higher than for the three CMIP3 scenarios, reflecting the larger range of radiative forcing. Otherwise, there do not appear to be any substantive differences between the CMIP3 and CMIP5 results, when considering differences in greenhouse gas concentrations. For example, the decreases for RCP8.5 are considerably larger than for A1B or A2, but RCP8.5 has considerably higher greenhouse gas concentrations out to the mid-21st century than either of those scenarios. As was the case with mean temperature changes, the changes in Fig. 12 for RCP6.0 are less than for RCP4.5, reflecting the fact that greenhouse gas concentrations are actually less in RCP6.0 than in RCP4.5 in this mid-21st century period.

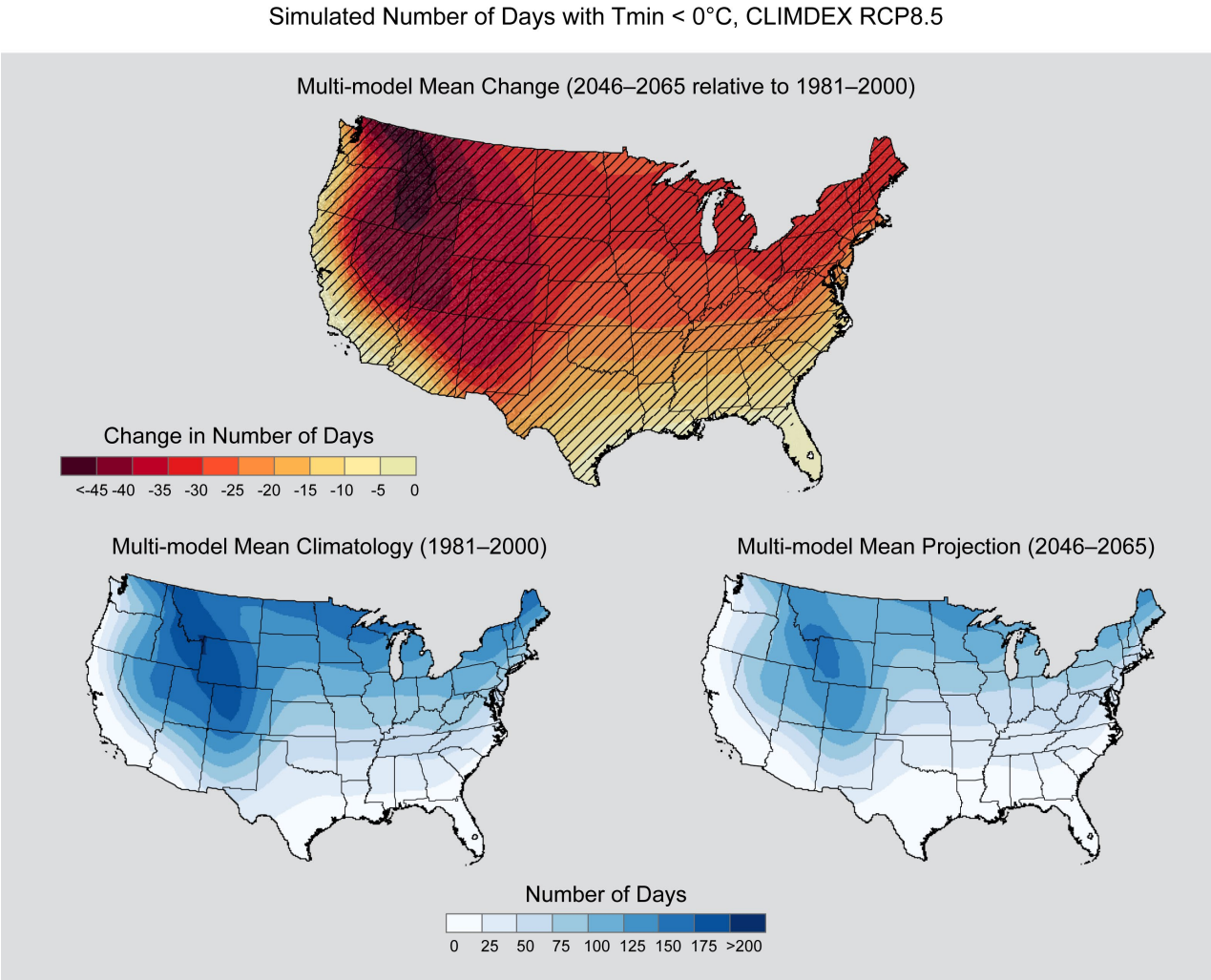

Figure 11a. *Simulated multi-model mean change in the mean annual number of days with a minimum temperature less than 0°C (T_{min} < 0°C) for the contiguous United States, for 2046–2065 with respect to the reference period of 1981–2000, using the CLIMDEX RCP8.5 scenario (top). Color only (category 1) indicates that less than 50% of the models show a statistically significant change. Color with hatching (category 3) indicates that more than 50% of the models show a statistically significant change, and more than 67% agree on the sign of the change (see Section 3). Multi-model mean climatology indicating the annual number of days with T_{min} < 0°C for 1981–2000 (bottom left). Multi-model mean projection indicating the annual number of days with T_{min} < 0°C for 2046–2065 (bottom right).*

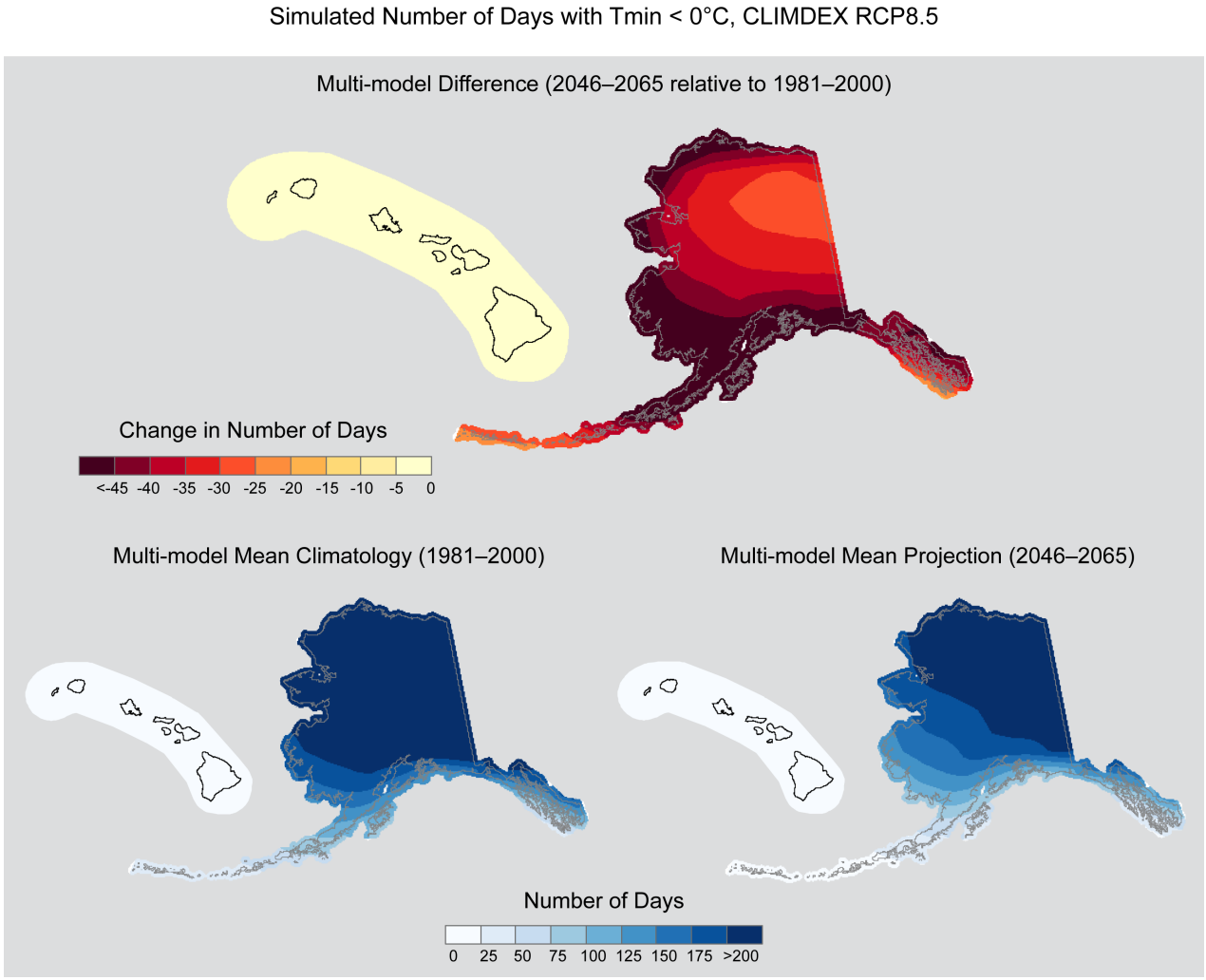

Figure 11b. *Simulated multi-model mean change in the mean annual number of days with a minimum temperature less than 0°C (T_{min} < 0°C) for Alaska and Hawai'i, for 2046–2065 with respect to the reference period of 1981–2000, using the CLIMDEX RCP8.5 scenario (top). Color only (category 1) indicates that less than 50% of the models show a statistically significant change (see Section 3). Multi-model mean climatology indicating the annual number of days with T_{min} < 0°C for 1981–2000 (bottom left). Multi-model mean projection indicating the annual number of days with T_{min} < 0°C for 2046–2065 (bottom right).*

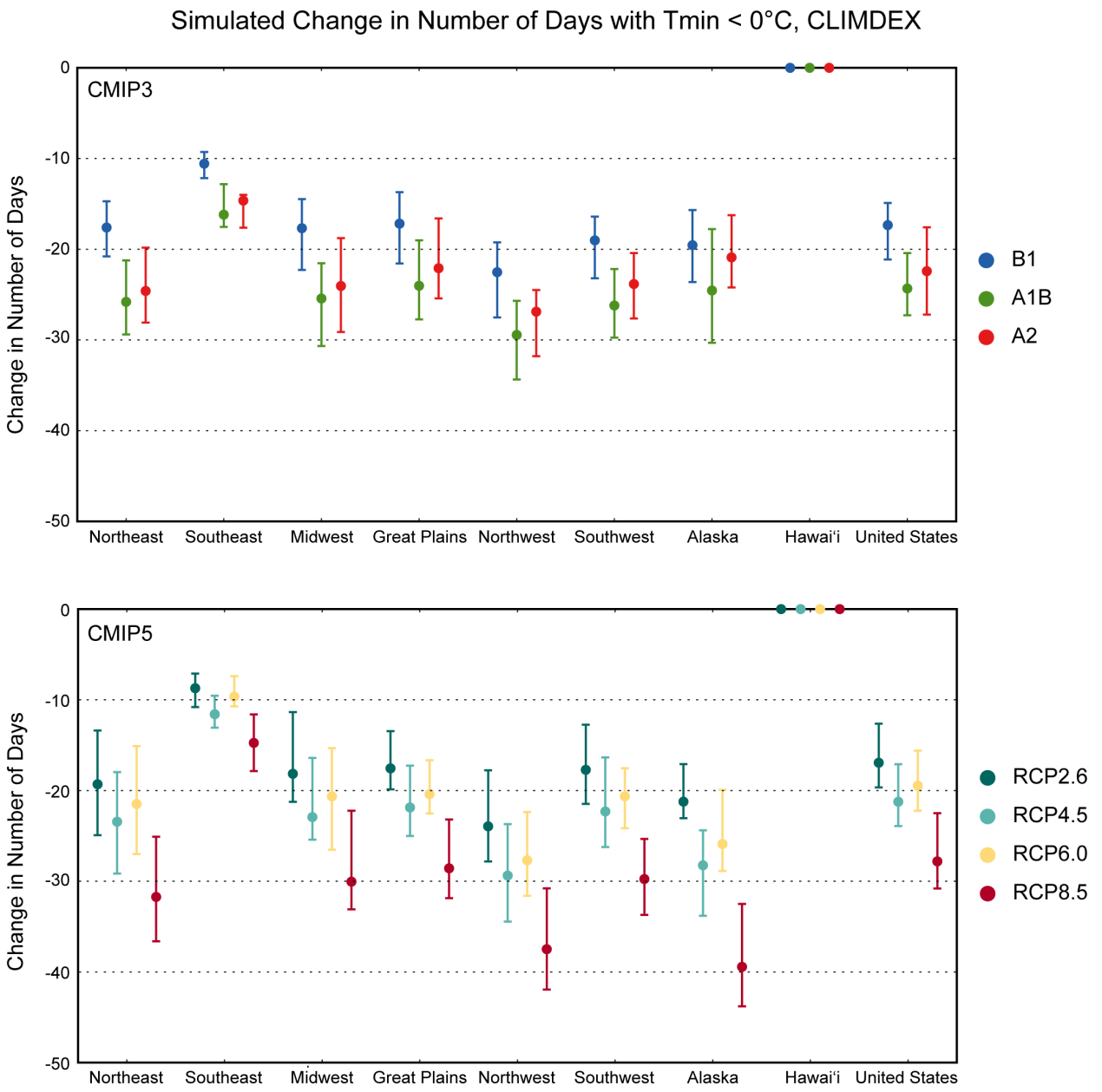

Figure 12. *Simulated change in the mean annual number of days with a minimum temperature less than 0°C for each region and the contiguous United States, for 2046–2065 with respect to the reference period of 1981–2000. The upper panel shows values for the CLIMDEX SRES B1 (blue), A1B (green), and A2 (red) scenarios. The lower panel shows values for the CLIMDEX RCP2.6 (dark teal), 4.5 (light teal), 6.0 (yellow), and 8.5 (dark red) scenarios. Bars indicate the interquartile ranges of model values and circles depict the multi-model means.*

For RCP8.5, simulations for 2046–2065 indicate increases of up to 40 more nights above 20°C across the majority of the contiguous United States, with larger increases across the south (Fig. 13a). This represents an increase of 25% to 50% in many areas. The models are in agreement on these increases, with all grid points satisfying category 3. For Hawai‘i (Fig. 13b), values range from 10 additional nights above 20°C in the south to 40 more in the north, however, these values are not statistically significant for most models (category 1). Alaska does not see any nights above 20°C, either presently or in the future. The dependence of regional changes on scenario (Fig. 14) roughly follows that of the temperature changes, as was the case for freezing nights. For CMIP3 (Fig. 14, top panel), the increases are smallest for the B1 scenario and roughly equal for the A1B and A2 scenarios. The interquartile range of increases of about 5 to 20 nights compares with the multi-model mean changes of 10 to 40 nights. The changes for Alaska are zero because future values are zero (that is, no nights above 20°C), even in a warmer climate. For CMIP5 (Fig. 14, bottom panel), the range of changes among the four RCPs is higher than for the three CMIP3 scenarios, reflecting the larger range of radiative forcing. Otherwise, there do not appear to be any substantive differences between the CMIP3 and CMIP5 results, when considering differences in greenhouse gas concentrations. For example, the increases for RCP8.5 are considerably larger than for A1B or A2, but RCP8.5 has considerably higher greenhouse gas concentrations out to the mid-21st century than either of those scenarios, as noted above. As was the case with mean temperature changes, the changes in Fig. 12 for RCP6.0 are less than for RCP4.5, reflecting the fact that greenhouse gas concentrations are actually less in RCP6.0 than in RCP4.5 in this mid-21st century period.

For RCP8.5, simulations for 2046–2065 indicate longer growing seasons, with increases of about 20 to 40 days over most of the contiguous U.S. and smaller increases in the far south and west (Fig. 15a). Most models agree that these increases are statistically significant everywhere (category 3) except for the far south and west where freezes in the present climate are relatively rare. Changes in growing season length cannot be quantified for Hawai‘i, as the average temperature does not get below freezing. The models also agree that the length of the growing season will increase throughout Alaska (Fig. 15b), with all grid points satisfying category 3. Values range from 20 to more than 40 additional days between the last frost in spring and the first frost in fall. The dependence of regional changes on scenario (Fig. 16) roughly follows that of the temperature changes, as was the case for freezing nights. For CMIP3 (Fig. 16, top panel), the increases are smallest for the B1 scenario and roughly equal for the A1B and A2 scenarios. The interquartile range of increases of about 5 to15 days compares with the multi-model mean changes of 10 to 25 days. The changes for Hawai‘i are zero because freezing temperatures do not occur in the present or future climate. For CMIP5 (Fig. 16, bottom panel), the range of changes among the four RCPs is higher than for the three CMIP3 scenarios, reflecting the larger range of radiative forcing. Otherwise, there do not appear to be any substantive differences between the CMIP3 and CMIP5 results, when considering differences in greenhouse gas concentrations. For example, the increases for RCP8.5 are considerably larger than for A1B or A2, but RCP8.5 has considerably higher greenhouse gas concentrations out to the mid-21st century than either of those scenarios. As was the case with mean temperature changes, the changes in Fig. 12 for RCP6.0 are less than for RCP4.5, reflecting the fact that greenhouse gas concentrations are actually less in RCP6.0 than in RCP4.5 in this mid-21st century period.

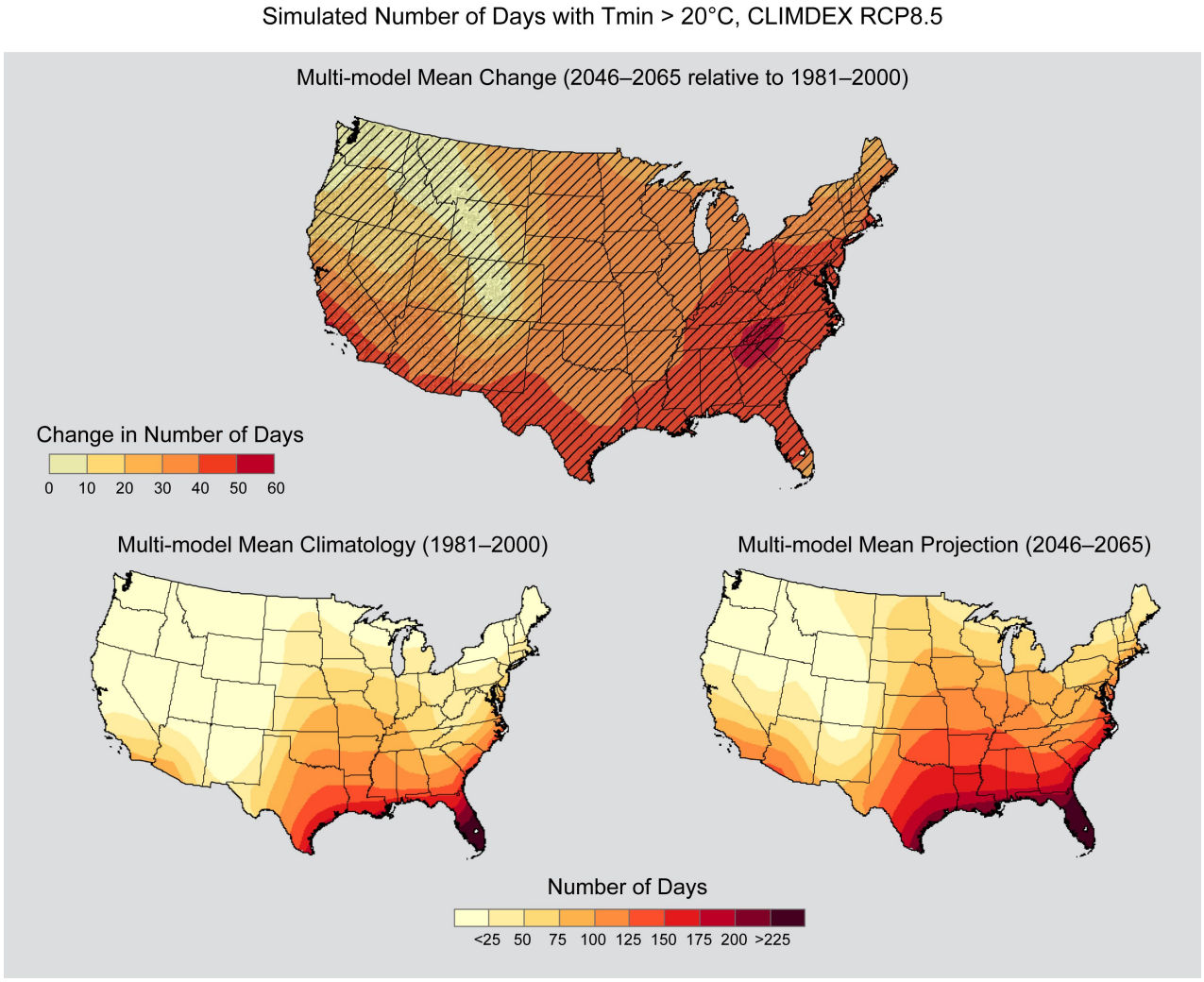

Figure 13a. *Simulated multi-model mean change in the mean annual number of days with a minimum temperature greater than 20°C (T_{min} > 20°C) for the contiguous United States, for 2046–2065 with respect to the reference period of 1981–2000, using the CLIMDEX RCP8.5 scenario (top). Color only (category 1) indicates that less than 50% of the models show a statistically significant change. Color with hatching (category 3) indicates that more than 50% of the models show a statistically significant change, and more than 67% agree on the sign of the change (see Section 3). Multi-model mean climatology indicating the annual number of days with T_{min} > 20°C for 1981–2000 (bottom left). Multi-model mean projection indicating the annual number of days with T_{min} > 20°C for 2046–2065 (bottom right).*

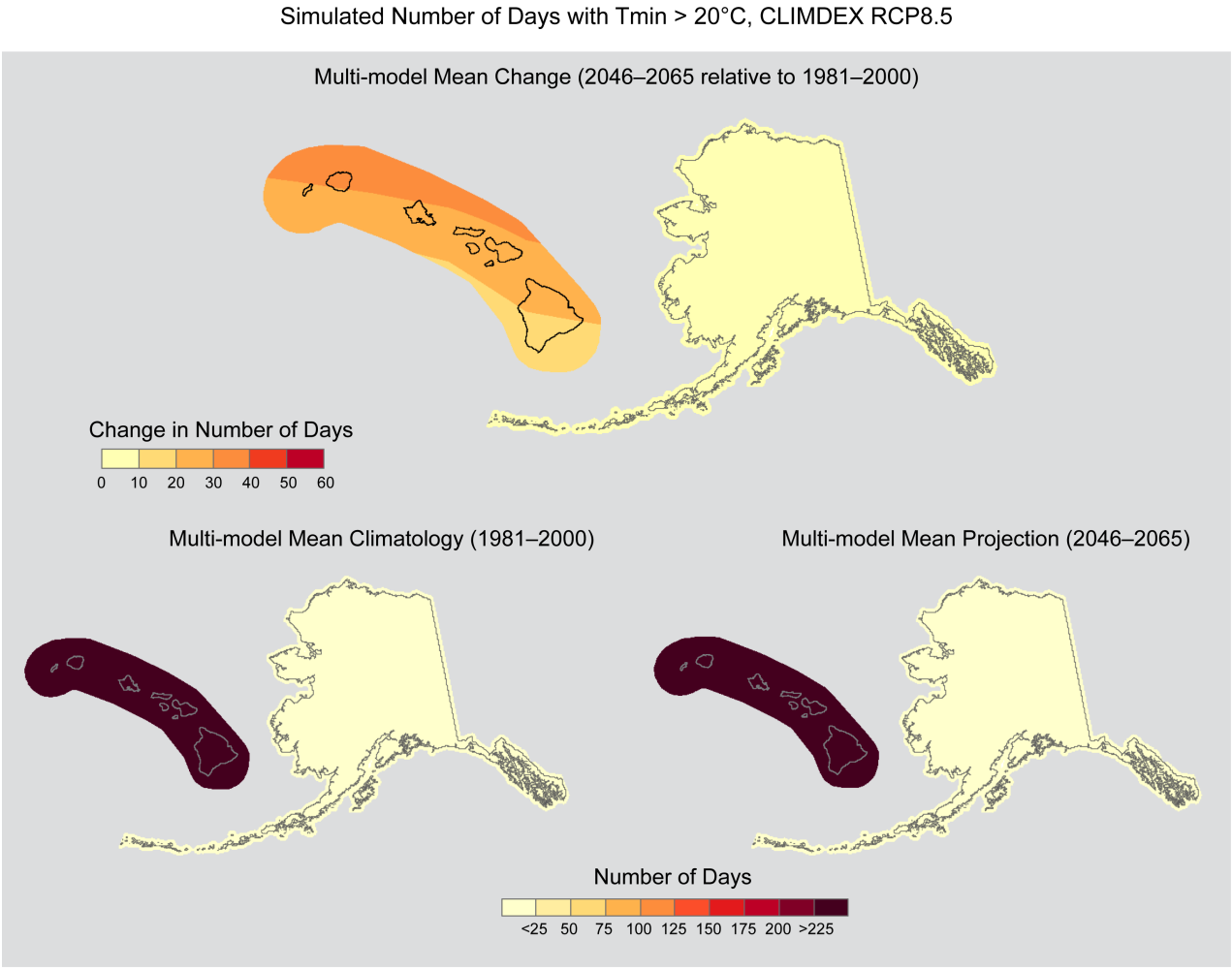

Figure 13b. *Simulated multi-model mean change in the mean annual number of days with a minimum temperature greater than 20°C (T_{min} > 20°C) for Alaska and Hawai'i, for 2046–2065 with respect to the reference period of 1981–2000, using the CLIMDEX RCP8.5 scenario (top). Color only (category 1) indicates that less than 50% of the models show a statistically significant change (see Section 3). Multi-model mean climatology indicating the annual number of days with T_{min} > 20°C for 1981–2000 (bottom left). Multi-model mean projection indicating the annual number of days with T_{min} > 20°C for 2046–2065 (bottom right).*

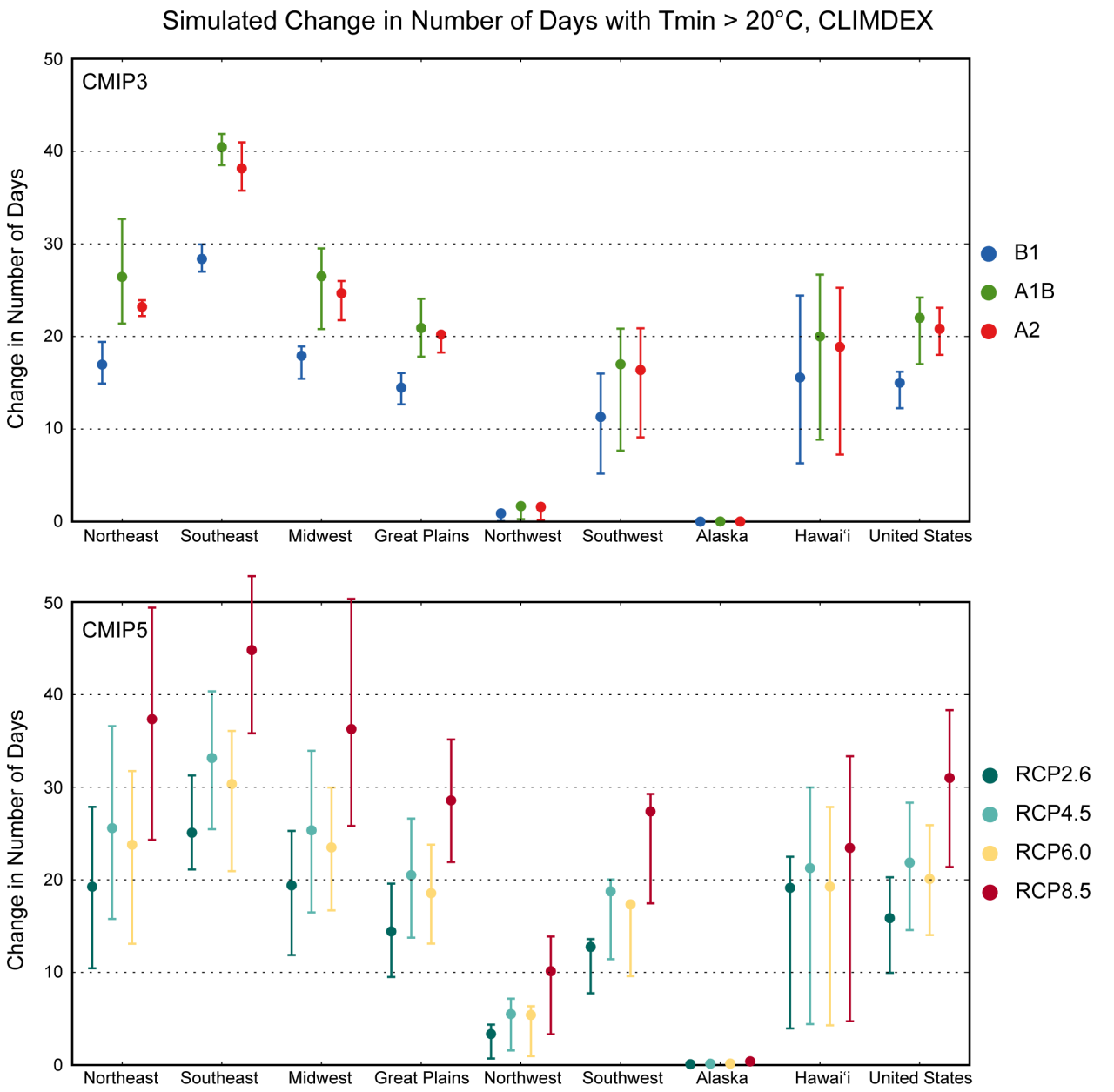

Figure 14. *Simulated change in the mean annual number of days with a minimum temperature greater than 20°C for each region and the contiguous United States, for 2046–2065 with respect to the reference period of 1981–2000. The upper panel shows values for the CLIMDEX SRES B1 (blue), A1B (green), and A2 (red) scenarios. The lower panel shows values for the CLIMDEX RCP2.6 (dark teal), 4.5 (light teal), 6.0 (yellow), and 8.5 (dark red) scenarios. Bars indicate the interquartile ranges of model values and circles depict the multi-model means.*

Simulated Growing Season Length, CLIMDEX RCP8.5

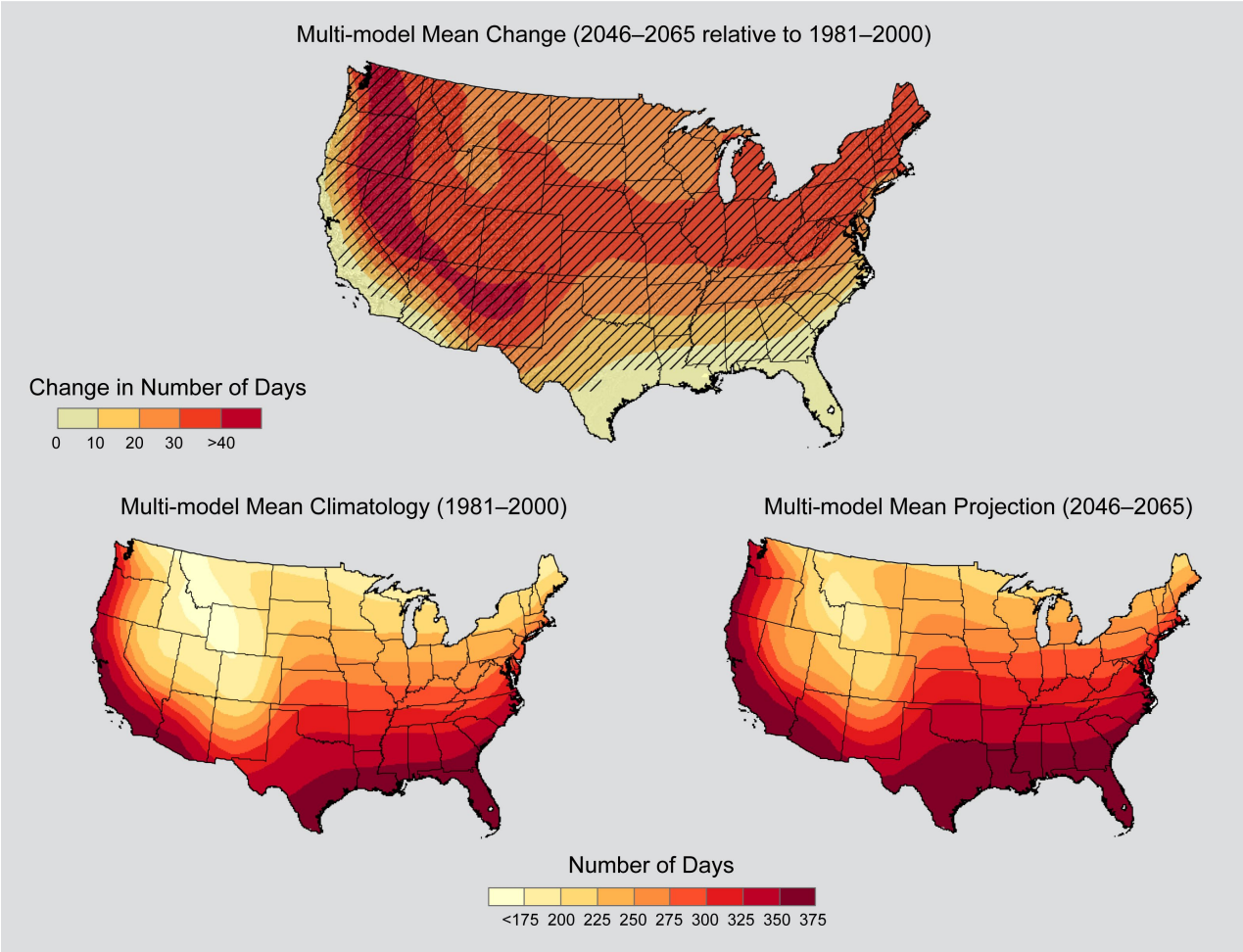

Figure 15a. *Simulated multi-model mean change in the growing season length (GSL) for the contiguous United States, for 2046–2065 with respect to the reference period of 1981–2000, using the CLIMDEX RCP8.5 scenario (top). Color only (category 1) indicates that less than 50% of the models show a statistically significant change. Color with hatching (category 3) indicates that more than 50% of the models show a statistically significant change, and more than 67% agree on the sign of the change (see Section 3). Multi-model mean climatology indicating the GSL for 1981–2000 (bottom left). Multi-model mean projection indicating the GSL for 2046–2065 (bottom right).*

Simulated Growing Season Length, CLIMDEX RCP8.5

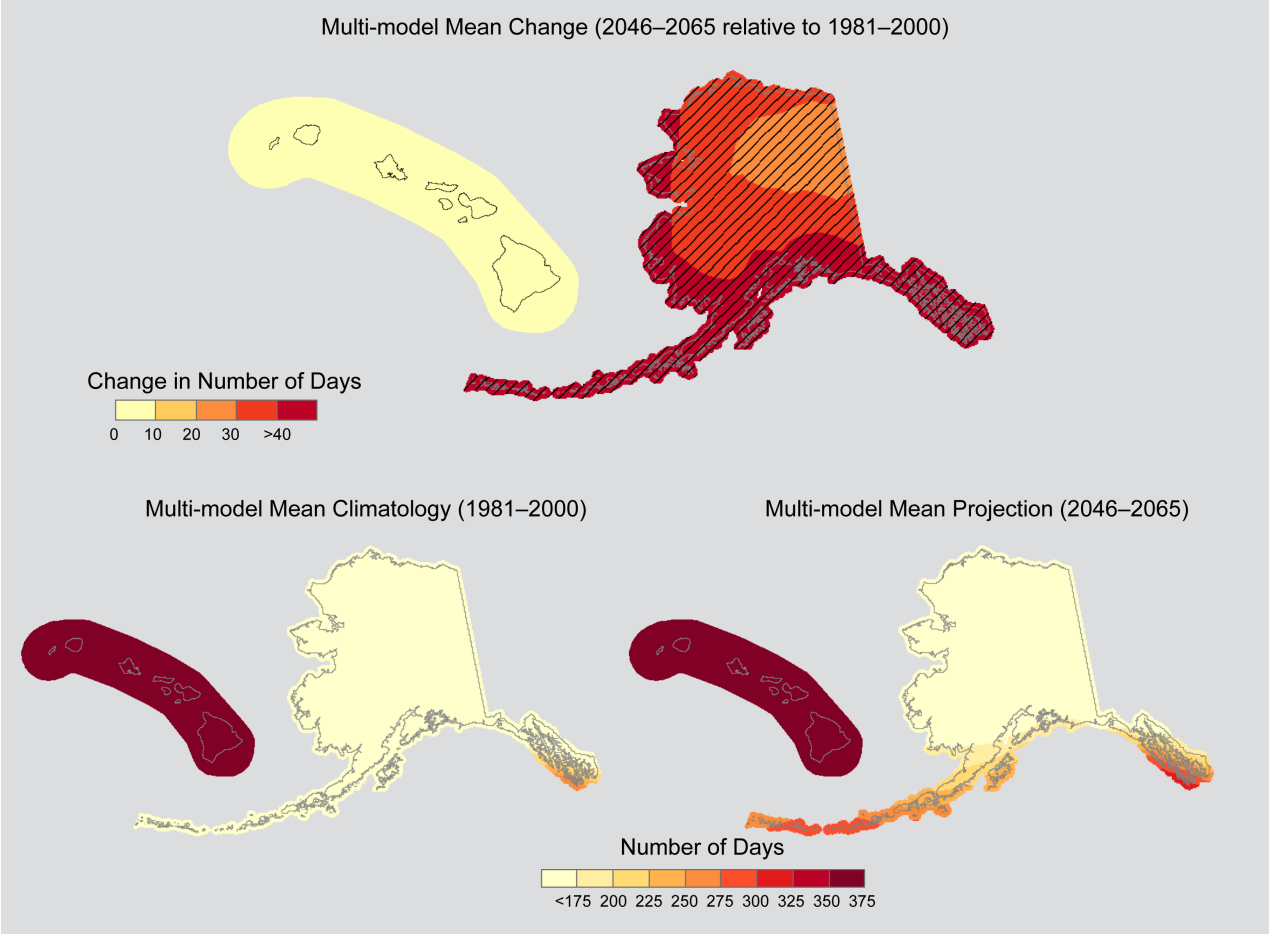

Figure 15b. *Simulated multi-model mean change in the growing season length (GSL) for Alaska and Hawai'i, for 2046–2065 with respect to the reference period of 1981–2000, using the CLIMDEX RCP8.5 scenario (top). Color only (category 1) indicates that less than 50% of the models show a statistically significant change. Color with hatching (category 3) indicates that more than 50% of the models show a statistically significant change, and more than 67% agree on the sign of the change (see Section 3). Multi-model mean climatology indicating the GSL for 1981–2000 (bottom left). Multi-model mean projection indicating the GSL for 2046–2065 (bottom right).*

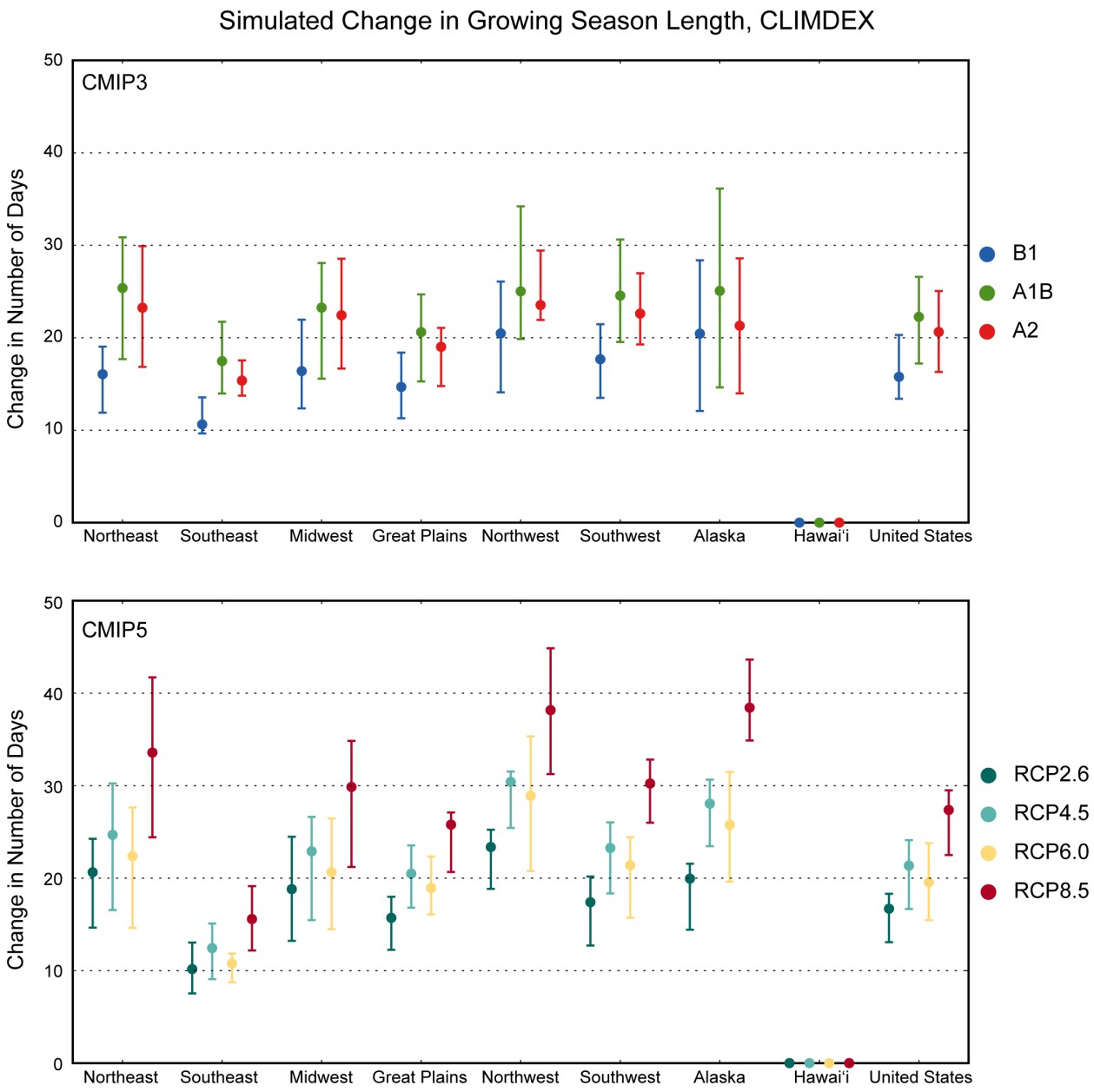

Figure 16. *Simulated change in the growing season length (GSL) for each region and the contiguous United States, for 2046–2065 with respect to the reference period of 1981–2000. The upper panel shows values for the CLIMDEX SRES B1 (blue), A1B (green), and A2 (red) scenarios. The lower panel shows values for the CLIMDEX RCP2.6 (dark teal), 4.5 (light teal), 6.0 (yellow), and 8.5 (dark red) scenarios. Bars indicate the interquartile ranges of model values and circles depict the multi-model means.*

For RCP8.5, simulations for 2046–2065 indicate increases of about 5°F to 9°F in the annual highest value of the daily maximum temperature over most of the contiguous U.S. (Fig. 17a). The models are in agreement on the sign of the change, with all grid points satisfying category 3. These increases tend to be somewhat larger away from the coasts and the moderating effect of the oceans. Statistically significant increases (category 3) are also seen for both Alaska and Hawai‘i (Fig. 17b), with values in the 5°–6°F range for the majority of Alaska, and 3°–4°F for Hawai‘i. The dependence of regional changes on scenario (Fig. 18) roughly follows that of the temperature changes, as was the case for freezing nights. For CMIP3 (Fig. 18, top panel), the increases are smallest for the B1 scenario and roughly equal for the A1B and A2 scenarios. The interquartile range of increases of about 3°F to 5°F is comparable to the multi-model mean changes of 3°F to 6°F. For CMIP5 (Fig. 18, bottom panel), the range of changes among the four RCPs is higher than for the three CMIP3 scenarios, reflecting the larger range of radiative forcing. Otherwise, there do not appear to be any substantive differences between the CMIP3 and CMIP5 results, when considering differences in greenhouse gas concentrations. For example, the increases for RCP8.5 are considerably larger than for A1B or A2, but RCP8.5 has considerably higher greenhouse gas concentrations out to the mid-21st century than either of those scenarios. As was the case with mean temperature changes, the changes in Fig. 12 for RCP6.0 are less than for RCP4.5, reflecting the fact that greenhouse gas concentrations are actually less in RCP6.0 than in RCP4.5 in this mid-21st century period.

For RCP8.5, simulations for 2046–2065 (Fig. 19a) indicate increases of about 4°F to 10°F in the annual lowest daily maximum temperatures over most of the contiguous United States, with the majority of models indicating statistically significant increases everywhere (category 3). In general, larger increases are seen for places that experience lower temperatures in the present-day climate, and vice-versa. This also holds true for Alaska and Hawai‘i (Fig. 19b), which see increases mostly above 10°F and below 4°F, respectively. The dependence of regional changes on emissions scenarios (Fig. 20) roughly follows temperature changes, as was the case for freezing nights. For CMIP3 (Fig. 20, top panel), the increases are smallest for the B1 scenario and roughly equal for the A1B and A2 scenarios. The interquartile range of increases of about 2°F to 3°F is smaller than the multi-model mean changes of 3°F to 7°F. For CMIP5 (Fig. 20, bottom panel), the range of changes among the four RCPs is higher than for the three CMIP3 scenarios, reflecting the larger range of radiative forcing. Otherwise, there do not appear to be any substantive differences between the CMIP3 and CMIP5 results when considering differences in greenhouse gas concentrations. For example, the increases for RCP8.5 are considerably larger than for A1B or A2, but RCP8.5 has considerably higher greenhouse gas concentrations out to the mid-21st century than either of those scenarios. As was the case with mean temperature changes, the changes in Fig. 12 for RCP6.0 are less than for RCP4.5, reflecting the fact that greenhouse gas concentrations are actually less in RCP6.0 than in RCP4.5 in this mid-21st century period.

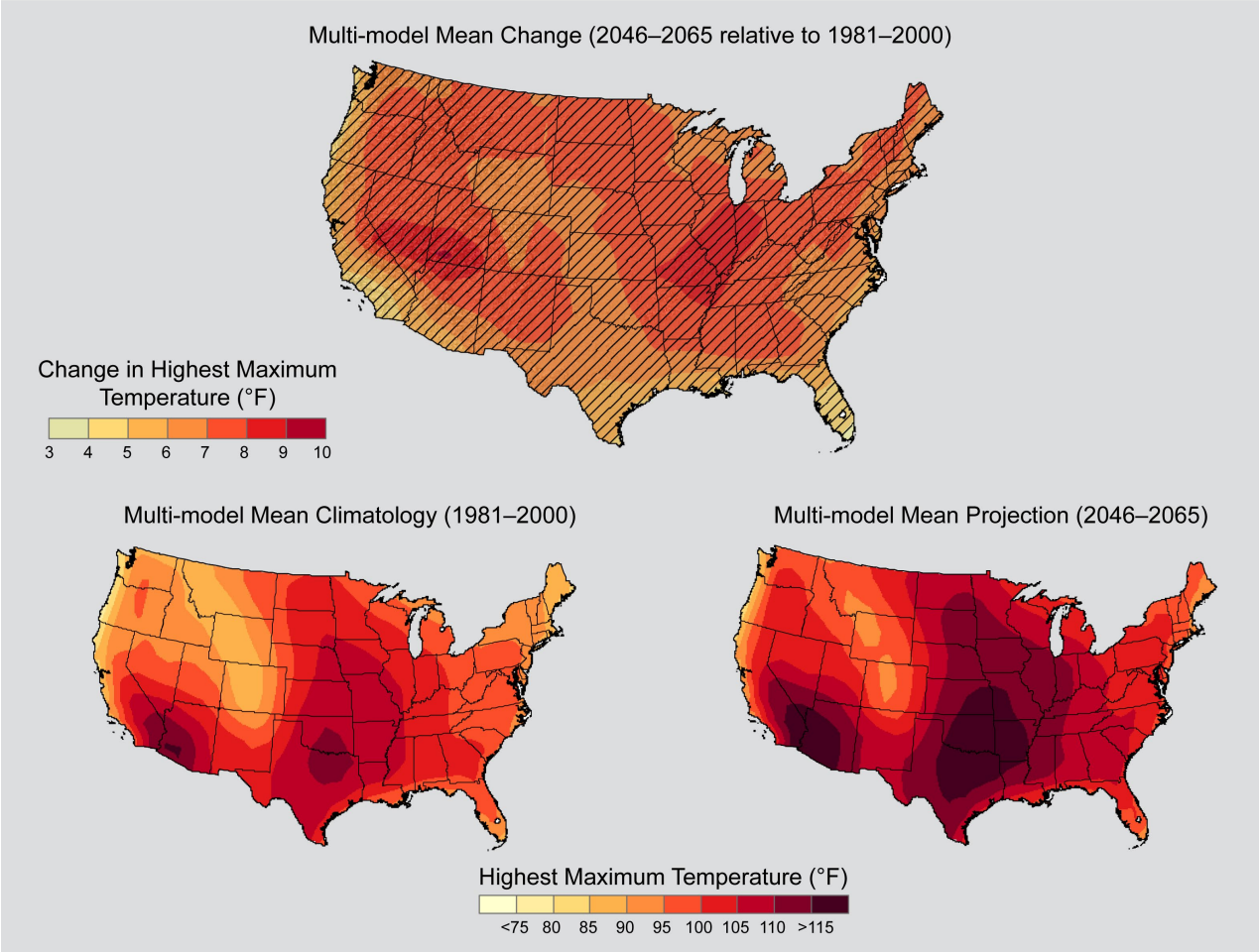

Figure 17a. *Simulated multi-model mean change in the annual highest value of daily maximum temperature (TXx) for the contiguous United States, for 2046–2065 with respect to the reference period of 1981–2000, using the CLIMDEX RCP8.5 scenario (top). Color with hatching (category 3) indicates that more than 50% of the models show a statistically significant change, and more than 67% agree on the sign of the change (see Section 3). Multi-model mean climatology indicating the TXx for 1981–2000 (bottom left). Multi-model mean projection indicating the TXx for 2046–2065 (bottom right).*

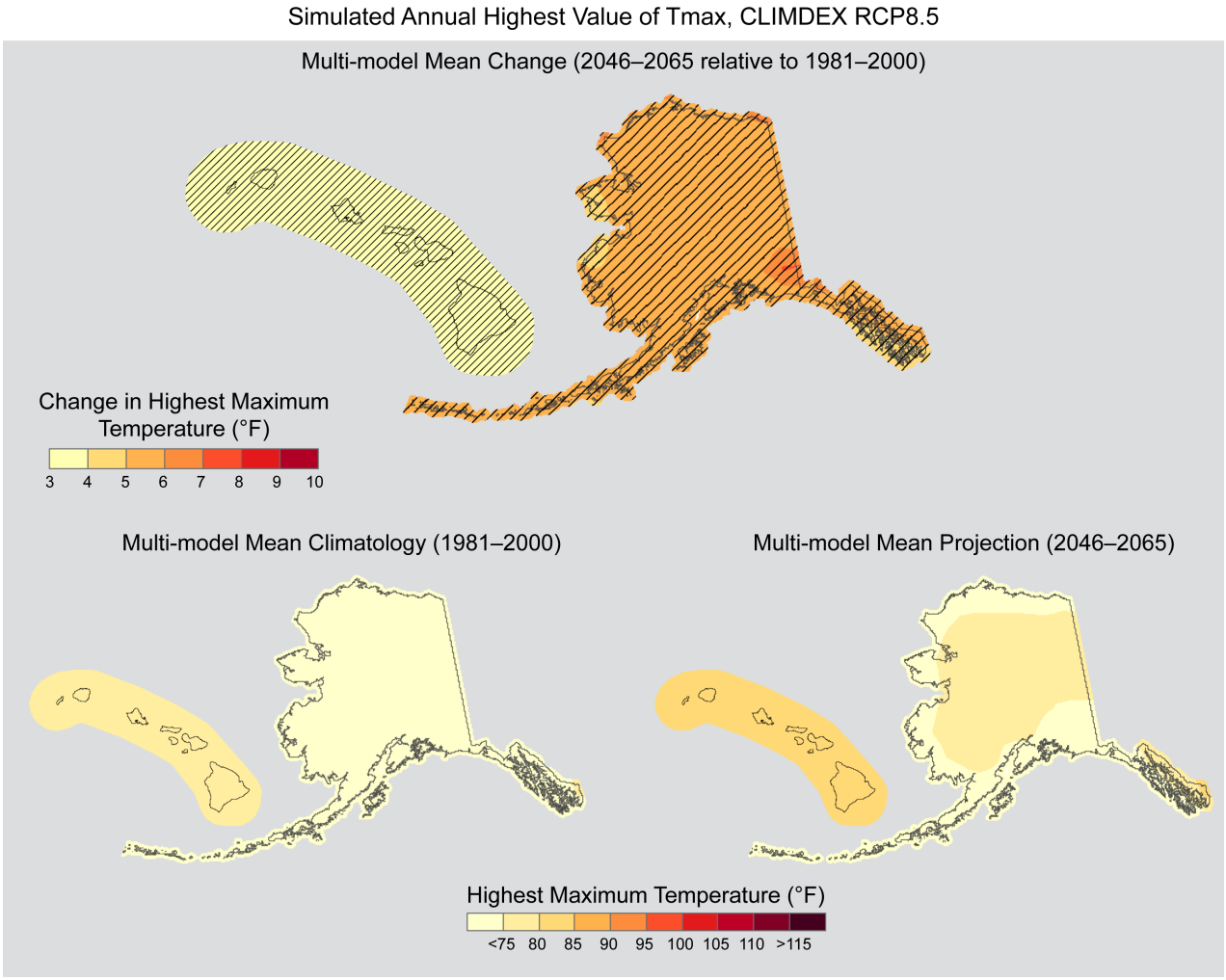

Figure 17b. *Simulated multi-model mean change in the annual highest value of daily maximum temperature (TXx) for Alaska and Hawai'i, for 2046–2065 with respect to the reference period of 1981–2000, using the CLIMDEX RCP8.5 scenario (top). Color with hatching (category 3) indicates that more than 50% of the models show a statistically significant change, and more than 67% agree on the sign of the change (see Section 3). Multi-model mean climatology indicating the TXx for 1981–000 (bottom left). Multi-model mean projection indicating the TXx for 2046–2065 (bottom right).*

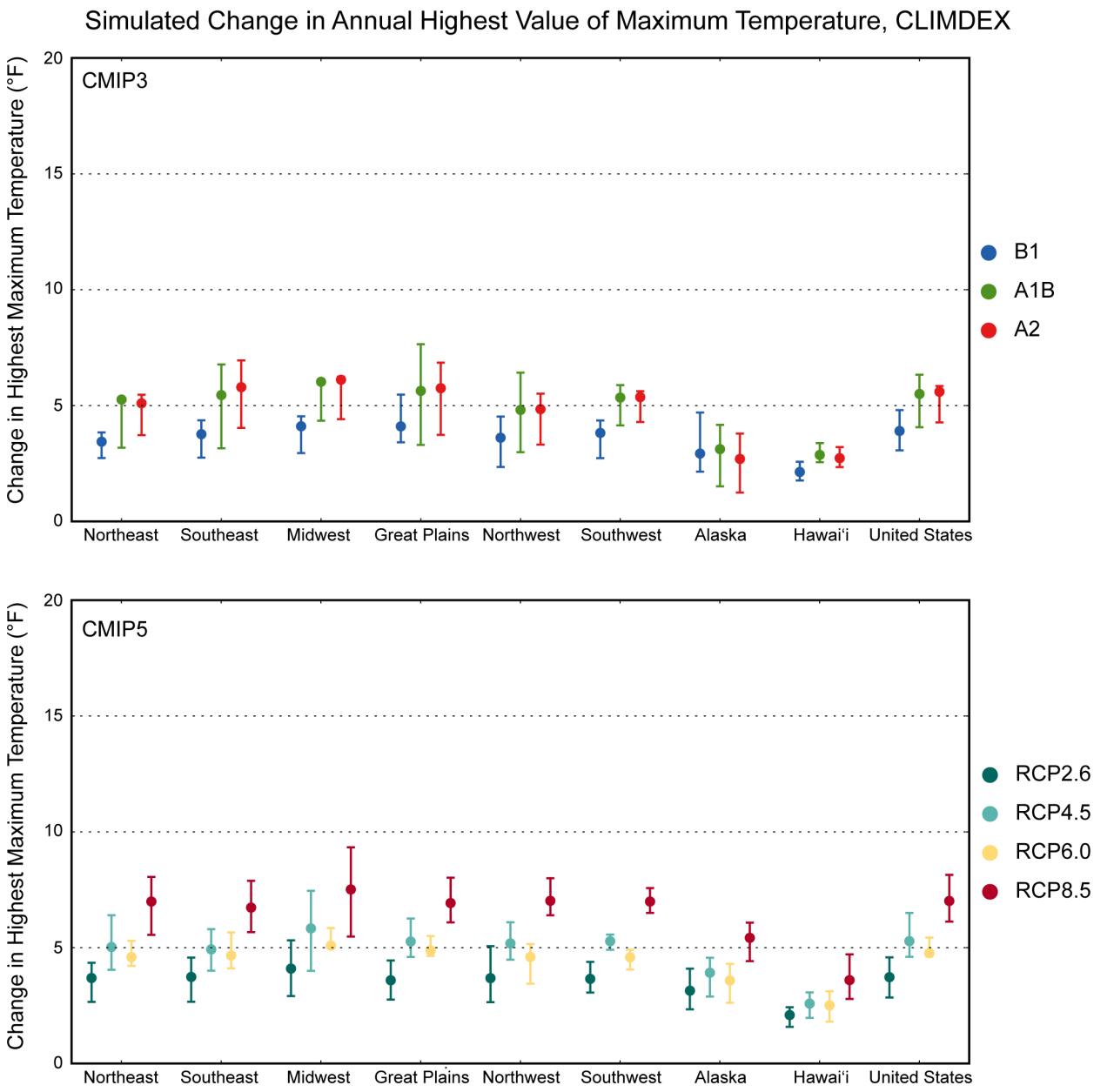

Figure 18. *Simulated change in the annual highest value of daily maximum temperature (TXx) for each region and the contiguous United States, for 2046–2065 with respect to the reference period of 1981–2000. The upper panel shows values for the CLIMDEX SRES B1 (blue), A1B (green), and A2 (red) scenarios. The lower panel shows values for the CLIMDEX RCP2.6 (dark teal), 4.5 (light teal), 6.0 (yellow), and 8.5 (dark red) scenarios. Bars indicate the interquartile ranges of model values and circles depict the multi-model means.*

Simulated Annual Lowest Value of Tmax, CLIMDEX RCP8.5

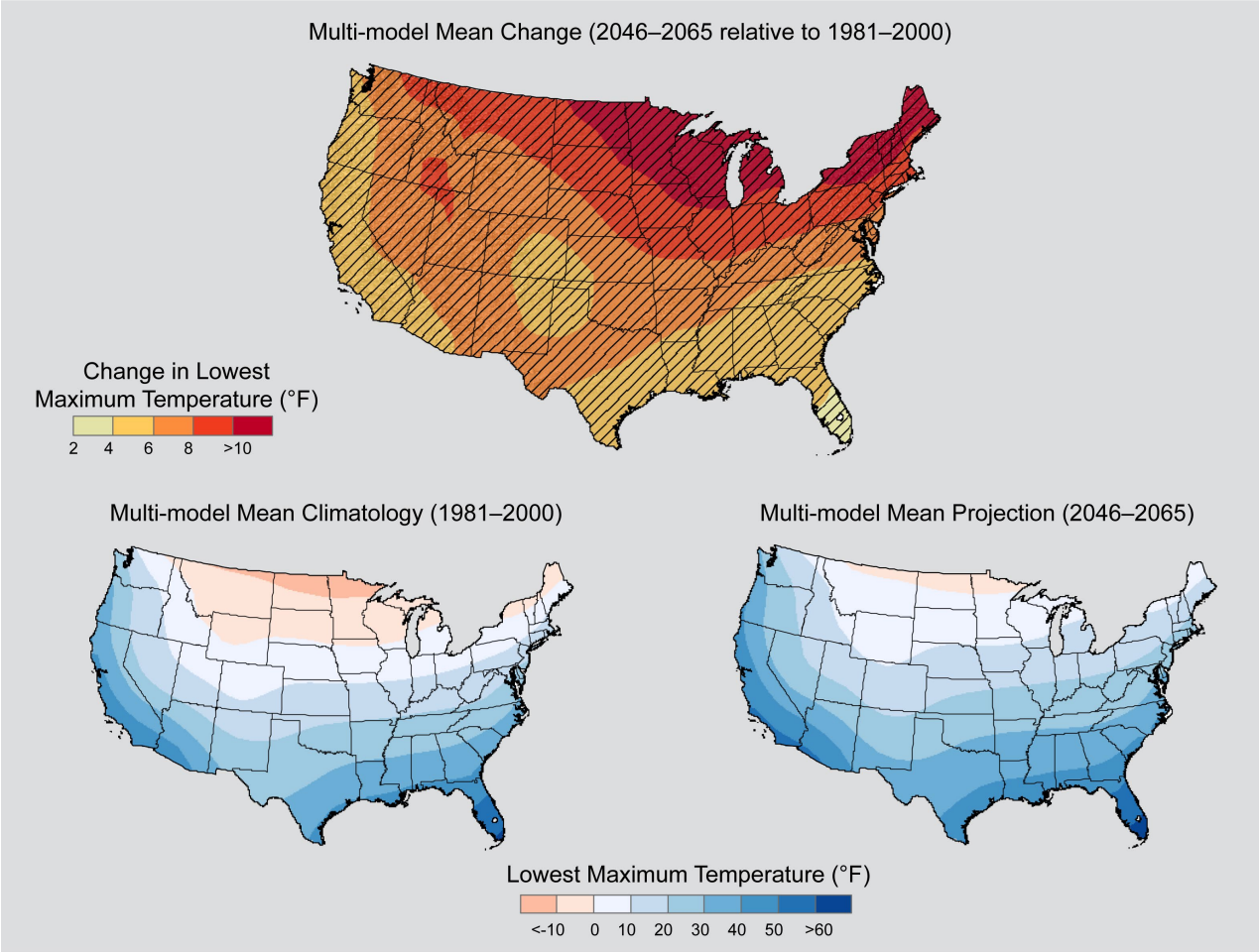

Figure 19a. *Simulated multi-model mean change in the annual lowest value of daily maximum temperature (TXn) for the contiguous United States, for 2046–2065 with respect to the reference period of 1981–2000, using the CLIMDEX RCP8.5 scenario (top). Color with hatching (category 3) indicates that more than 50% of the models show a statistically significant change, and more than 67% agree on the sign of the change (see Section 3). Multi-model mean climatology indicating the TXn for 1981–2000 (bottom left). Multi-model mean projection indicating the TXn for 2046–2065 (bottom right).*

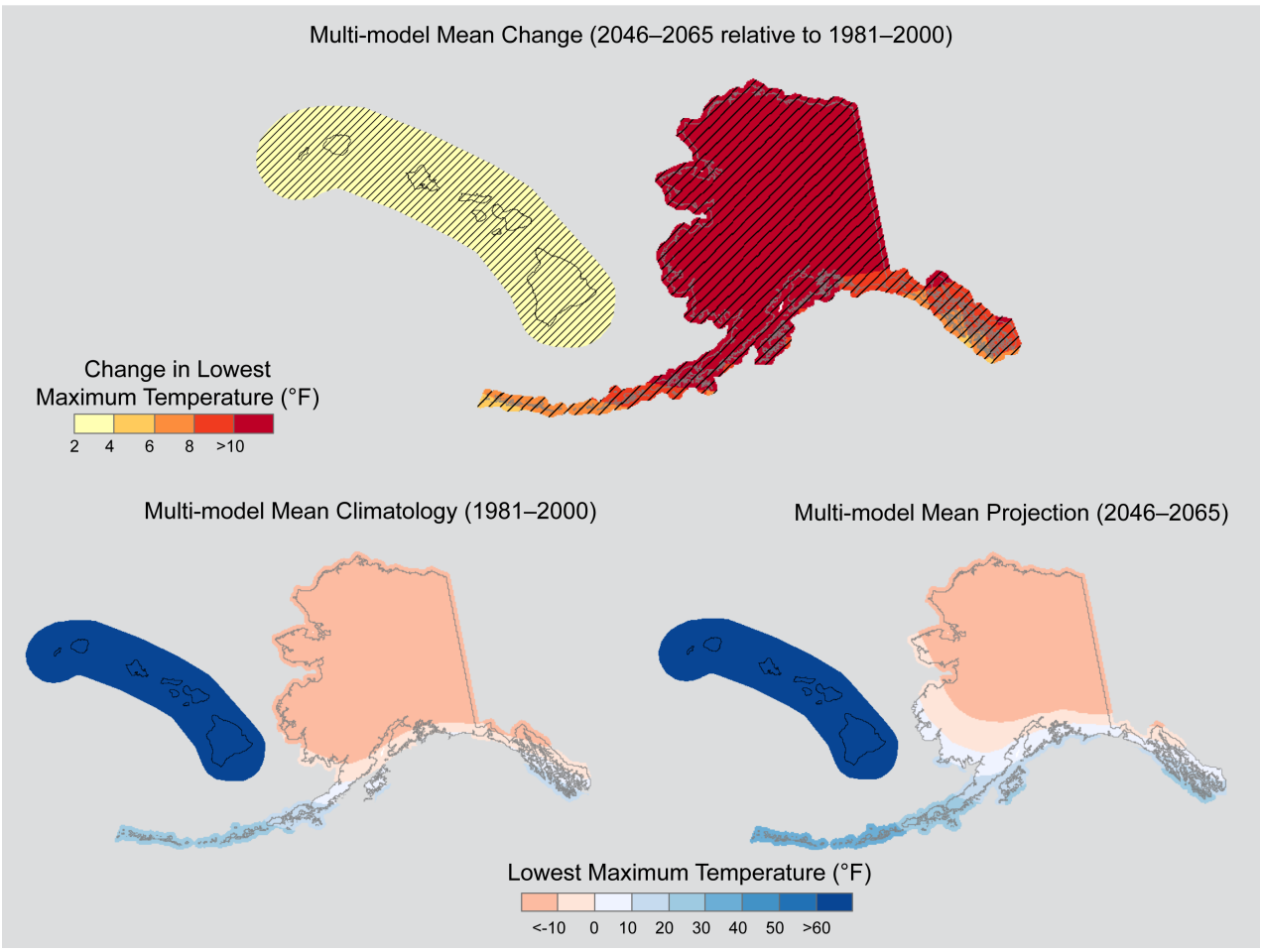

Figure 19b. *Simulated multi-model mean change in the annual lowest value of daily maximum temperature (TXn) for Alaska and Hawai'i, for 2046–2065 with respect to the reference period of 1981–2000, using the CLIMDEX RCP8.5 scenario (top). Color with hatching (category 3) indicates that more than 50% of the models show a statistically significant change, and more than 67% agree on the sign of the change (see Section 3). Multi-model mean climatology indicating the TXn for 1981–2000 (bottom left). Multi-model mean projection indicating the TXn for 2046–2065 (bottom right).*

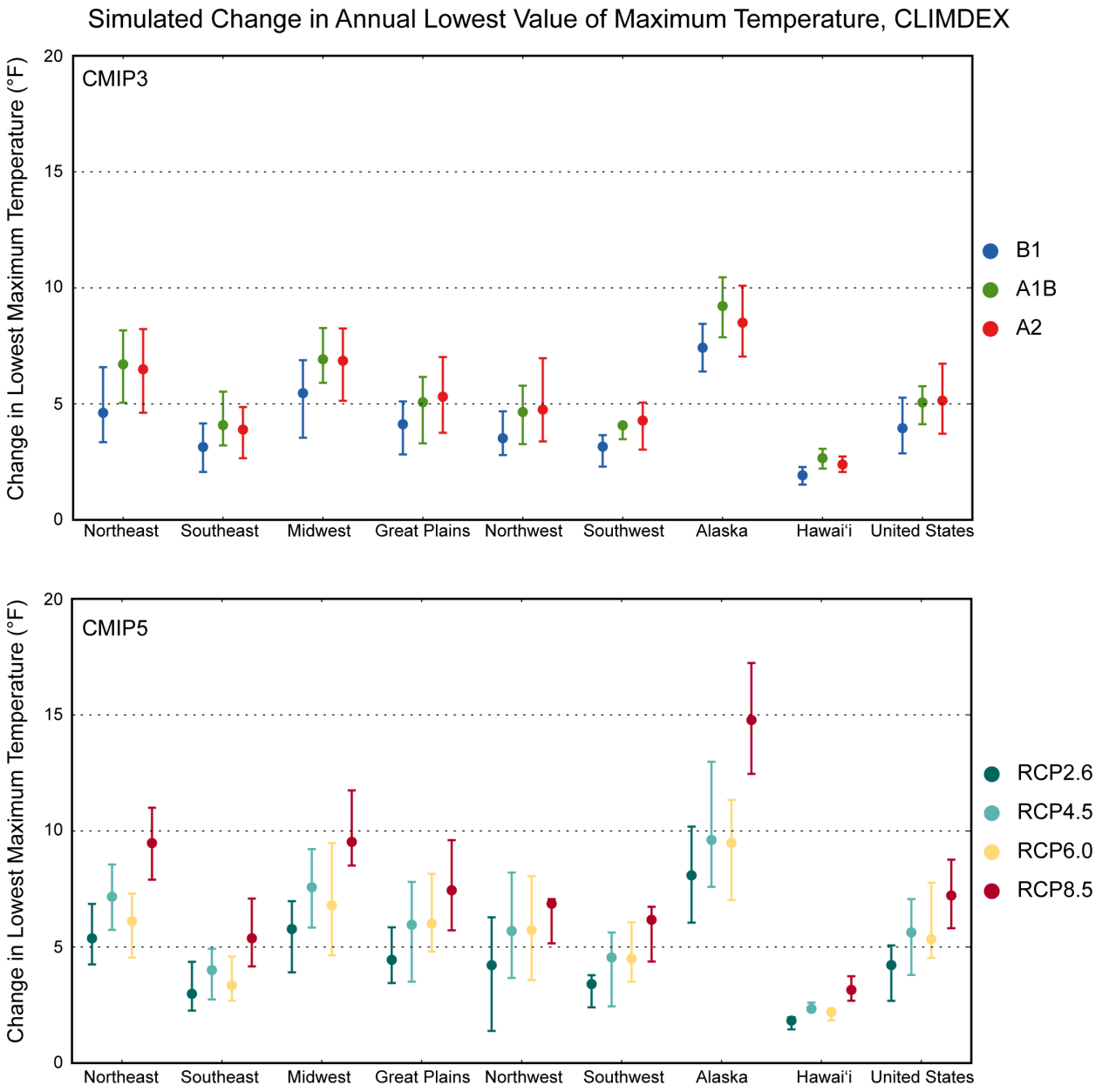

Figure 20. *Simulated change in the annual lowest value of daily maximum temperature (TXn) for each region and the contiguous United States, for 2046–2065 with respect to the reference period of 1981–2000. The upper panel shows values for the CLIMDEX SRES B1 (blue), A1B (green), and A2 (red) scenarios. The lower panel shows values for the CLIMDEX RCP2.6 (dark teal), 4.5 (light teal), 6.0 (yellow), and 8.5 (dark red) scenarios. Bars indicate the interquartile ranges of model values and circles depict the multi-model means.*

For daily minimum temperatures, RCP8.5 simulations for 2046–2065 (Fig. 21a) indicate increases of about 4°F to more than 12°F over most of the United States, with slightly smaller increases of 2°F to 4°F in parts of the southeast United States. The increases are larger across the northeastern U.S. and the models agree on the sign of the change (grid points satisfy category 3) everywhere. Increases for Alaska (Fig. 21b) range from 6°F in the south to more than 12°F in the north. Hawai‘i sees increases of 2°–4°F, with most models indicating statistically significant increases (category 3) for both states. The dependence of regional changes on emissions scenarios (Fig. 22) roughly follows temperature changes, as was the case for freezing nights. For CMIP3 (Fig. 22, top panel), the increases are smallest for the B1 scenario and roughly equal for the A1B and A2 scenarios. The interquartile range of increases of about 3°F to 4°F is smaller than the multi-model mean changes of 3°F to 8°F. For CMIP5 (Fig. 22, bottom panel), the range of changes among the four RCPs is higher than for the three CMIP3 scenarios, reflecting the larger range of radiative forcing. Otherwise, there do not appear to be any substantive differences between the CMIP3 and CMIP5 results when considering differences in greenhouse gas concentrations. For example, the increases for RCP8.5 are considerably larger than for A1B or A2, but RCP8.5 has considerably higher greenhouse gas concentrations out to the mid-21st century than either of those scenarios. As was the case with mean temperature changes, the changes in Fig. 12 for RCP6.0 are less than for RCP4.5, reflecting the fact that greenhouse gas concentrations are actually less in RCP6.0 than in RCP4.5 in this mid-21st century period.

In the CLIMDEX set of indices, a warm spell at a specific location is defined as a period of at least six days in length when the maximum temperature on each day is above the 90th percentile threshold for that calendar day. The warm spell duration index (WSDI) is the longest such period in a calendar year. Some years do not have any warm spells and the value of the WSDI in those years is zero. The 90th percentile threshold for the present climate is applied to the future climate simulations as well. The simulated change in the annual average WSDI for 2046–2065 for RCP8.5 (Fig. 23a) indicates increases of about 60 days in the northern contiguous U.S. to more than 100 days in the intermountain west. These changes are much larger than the 1981–2000 climatological values of 5 to 20 days. The increases are indicated by most models to be statistically significant everywhere (all grid points satisfy category 3). Values for Alaska (Fig. 23b) are greater for coastal areas than inland, ranging from less than 60 days in the interior of the state, to more than 220 days in the Aleutian Islands. The models are once again in agreement on these increases (category 3), as they also are for Hawai‘i, which sees the WSDI lengthen by more than 220 days. The largest changes of greater than 100 days occur in southern Florida, the Aleutian Islands, and Hawai’i, where the adjacent oceans damp the amplitude of the daily and seasonal temperature cycle. In these cases, the future mean changes in climate are large compared to the daily variability and result in many days being over the 90th percentile threshold in the future.

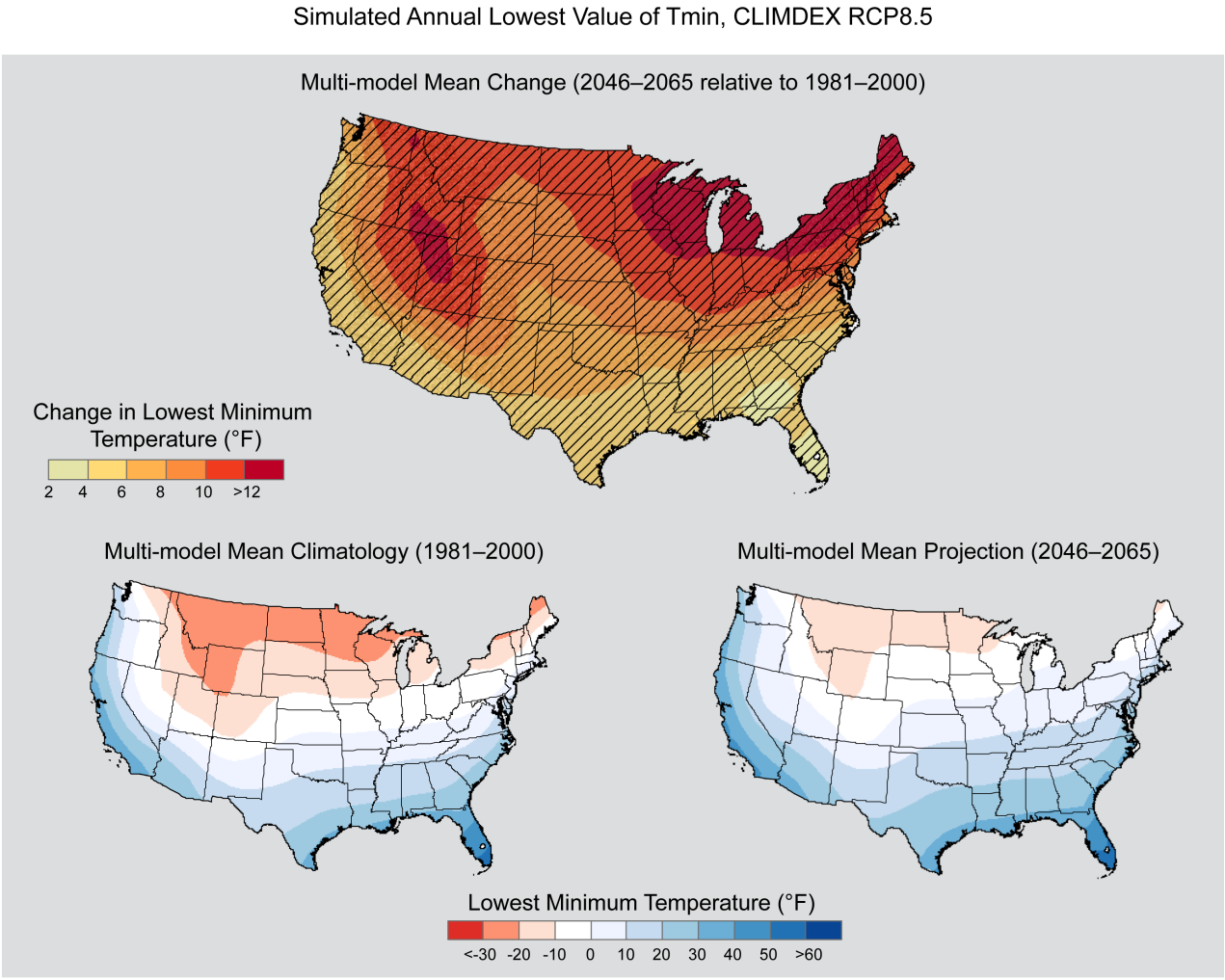

Figure 21a. *Simulated multi-model mean change in the annual lowest value of daily minimum temperature (TNn) for the contiguous United States, for 2046–2065 with respect to the reference period of 1981–2000, using the CLIMDEX RCP8.5 scenario (top). Color with hatching (category 3) indicates that more than 50% of the models show a statistically significant change, and more than 67% agree on the sign of the change (see Section 3). Multi-model mean climatology indicating the TNn for 1981–2000 (bottom left). Multi-model mean projection indicating the TNn for 2046–2065 (bottom right).*

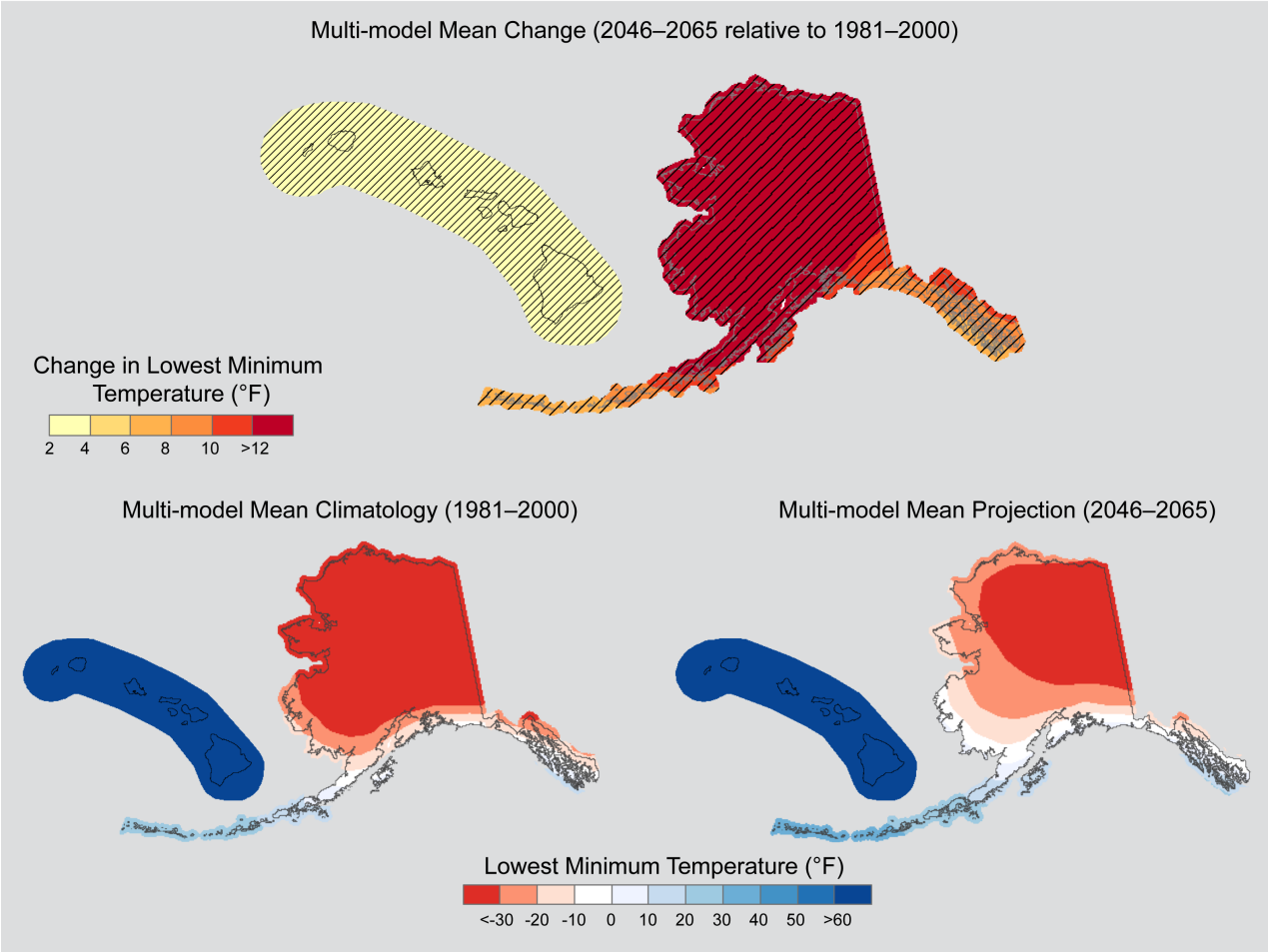

Figure 21b. *Simulated multi-model mean change in the annual lowest value of daily minimum temperature (TNn) for Alaska and Hawai'i, for 2046–2065 with respect to the reference period of 1981–2000, using the CLIMDEX RCP8.5 scenario (top). Color with hatching (category 3) indicates that more than 50% of the models show a statistically significant change, and more than 67% agree on the sign of the change (see Section 3). Multi-model mean climatology indicating the TNn for 1981–2000 (bottom left). Multi-model mean projection indicating the TNn for 2046–2065 (bottom right).*

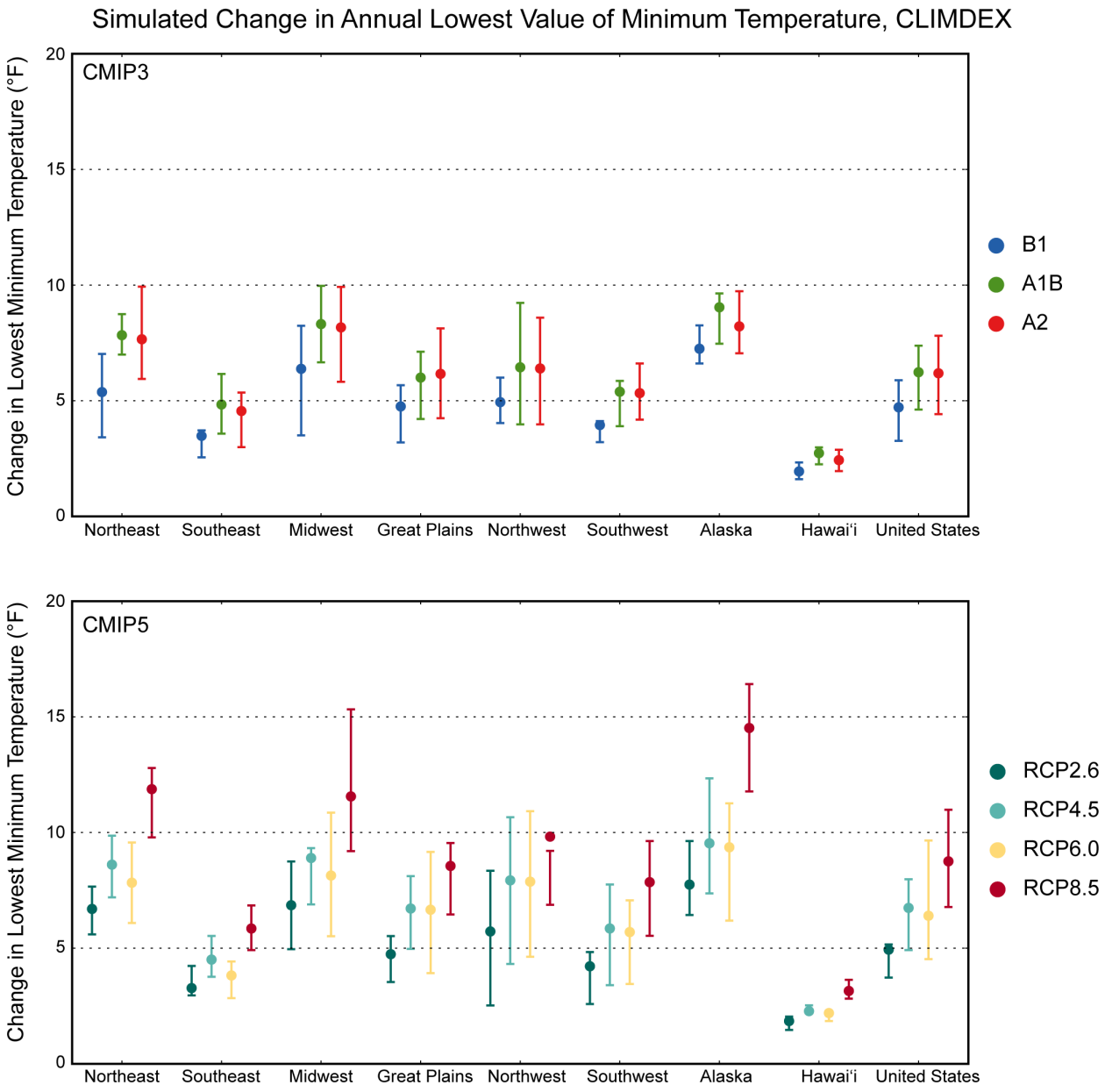

Figure 22. *Simulated change in the annual lowest value of daily minimum temperature (TNn) for each region and the contiguous United States, for 2046–2065 with respect to the reference period of 1981–2000. The upper panel shows values for the CLIMDEX SRES B1 (blue), A1B (green), and A2 (red) scenarios. The lower panel shows values for the CLIMDEX RCP2.6 (dark teal), 4.5 (light teal), 6.0 (yellow), and 8.5 (dark red) scenarios. Bars indicate the interquartile ranges of model values and circles depict the multi-model means.*

Simulated Warm Spell Duration Index, CLIMDEX RCP8.5

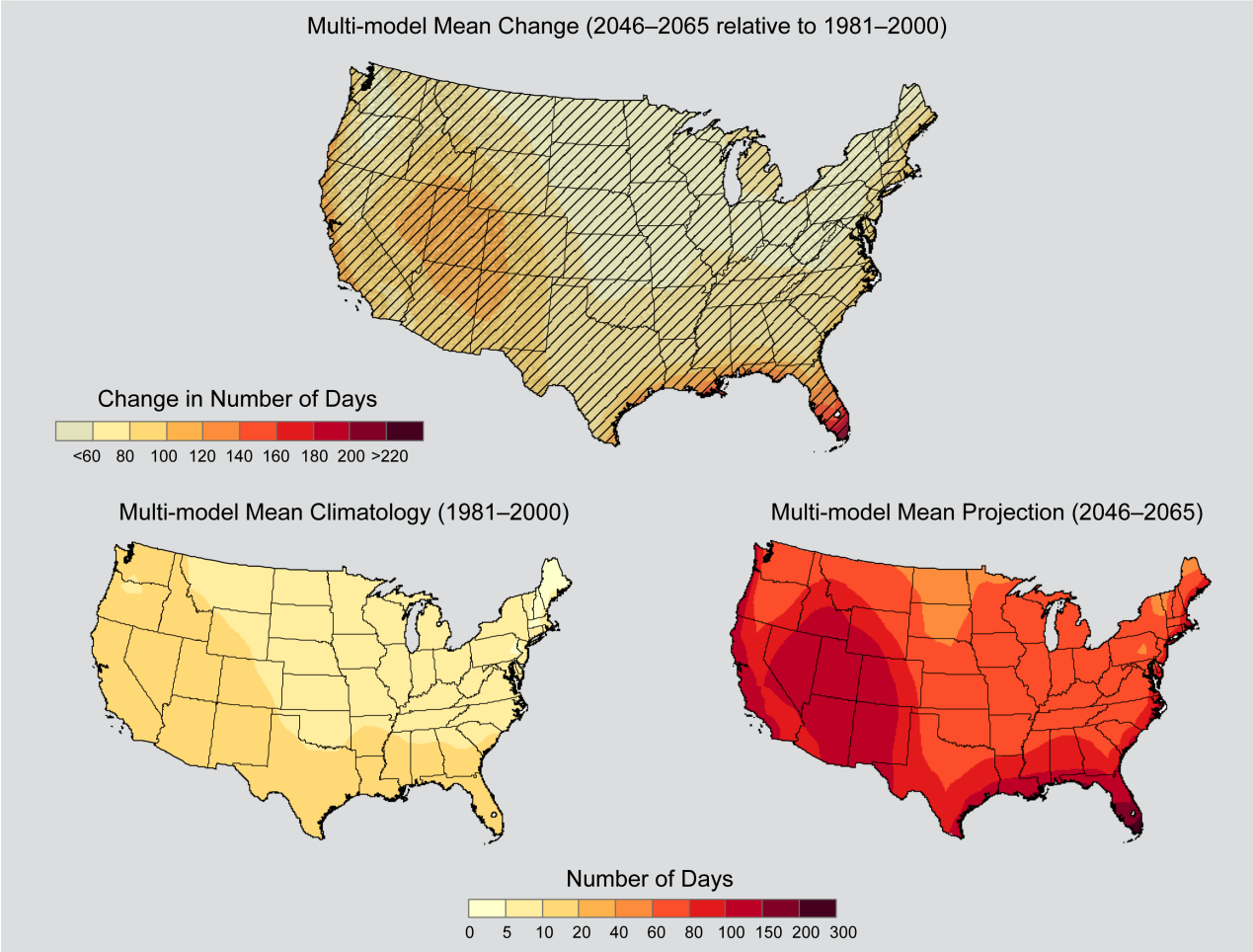

Figure 23a. *Simulated multi-model mean change in warm spell duration index (WSDI) for the contiguous United States, for 2046–2065 with respect to the reference period of 1981–2000, using the CLIMDEX RCP8.5 scenario (top). Color with hatching (category 3) indicates that more than 50% of the models show a statistically significant change, and more than 67% agree on the sign of the change (see Section 3). Multi-model mean climatology indicating the WSDI for 1981–2000 (bottom left). Multi-model mean projection indicating the WSDI for 2046–2065 (bottom right).*

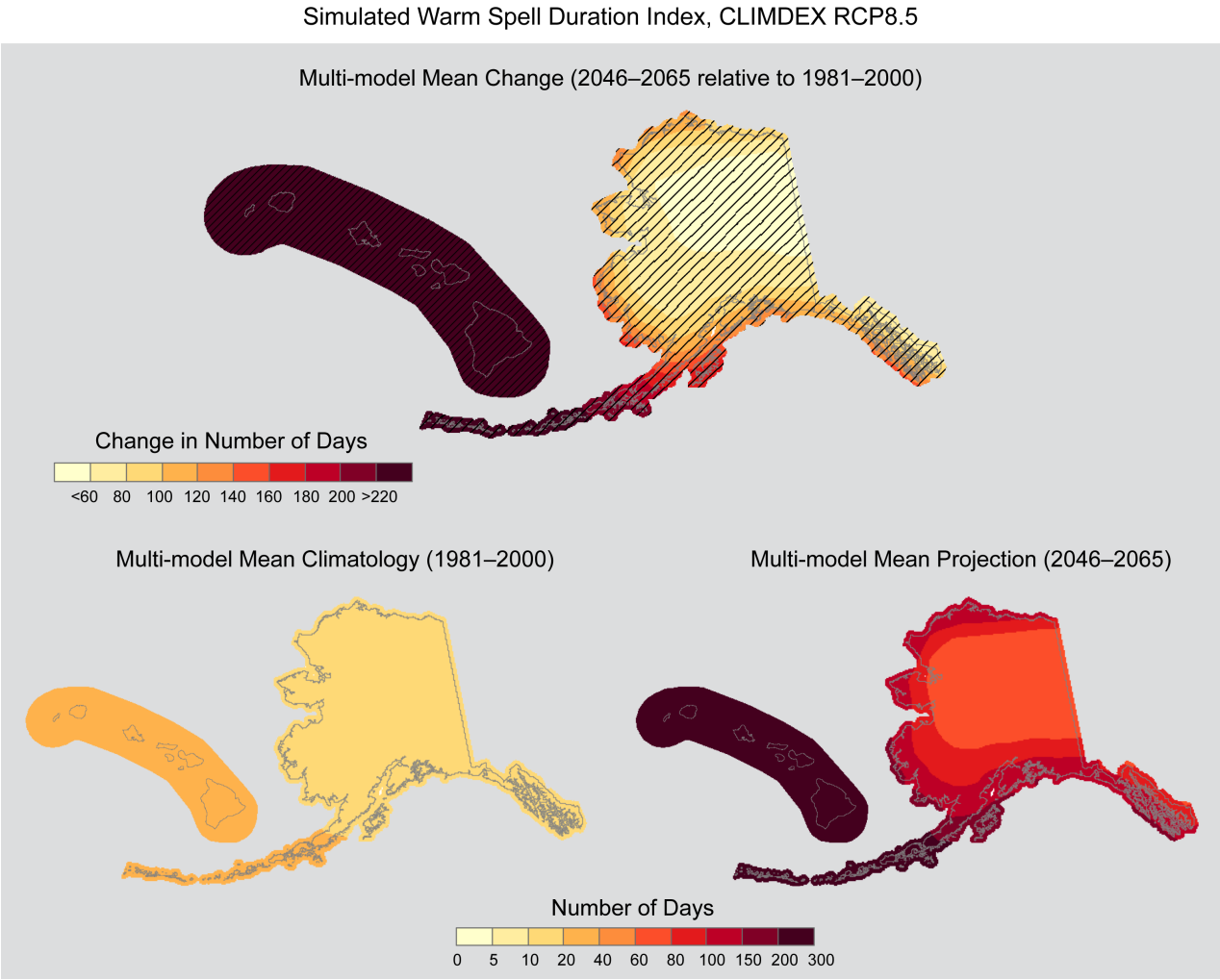

Figure 23b. *Simulated multi-model mean change in warm spell duration index (WSDI) for Alaska and Hawai'i, for 2046–2065 with respect to the reference period of 1981–2000, using the CLIMDEX RCP8.5 scenario (top). Color with hatching (category 3) indicates that more than 50% of the models show a statistically significant change, and more than 67% agree on the sign of the change (see Section 3). Multi-model mean climatology indicating the WSDI for 1981–2000 (bottom left). Multi-model mean projection indicating the WSDI for 2046–2065 (bottom right).*

The dependence of regional changes on emissions scenarios (Fig. 24) roughly follows temperature changes, as was the case for freezing nights. For CMIP3 (Fig. 24, top panel), the increases are smallest for the B1 scenario and roughly equal for the A1B and A2 scenarios. The interquartile range of increases of about 15 to more than 30 days compares with the multi-model mean changes of 20 to 60 days. For CMIP5 (Fig. 24, bottom panel), the range of changes among the four RCPs is higher than for the three CMIP3 scenarios, reflecting the larger range of radiative forcing. Otherwise, there do not appear to be any substantive differences between the CMIP3 and CMIP5 results when considering differences in greenhouse gas concentrations. For example, the increases for RCP8.5 are considerably larger than for A1B or A2, but RCP8.5 has considerably higher greenhouse gas concentrations out to the mid-21st century than either of those scenarios. As was the case with mean temperature changes, the changes in Fig. 12 for RCP6.0 are less than for RCP4.5, reflecting the fact that greenhouse gas concentrations are actually less in RCP6.0 than in RCP4.5 in this mid-21st century period.

In the CLIMDEX set of indices, a cold spell at a specific location is defined as a period of at least six days in length when the minimum temperature on each day is below the 10th percentile threshold for that calendar day. The cold spell duration index (CSDI) is the longest such period in a calendar year. As with the WSDI, the 10th percentile threshold for the present climate is applied to the future climate simulations as well. Some years do not have any cold spells and the value of the CSDI in those years is zero. The simulated change in the annual CSDI for 2046–2065 for RCP8.5 (Fig. 25a) indicates decreases of up to 5 days, with the smallest changes in the eastern contiguous U.S. and the largest changes along the west coast. The 1981–2000 climatological values are about 2 to 6 days; thus these changes mean that cold spells become very rare in the future period. The models are in agreement regarding these decreases, i.e., grid points satisfy category 3, in most of the western and central United States. Statistically significant decreases are indicated by most models (category 3) for Alaska and Hawai‘i (Fig. 25b). For both states, values of CSDI are simulated to be not much greater than zero for the future period of 2046–2065, with decreases ranging from 4 to 7 days for the majority of Alaska, and greater than 7 days across the Hawaiian Islands. The dependence of regional changes on emissions scenarios (Fig. 26) is quite small. For CMIP3 (Fig. 26, top panel), the decreases are comparable for all three scenarios. The interquartile range of increases of about 2 days compares with the multi-model mean changes of 2 to 3 days. For CMIP5 (Fig. 26, bottom panel), the range of changes among the four RCPs is slightly higher than for the three CMIP3 scenarios, but still quite small overall. The differences between the CMIP3 and CMIP5 results are not substantive. As was the case with mean temperature changes, the changes in Fig. 12 for RCP6.0 are less than for RCP4.5, reflecting the fact that greenhouse gas concentrations are actually less in RCP6.0 than in RCP4.5 in this mid-21st century period.

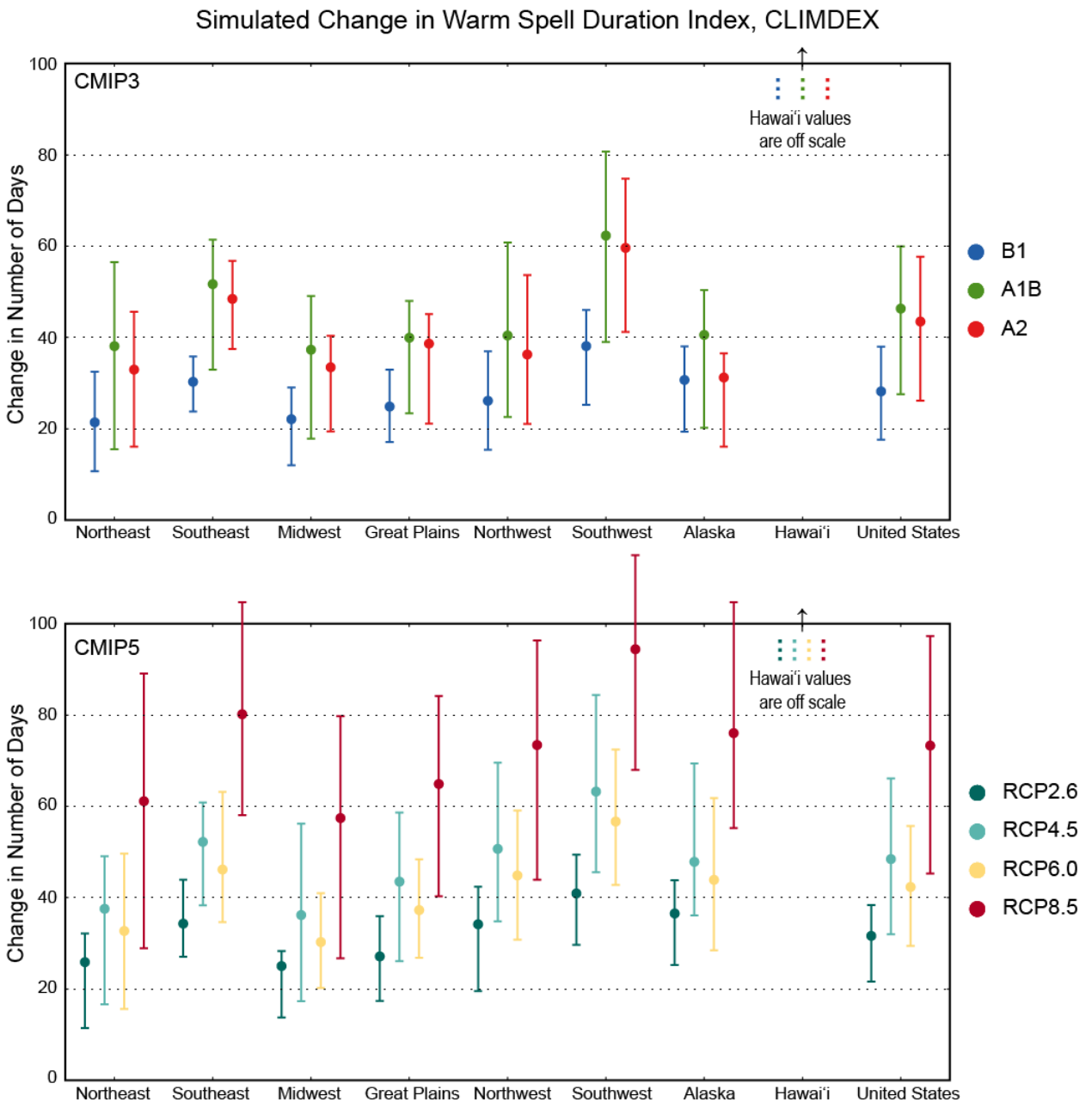

Figure 24. *Simulated change in warm spell duration index (WSDI) for each region and the contiguous United States, for 2046–2065 with respect to the reference period of 1981–2000. The upper panel shows values for the CLIMDEX SRES B1 (blue), A1B (green), and A2 (red) scenarios. The lower panel shows values for the CLIMDEX RCP2.6 (dark teal), 4.5 (light teal), 6.0 (yellow), and 8.5 (dark red) scenarios. Bars indicate the interquartile ranges of model values and circles depict the multi-model means. Note: values for Hawai'i lie off the scale, with multi-model means ranging from 184.4 days for the RCP2.6 scenario, to 271.3 days for RCP8.5.*

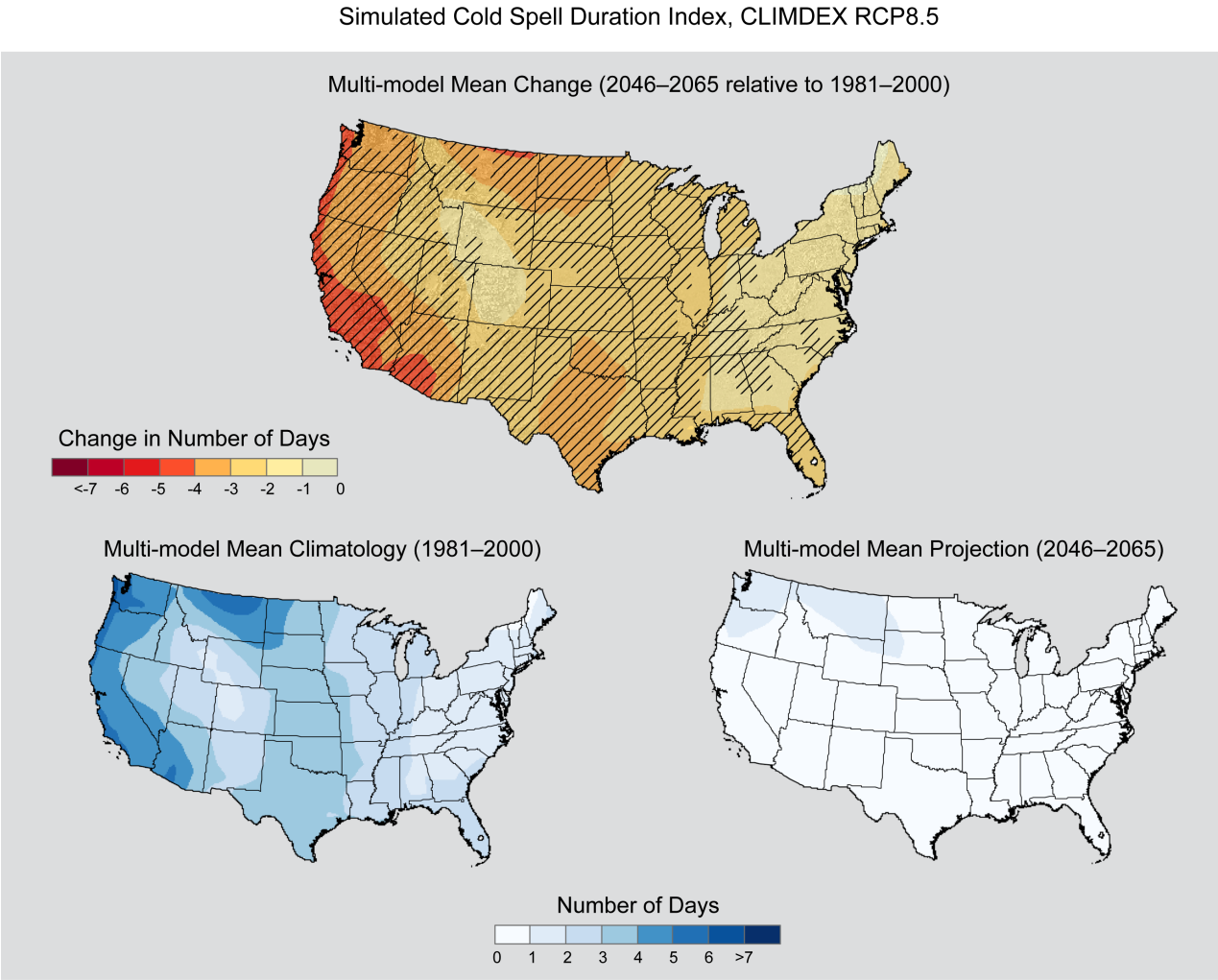

Figure 25a. *Simulated multi-model mean change in cold spell duration index (CSDI) for the contiguous United States, for 2046–2065 with respect to the reference period of 1981–2000, using the CLIMDEX RCP8.5 scenario (top). Color only (category 1) indicates that less than 50% of the models show a statistically significant change. Color with hatching (category 3) indicates that more than 50% of the models show a statistically significant change, and more than 67% agree on the sign of the change (see Section 3). Multi-model mean climatology indicating the CSDI for 1981–2000 (bottom left). Multi-model mean projection indicating the CSDI for 2046–2065 (bottom right).*

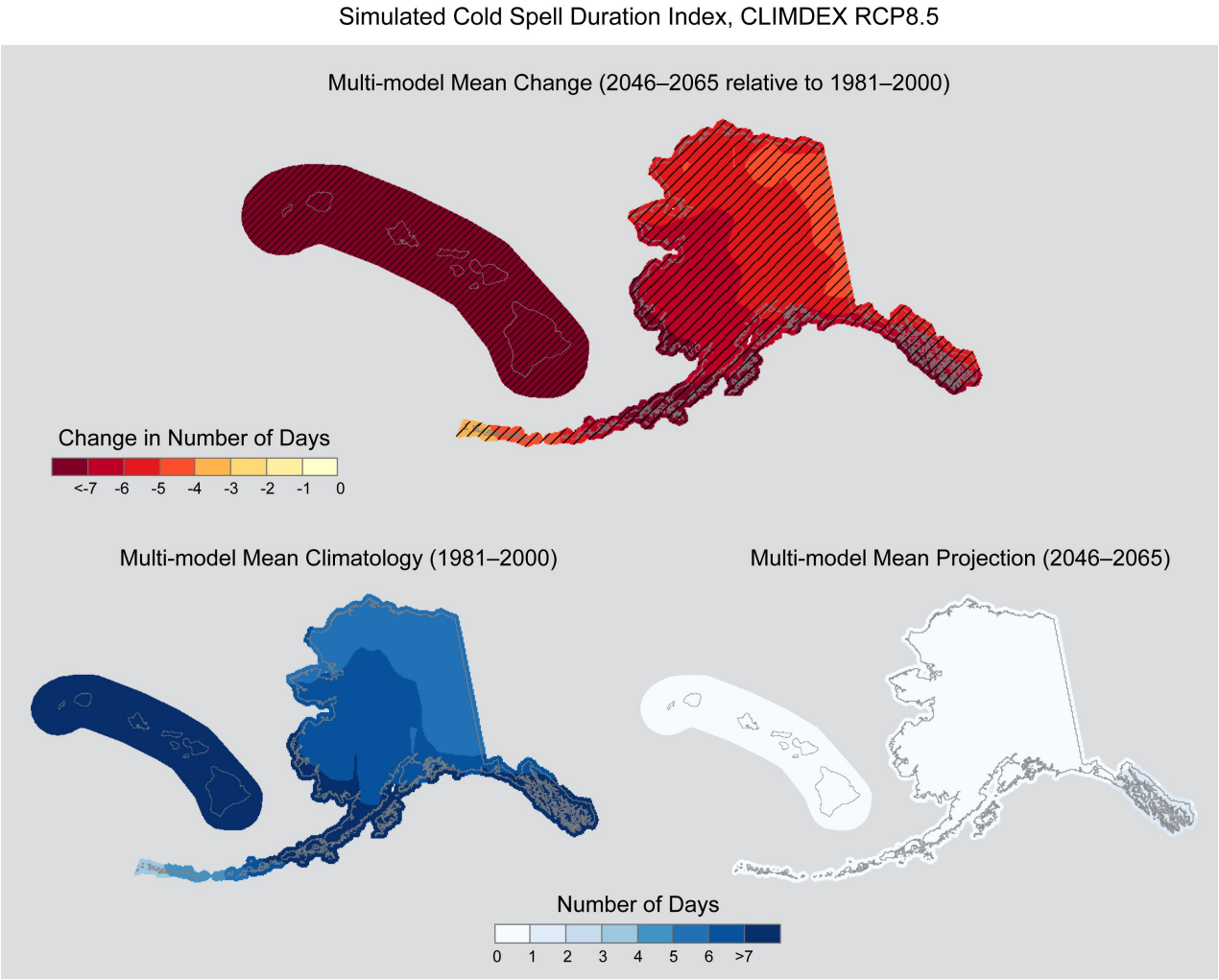

Figure 25b. *Simulated multi-model mean change in cold spell duration index (CSDI) for Alaska and Hawai'i, for 2046–2065 with respect to the reference period of 1981–2000, using the CLIMDEX RCP8.5 scenario (top). Color with hatching (category 3) indicates that more than 50% of the models show a statistically significant change, and more than 67% agree on the sign of the change (see Section 3). Multi-model mean climatology indicating the CSDI for 1981–2000 (bottom left). Multi-model mean projection indicating the CSDI for 2046–2065 (bottom right).*

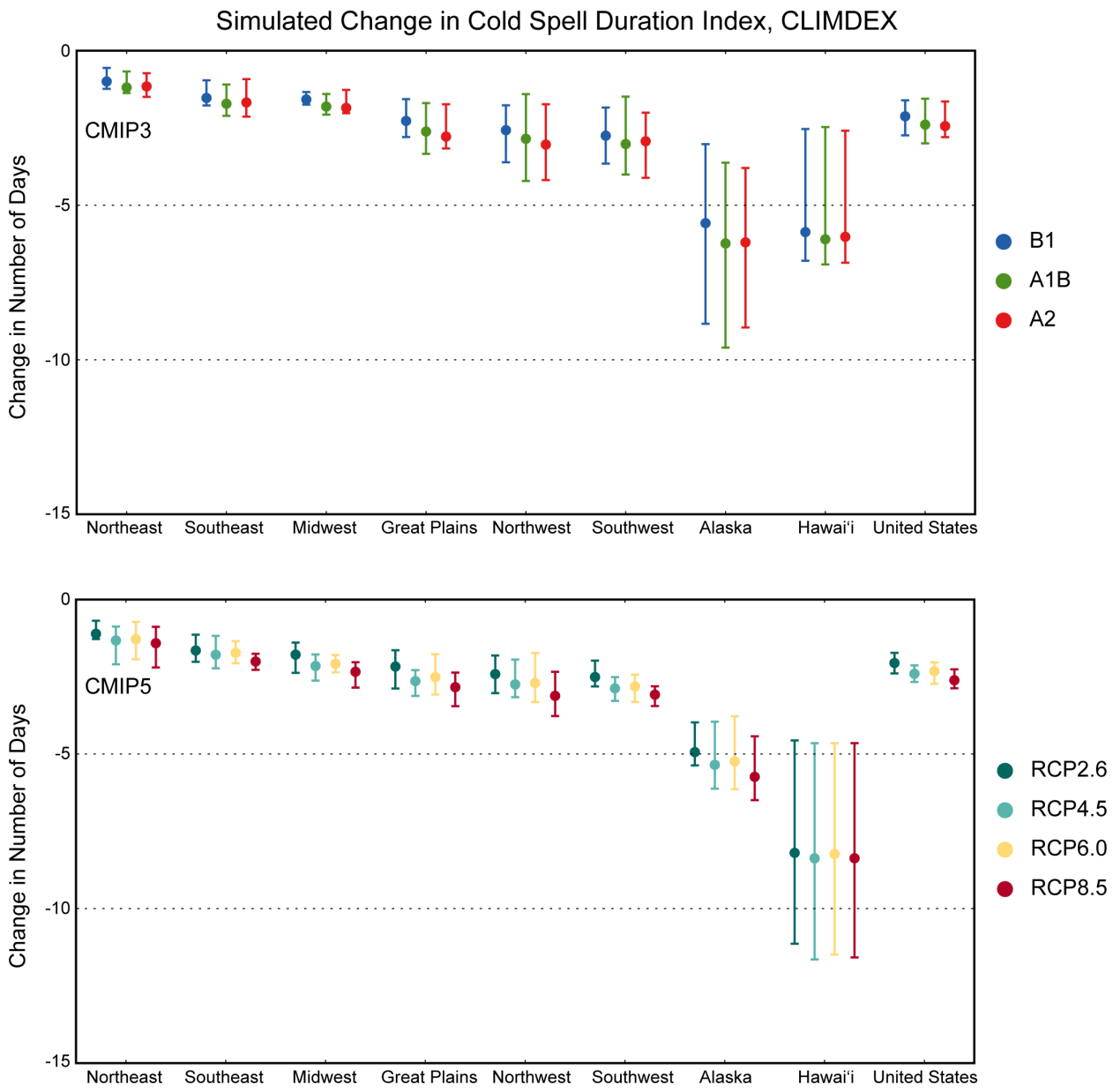

Figure 26. *Simulated change in cold spell duration index (CSDI) for each region and the contiguous United States, for 2046–2065 with respect to the reference period of 1981–2000. The upper panel shows values for the CLIMDEX SRES B1 (blue), A1B (green), and A2 (red) scenarios. The lower panel shows values for the CLIMDEX RCP2.6 (dark teal), 4.5 (light teal), 6.0 (yellow), and 8.5 (dark red) scenarios. Bars indicate the interquartile ranges of model values and circles depict the multi-model means.*

5. PRECIPITATION

5.1. Historical Simulations

Analyses of precipitation simulated for the period of 1901–2000, with changes calculated with respect to a reference period (1901–1960), were done for each NCA region in the contiguous United States.

Figure 27 shows observed and simulated annual mean precipitation for the six NCA regions and the contiguous U.S. for 1901–2000 (Alaska and Hawai‘i are omitted due to a lack of sufficient observational data). Three time series are shown for each region: nClimDiv observations (black line), CMIP3 simulations (blue line), and CMIP5 simulations (red line). The shaded regions indicate the 5th to 95th percentile range of individual annual model values. Both the observations and CMIP simulations are smoothed with a 10-year moving boxcar filter. The observations show much more interannual variability than either the CMIP3 or CMIP5 precipitation time series. Comparing the CMIP3 to the CMIP5 time series in each region, there is slightly more interannual variability in the CMIP5 simulations than CMIP3. However, there is little trend in the CMIP3 or CMIP5 simulated precipitation time series for any region, and there is little difference between the CMIP3 and CMIP5 time series. The observed values indicate that the Southwest region shows a slight drying, and the Northeast appears to show a slight increase, however statistical significance is not evaluated.

5.2. Projections

CMIP3 and CMIP5 analyses are provided for the periods of 2021–2050, 2041–2070, and 2070–2099, with changes calculated with respect to an historical climate reference period (1971–2000). These future periods will sometimes be denoted in the text by their midpoints of 2035, 2055, and 2085, respectively.

5.2.1. Mean Precipitation

Figure 28 shows mean annual precipitation time series for the northeastern United States. The Northeast region was chosen to illustrate temporal changes because the forced precipitation change is larger than the other contiguous U.S. regions. The upper panel shows nClimDiv observations (green line) and historical CMIP3 simulations (black line) for 1901–2000, as well as simulated mean annual precipitation for each CMIP3 scenario (colored lines) for 2001–2100. The lower panel shows nClimDiv observations (orange line), and historical CMIP5 simulations (orange line) for 1901–2005, as well as simulated mean annual precipitation for each CMIP5 scenario (colored lines) for 2006–2100. The shaded regions indicate the 5th to 95th percentile range of individual annual model values. Both the observations and CMIP simulations are smoothed with a 10-year moving boxcar filter. For the historical simulations, the multi-model mean time series for both CMIP3 and CMIP5 show a very small increase over the simulated 20th century. However, the difference between the 5th and 95th percentiles in the CMIP5 historical simulations is larger than in the CMIP3 simulations, indicating that there is more spread in the CMIP5 simulations of precipitation than in CMIP3.

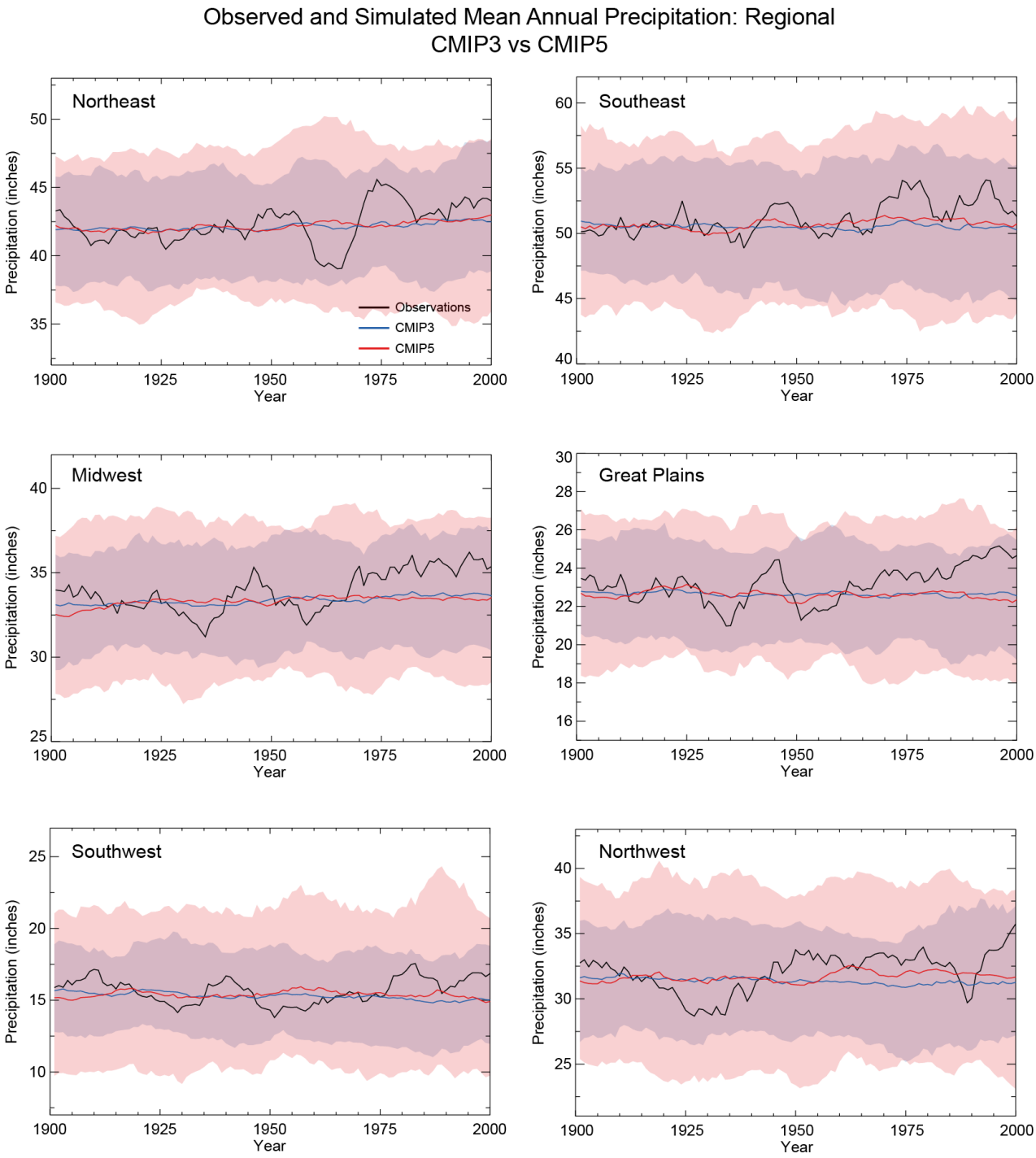

Figure 27. *Observed and simulated mean annual precipitation (inches) for the six contiguous U.S. NCA regions for 1901–2000. Observational data are from NCEI's Climate Divisional Dataset (nClimDiv, black); simulations are multi-model means from CMIP3 (blue) and CMIP5 (red). Shaded areas represent the 5–95th percentile range of the model simulations. Data are smoothed with a 10-year moving boxcar average. Note: these time series are on unique scales for each region.*

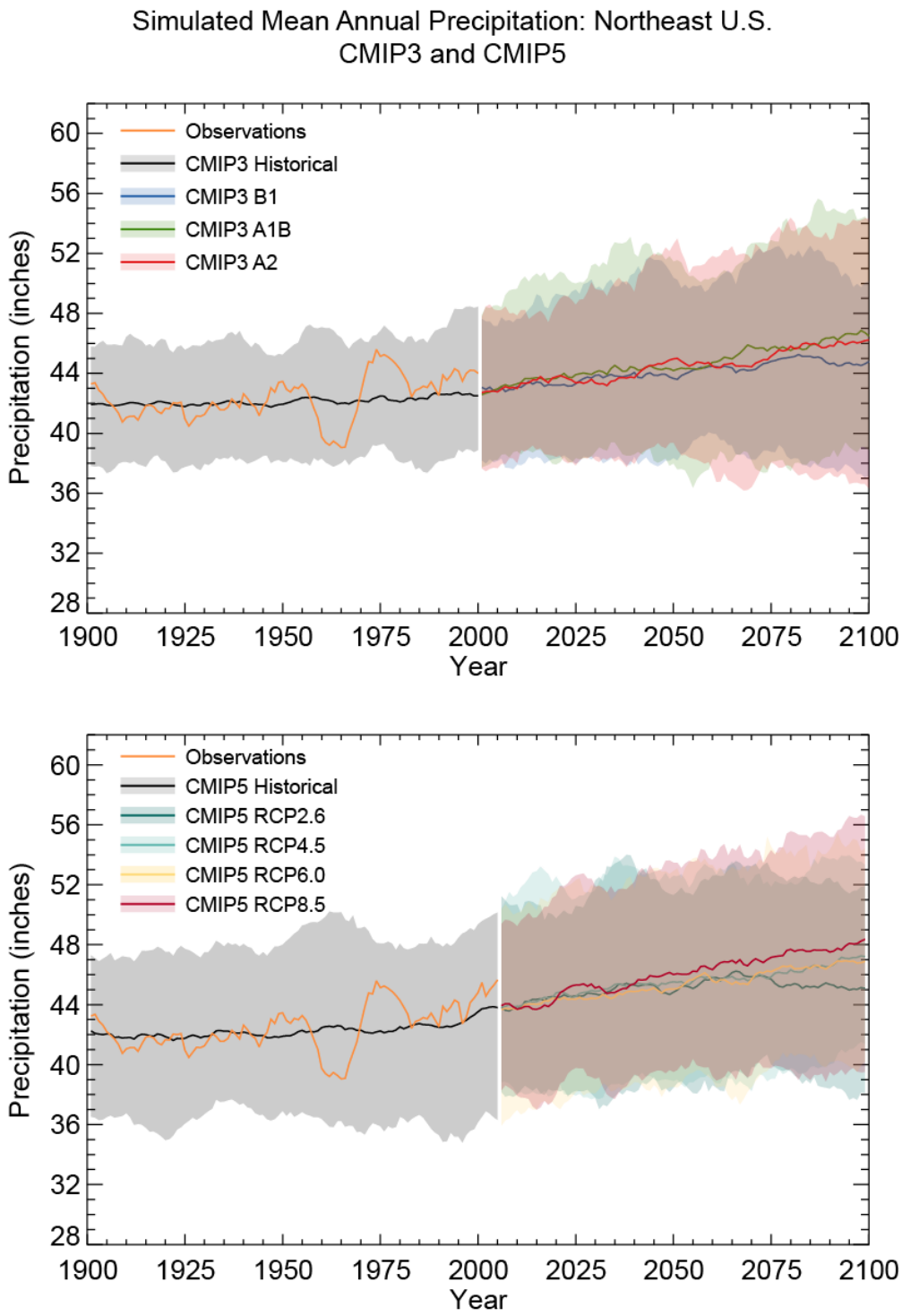

Figure 28. *Simulated mean annual precipitation (inches) for the northeast U.S. for 1900–2100. The upper panel shows observations from NCEI's Climate Divisional Dataset (nClimDiv, orange), multi-model mean simulations from CMIP3 for the historical period (black), and under the SRES B1 (blue), A1B (green), and A2 (red) scenarios. The lower panel shows observations from NCEI's Climate Divisional Dataset (nClimDiv, orange), multi-model mean simulations from CMIP5 for the historical period (black), and under the RCP2.6 (dark teal), 4.5 (light teal), 6.0 (yellow), and 8.5 (dark red) scenarios. Shaded areas represent the 5th–95th percentile range of the model simulations. Data are smoothed with a 10-year moving boxcar average.*

The multi-model means of the simulations for the future for CMIP3 show increases for each of the three forcing scenarios by the end of the 21st century. The B1 scenario shows a slightly smaller increase, but the 5th to 95th percentile spread indicates there is little statistical difference. Three of the multi-model mean time series for the CMIP5 simulations show increases, while the RCP2.6 forcing shows an increase to mid-century, then a decline ending at approximately the value for the beginning of the 21st century.

Figures 29a–31b show the percent change in mean annual precipitation for three time periods using both the CMIP3 and CMIP5 simulations. For CMIP3 the SRES B1, A1B, and A2 forcing scenarios are used and for CMIP5 the RCP2.6, 4.5, 6.0, and 8.5 are shown. For the three time periods 2021–2050, 2041–2070, and 2070–2099, the maps show the difference between the average for that period and the average of the 1971–2000 model period.

Each time period and forcing scenario shows the same broad-scale patterns of drying in the western and southwestern part of the country and increased wetness across the northern and northeast tier. For the near-term period (2021–2050), the largest increases are for the CMIP5 scenarios where each scenario produces increases of 5% to 10% in the northeastern contiguous United States (Fig. 29a). Most models agree on the sign of change, with all grid points in that region satisfying category 3 (see Section 3), i.e., the models are in agreement on precipitation increases. The RCP8.5 scenario produces the largest area of precipitation increases, and the RCP6.0 scenario has the smallest area. The three CMIP3 scenarios show a similar pattern, but the changes are modest in both the areas getting wetter and getting drier. Each CMIP3 scenario produces statistically significant wetness increases (category 3), but changes lie between +5% and −5% almost everywhere. For Alaska (Fig. 29b), increases in precipitation are seen across the state, with all grid points again satisfying category 3. Values range from 0% to 5% in southeastern parts of the state under the CMIP3 B1 scenario to greater than 15% in northern areas under the CMIP5 scenarios. Hawai‘i sees increased dryness in the north and wetness in the south for the A1B, A2, and RCP 8.5 scenarios. The B1, RCP4.5, and RCP6.0 scenarios indicate only a decrease in precipitation, and the RCP2.6 scenario sees increases across all the islands. These changes are small for all scenarios, however, and mostly not statistically significant (the majority of grid points satisfy category 1).

For the middle of the 21st century (2041–2070), the overall spatial pattern of wetting or drying remains similar, with drying in the western and southwestern parts of the contiguous U.S. and increased wetness in the northern and eastern parts (Fig. 30a). The CMIP5 simulations show broad spatial consistency with this pattern. However, the CMIP3 simulations produce a more complicated spatial pattern, with a number of smaller regions showing model disagreement on the sign of the change (category 2). The CMIP3 A2 scenario produces a large area of drying across much of the southern and southwestern part of the country, with the models being in agreement with these decreases in precipitation in several areas (these grid points satisfy category 3). None of the CMIP5 scenarios produce statistically significant drying in any region, however. An increase in precipitation is seen in northeastern areas, with statistically significant increases (category 3) under all CMIP3 and CMIP5 scenarios. The B1 and A2 scenarios also show statistically significant increases for a small portion of the northwestern contiguous United States. The models agree that precipitation will increase throughout Alaska (Fig. 30b), i.e., all grid points satisfy category 3. Values increase from south to north, reaching more then +15% across a large portion of the state under the RCP8.5 scenario. The spatial pattern of precipitation for Hawai‘i is similar to that for the early part of the century (Fig. 29b), with only RCP4.5 containing grid points that satisfy category 3.

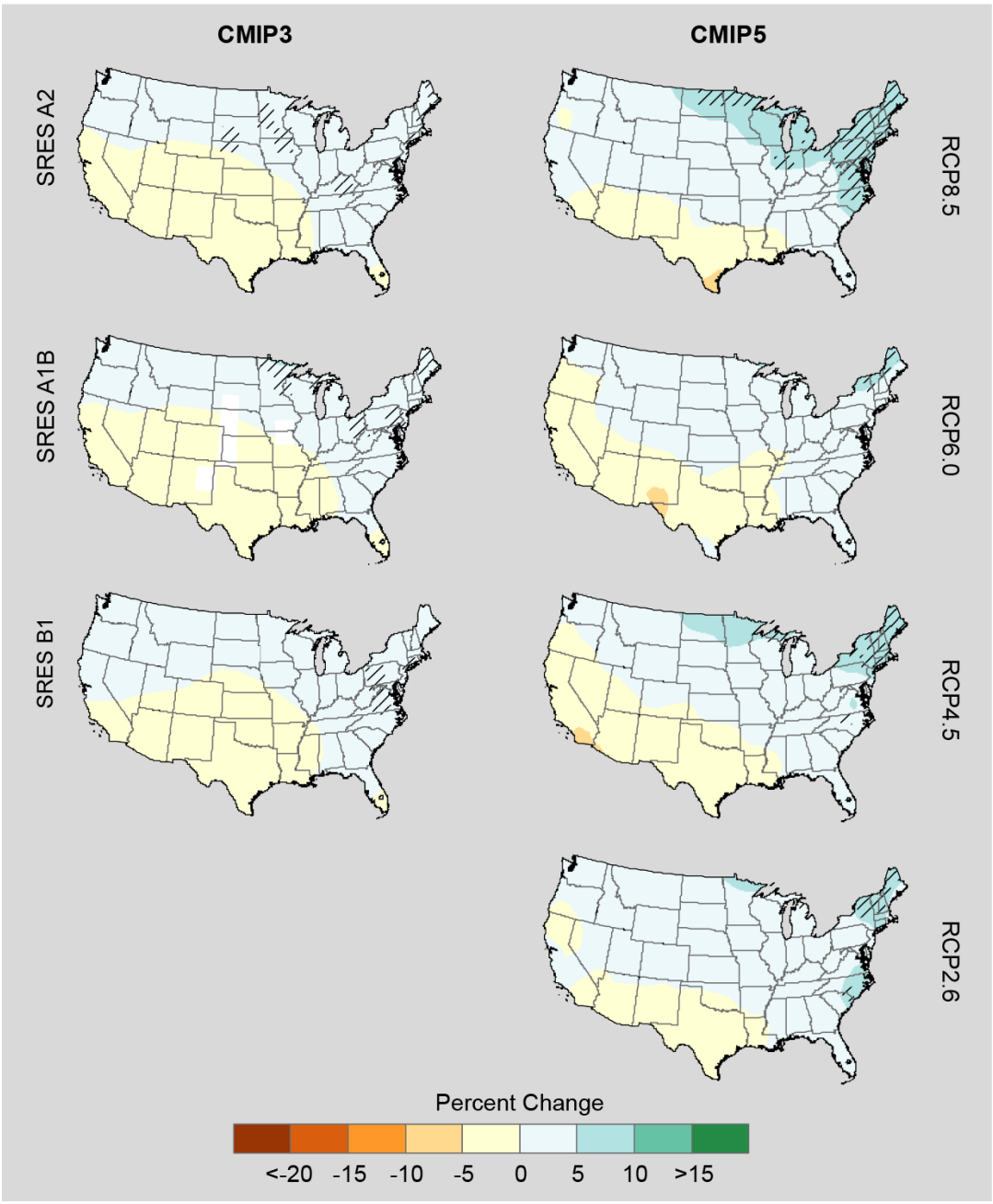

Figure 29a. *Projected change in mean annual precipitation (%) for the contiguous United States, for 2021–2050 with respect to the reference period of 1971–2000. These are multi-model means using CMIP3 SRES A2, A1B, and B1 scenarios (left column), and CMIP5 RCP8.5, 6.0, 4.5, and 2.6 scenarios (right column). Color only (category 1) indicates that less than 50% of the models show a statistically significant change. Whited out areas (category 2) indicate that more than 50% of the models show a statistically significant change, but less than 67% agree of the sign of the change. Color with hatching (category 3) indicates that more than 50% of the models show a statistically significant change, and more than 67% agree on the sign of the change (see Section 3).*

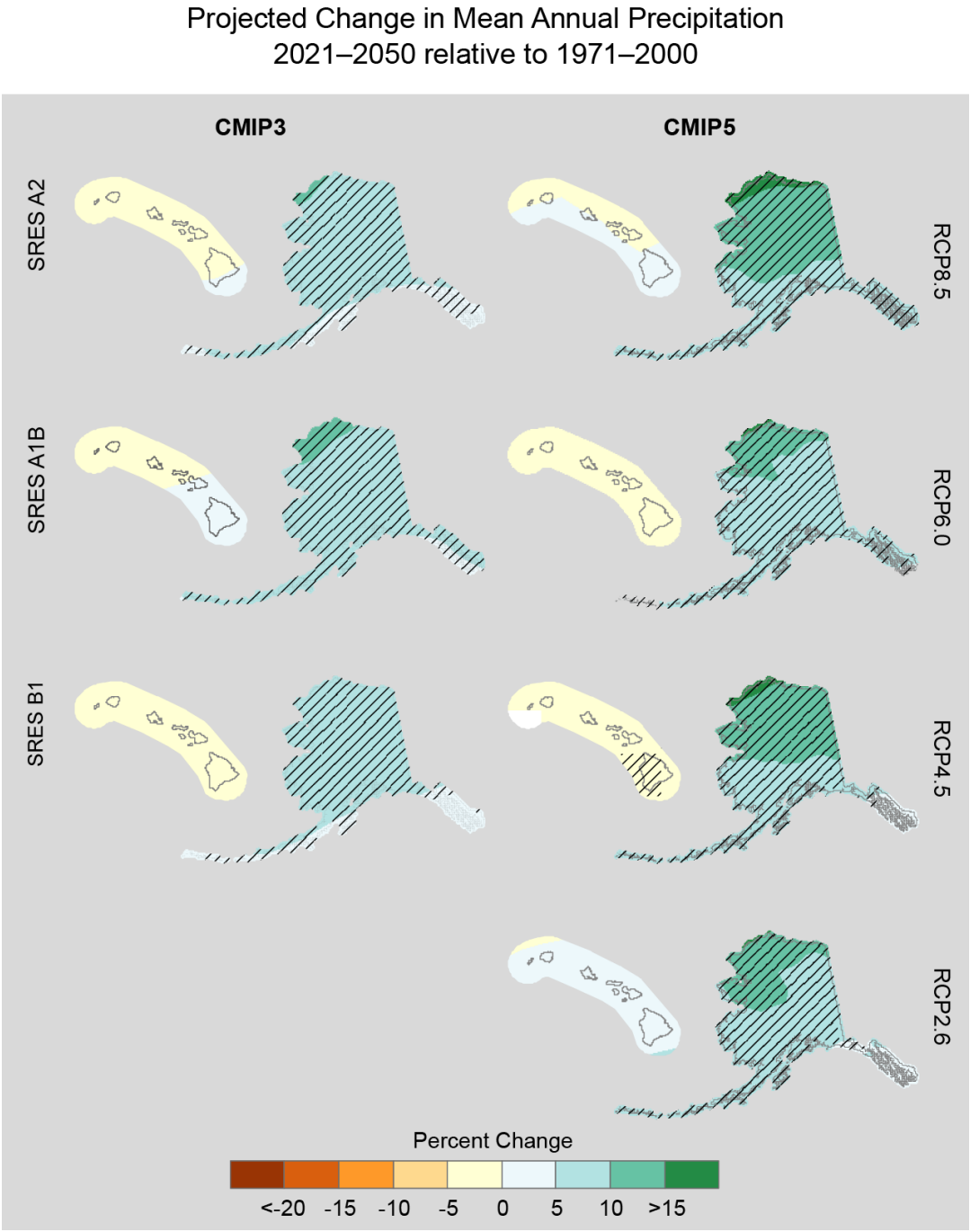

Figure 29b. *Projected change in mean annual precipitation (%) for Alaska and Hawai'i, for 2021–2050 with respect to the reference period of 1971–2000. These are multi-model means using CMIP3 SRES A2, A1B, and B1 scenarios (left column), and CMIP5 RCP8.5, 6.0, 4.5, and 2.6 scenarios (right column). Color only (category 1) indicates that less than 50% of the models show a statistically significant change. Whited out areas (category 2) indicate that more than 50% of the models show a statistically significant change, but less than 67% agree of the sign of the change. Color with hatching (category 3) indicates that more than 50% of the models show a statistically significant change, and more than 67% agree on the sign of the change (see Section 3).*

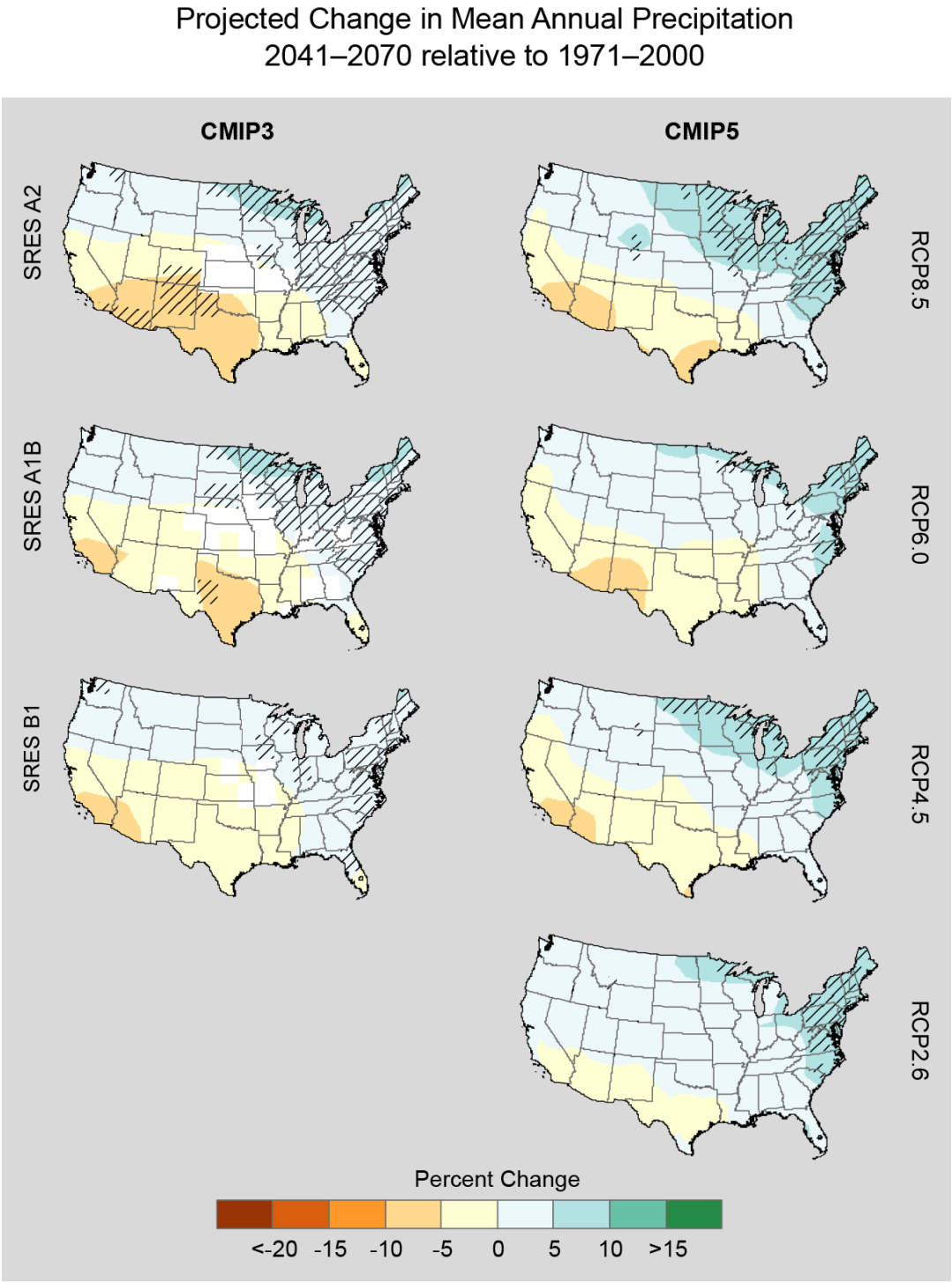

Figure 30a. *Projected change in mean annual precipitation (%) for the contiguous United States, for 2041–2070 with respect to the reference period of 1971–2000. These are multi-model means using CMIP3 SRES A2, A1B, and B1 scenarios (left column), and CMIP5 RCP8.5, 6.0, 4.5, and 2.6 scenarios (right column). Color only (category 1) indicates that less than 50% of the models show a statistically significant change. Whited out areas (category 2) indicate that more than 50% of the models show a statistically significant change, but less than 67% agree of the sign of the change. Color with hatching (category 3) indicates that more than 50% of the models show a statistically significant change, and more than 67% agree on the sign of the change (see Section 3).*

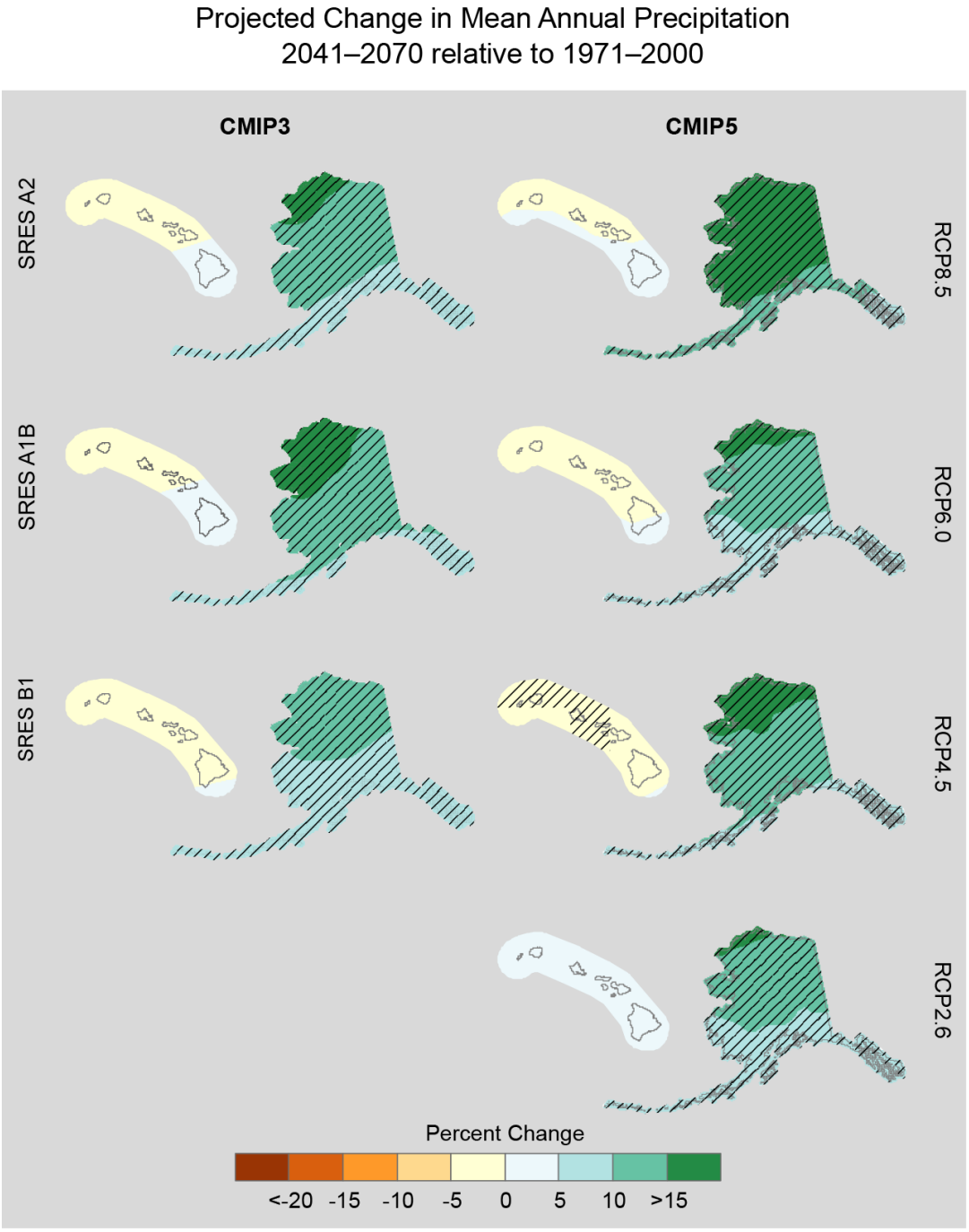

Figure 30b. *Projected change in mean annual precipitation (%) for Alaska and Hawai'i, for 2041–2070 with respect to the reference period of 1971–2000. These are multi-model means using CMIP3 SRES A2, A1B, and B1 scenarios (left column), and CMIP5 RCP8.5, 6.0, 4.5, and 2.6 scenarios (right column). Color only (category 1) indicates that less than 50% of the models show a statistically significant change. Color with hatching (category 3) indicates that more than 50% of the models show a statistically significant change, and more than 67% agree on the sign of the change (see Section 3).*

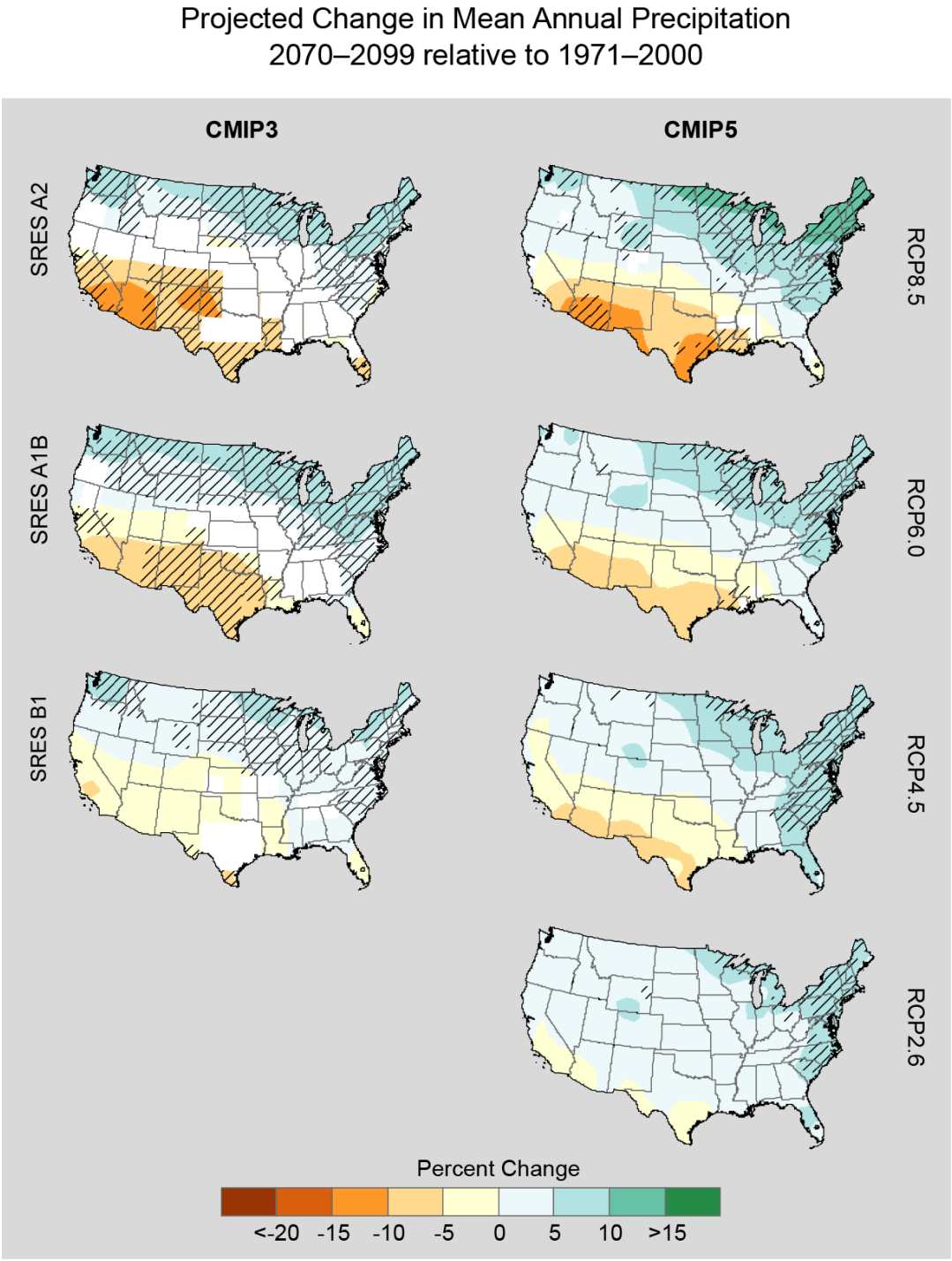

Figure 31a. *Projected change in mean annual precipitation (%) for the contiguous United States, for 2070–2099 with respect to the reference period of 1971–2000. These are multi-model means using CMIP3 SRES A2, A1B, and B1 scenarios (left column), and CMIP5 RCP8.5, 6.0, 4.5, and 2.6 scenarios (right column). Color only (category 1) indicates that less than 50% of the models show a statistically significant change. Whited out areas (category 2) indicate that more than 50% of the models show a statistically significant change, but less than 67% agree of the sign of the change. Color with hatching (category 3) indicates that more than 50% of the models show a statistically significant change, and more than 67% agree on the sign of the change (see Section 3).*

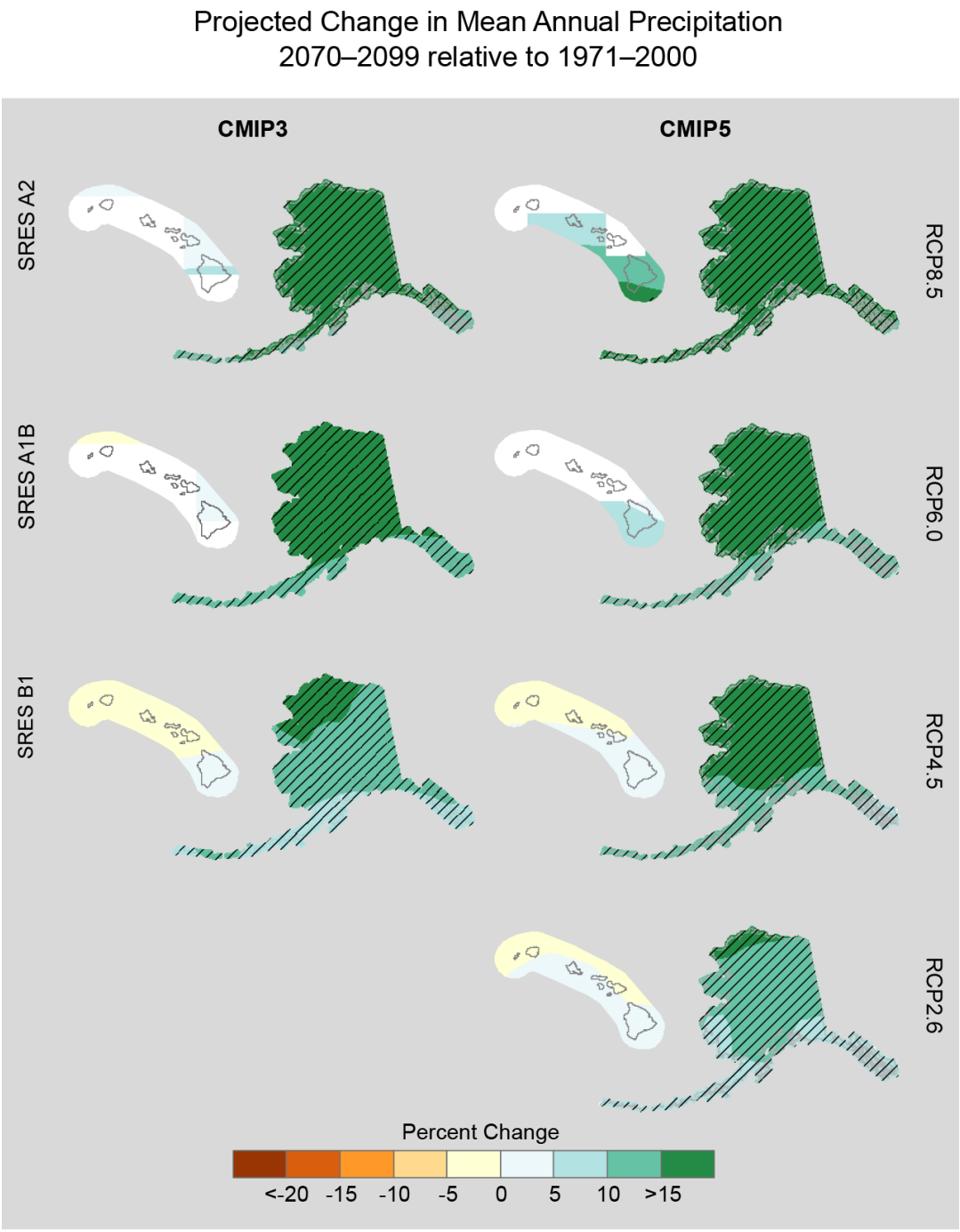

Figure 31b. *Projected change in mean annual precipitation (%) for Alaska and Hawai'i, for 2070–2099 with respect to the reference period of 1971–2000. These are multi-model means using CMIP3 SRES A2, A1B, and B1 scenarios (left column), and CMIP5 RCP8.5, 6.0, 4.5, and 2.6 scenarios (right column). Color only (category 1) indicates that less than 50% of the models show a statistically significant change. Whited out areas (category 2) indicate that more than 50% of the models show a statistically significant change, but less than 67% agree of the sign of the change. Color with hatching (category 3) indicates that more than 50% of the models show a statistically significant change, and more than 67% agree on the sign of the change (see Section 3).*

For the last period of the 21st century (2070–2099), the same general pattern of wetter in the northern portions and drier in the south and southwest are apparent, with the exception being the CMIP5 RCP2.6 scenario (Fig. 31a). In this scenario, the slight drying seen in the earlier periods in the south and southwest contiguous U.S. becomes much more spotty—only three areas, southern Texas, western Texas extending into southern New Mexico, and western Arizona/southern California show slight drying, the remainder of the country shows slight to moderate increases in annual precipitation. Moderate to large increases in precipitation are seen for the northeastern U.S. under all scenarios, with statistically significant increases across many grid points in this region (category 3). Some of the most intense drying occurs in both the CMIP3 A2 and CMIP5 RCP8.5 scenarios, with decreases of 10% or more occurring in Texas and the southwestern United States. The models agree on these decreases, with grid points satisfying category 3 for a large portion of the southern U.S. under the A1B and A2 scenarios. Across parts of the central and southern states, however, several grid points satisfy category 2 under the CMIP3 scenarios, i.e., the majority of models disagree on the sign of the change. Once again, increases in precipitation are seen for Alaska (Fig. 31b), with grid points satisfying category 3 everywhere. Values of more than +15% now cover the majority of the state for five of the seven scenarios (all except B1 and RCP2.6). For Hawai‘i, the B1, RCP2.6, and RCP4.5 scenarios show wetter conditions in the south and dryer in the north. The other scenarios show only increases in precipitation, but a large proportion of grid points satisfy category 2.

Seasonal changes in precipitation for the middle of the 21st century for the contiguous U.S. are shown in Fig. 32a. Only the CMIP3 A2 and CMIP5 RCP8.5 scenarios are shown. Results for winter show similar patterns between the CMIP3 and CMIP5 simulations, with increasing wetness across most of the contiguous United States, with the exception of the south and southwest. CMIP5 simulations show increases of more than 15% in the northern Great Plains into the upper Midwest. These increases are more pronounced than those indicated by the CMIP3 simulations. Areas of statistically significant changes (category 3) extend across the northeast and in parts of the central United States, covering a larger extent for the RCP8.5 scenario than for A2. The southern tier of states, from southern California to the Deep South, shows drying, with the most intense drying occurring in the southernmost parts of Texas, although these changes in precipitation are not statistically significant for most models (category 1).

Spring precipitation changes are also similar between CMIP3 and CMIP5, but there is a larger area of intense drying in the southwest in the CMIP3 simulations relative to CMIP5. For CMIP5, there is a larger area of moderately increasing wetness (>15%) in the upper Great Plains extending into the central United States. Grid points satisfy category 3 for each of these regions.

The spatial pattern of precipitation changes in the summer are different from the other three seasons, with most of the country (with the exception of the east coast) exhibiting a drying trend. Drying is most intense in CMIP3, and occurs along the west coast into the interior of the northwest, where grid points satisfy category 3. CMIP5 shows a similar pattern but with less intense drying. Both CMIP3 and CMIP5 also show drying in the Florida peninsula.

Precipitation changes in the fall are more modest than the other seasons, with the exception of strong, somewhat localized drying along the California coast. This area extends inland, with slight drying into the interior and across most of Texas. Most of the rest of the country shows some increasing wetness, and Florida shows an increase of more than 10%. Grid points satisfy category 1 throughout the country under both scenarios.

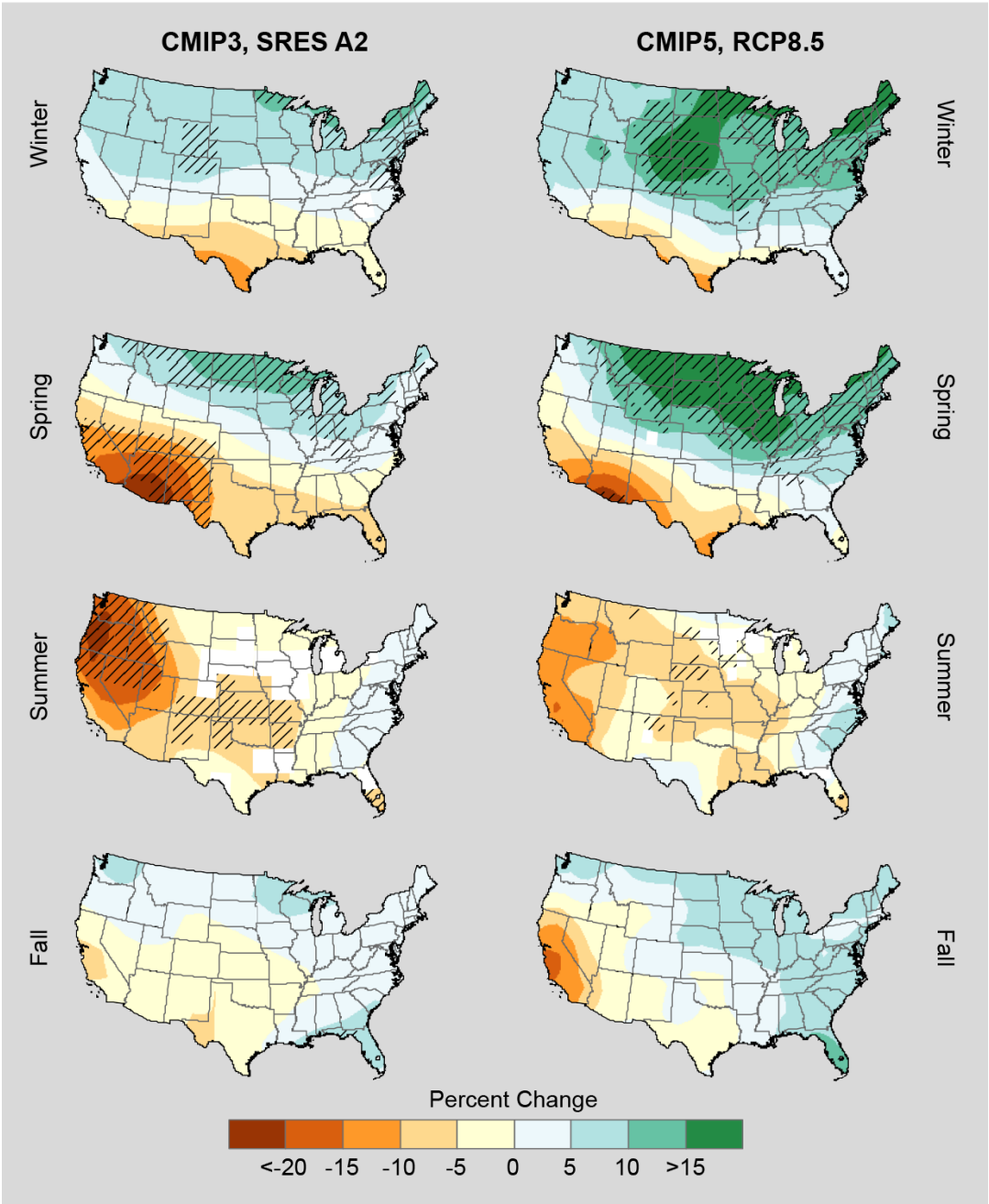

Figure 32a. *Projected change in mean seasonal precipitation (%) for the contiguous United States, for 2041–2070 with respect to the reference period of 1971–2000. These are multi-model means using CMIP3 SRES A2 (left column), and CMIP5 RCP8.5 (right column). Color only (category 1) indicates that less than 50% of the models show a statistically significant change. Whited out areas (category 2) indicate that more than 50% of the models show a statistically significant change, but less than 67% agree of the sign of the change. Color with hatching (category 3) indicates that more than 50% of the models show a statistically significant change, and more than 67% agree on the sign of the change (see Section 3).*

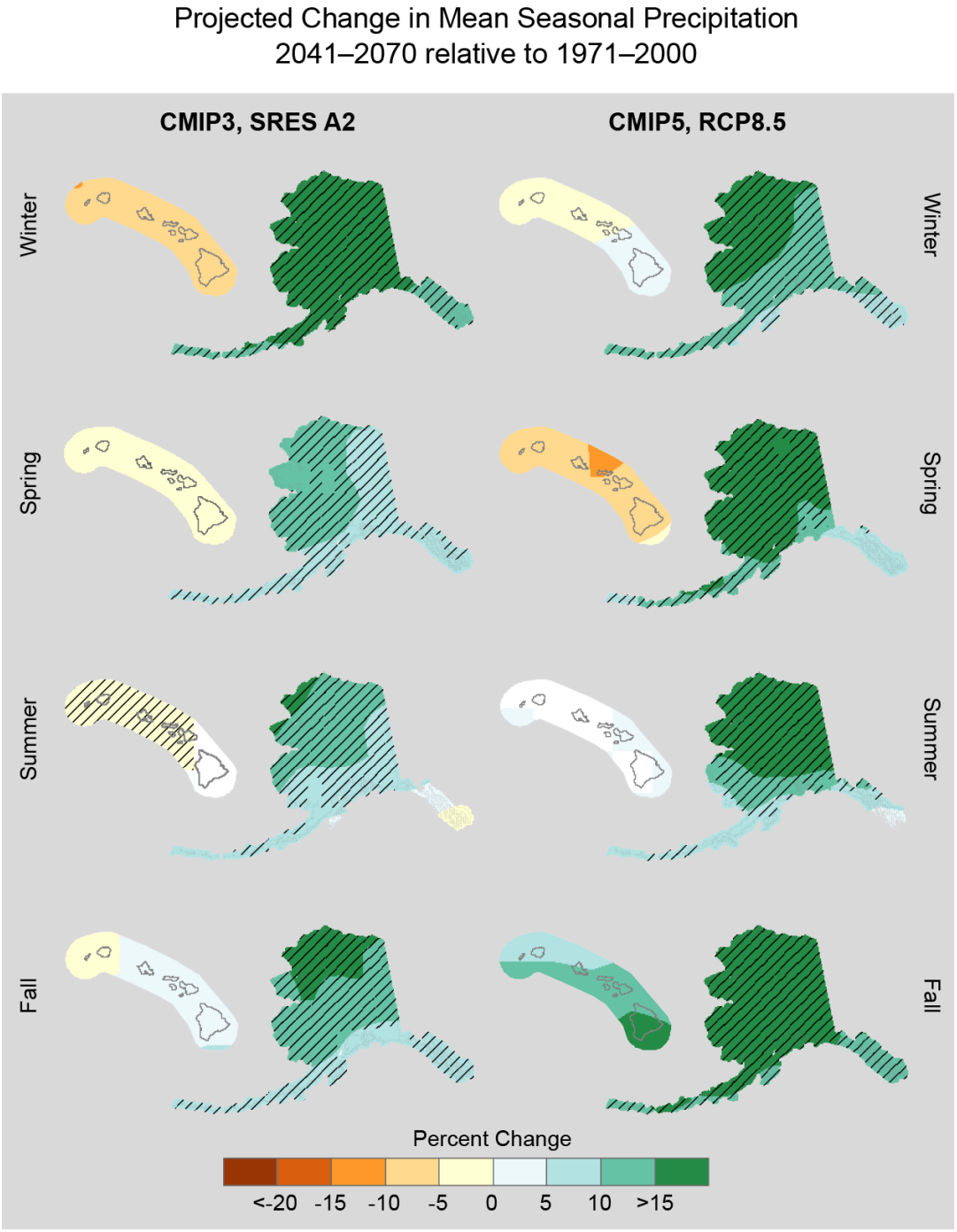

Figure 32b. *Projected change in mean seasonal precipitation (%) for Alaska and Hawai'i, for 2041–2070 with respect to the reference period of 1971–2000. These are multi-model means using CMIP3 SRES A2 (left column), and CMIP5 RCP8.5 (right column). Color only (category 1) indicates that less than 50% of the models show a statistically significant change. Whited out areas (category 2) indicate that more than 50% of the models show a statistically significant change, but less than 67% agree of the sign of the change. Color with hatching (category 3) indicates that more than 50% of the models show a statistically significant change, and more than 67% agree on the sign of the change (see Section 3).*

Mid-21st century seasonal precipitation changes for Alaska and Hawai‘i are shown in Fig. 32b. For Alaska, an increase in precipitation is seen for all seasons under both scenarios, with the exception of a small part of southeastern Alaska for the A2 scenario in summer. Values for RCP8.5 are greater than +15% across the majority of the state for all seasons, compared to increases generally in the 10%–15% range for A2. Greater increases are seen for the winter and fall season under both scenarios. Grid points satisfy category 3 almost everywhere for all seasons. For Hawai‘i, the majority of the state sees a decrease in precipitation for winter and spring under both scenarios and for summer under the A2 scenario. Wetter conditions are seen, however, for summer under the RCP8.5 scenario and for fall under both scenarios. The largest decreases in precipitation are in the 10%–15% range for spring under the RCP8.5 scenario. The largest increases are greater than 15% for fall, again under RCP8.5. The only grid points satisfying category 3 are for summer under the A2 scenario, however, the summer simulations also see grid points satisfying category 2 under both scenarios.

A scatter plot of individual model simulations and the multi-model means for annual precipitation change are shown in Fig. 33 for the southwest for the three time periods, 2021–2050, 2041–2070, and 2070–2099. The southwest consistently shows drying in the multi-model means shown in previous figures. The same is true on this scatter plot, with all of the multi-model means falling below the zero line. However, several individual model simulations show increasing wetness in each period. Some simulations have increases of 10% or more in each time period. The CMIP3 SRES simulations, especially A2, tend to produce the largest spread between simulations, with differences of almost 50% for the extremes of the A2 for the middle period. Generally the CMIP5 simulations show a tighter dispersion than CMIP3 for all three periods. However, both CMIP3 and CMIP5 have both decreases and increases in precipitation for each period.

Analyses of the distribution of simulated change in mean seasonal precipitation for the 2041–2070 period with respect to 1971–2000 for both CMIP3 (using the SRES B1 and A2 scenarios) and for CMIP5 (using RCP2.6 and 8.5) were done for each region. Tables 7–10 show the lowest, median, highest, and 25th and 75th percentile changes (in %) for each season.

For winter, spring, and fall, with the exception of the Southwest and Hawai‘i, the median values for the RCP8.5 for CMIP5 show the largest increases in each region and for the contiguous United States. However, there are some notable differences. In winter, the largest median increase in the Southwest (+7.3%) is for the CMIP5 RCP2.6, but the CMIP3 SRES B1 median shows a slight decrease, with the other two forcing scenarios showing modest increases. Hawai‘i is the only region to show consistent decreases in median values across both CMIP3 and CMIP5.

The lowest values across the regions show a mixture from small increases to large decreases. The largest decrease, more than −40%, is in Hawai‘i for the CMIP5 RCP8.5 forcing scenario, while the CMIP3 A2 scenario shows a more modest decline of −16%. The other region with large decreases in the lowest values are in the Southeast, where both the CMIP3 SRES A2 and CMIP5 RCP8.5 show large decreases in the lowest values. For the contiguous United States, both CMIP3 and CMIP5 show modest decreases in the lowest values.

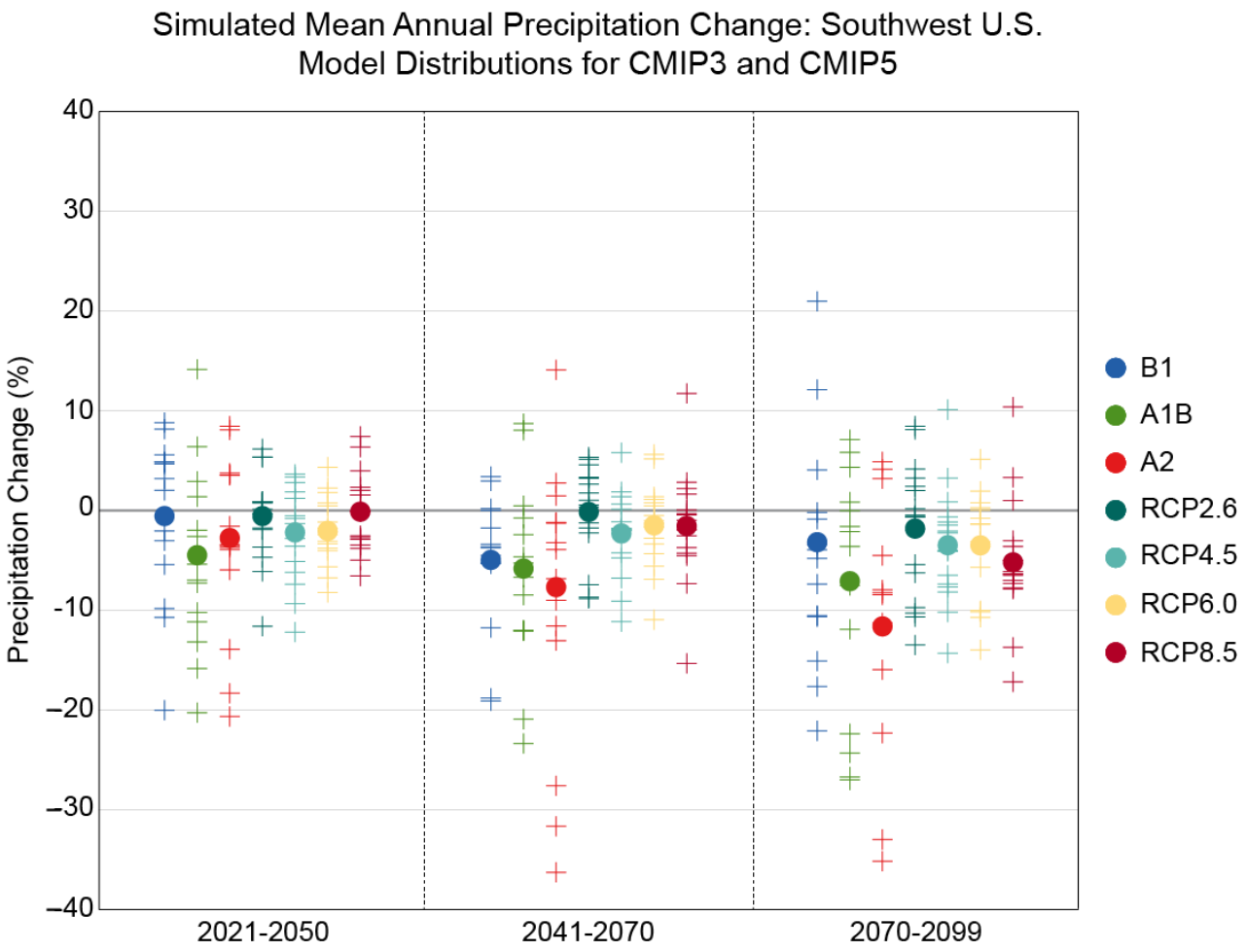

Figure 33. *Model distributions of simulated mean annual precipitation change (%) for the southwest United States, for each future time period (2021–2050, 2041–2070, and 2070–2099) with respect to the reference period of 1971–2000 for each CMIP3 and CMIP5 scenario. The small plus signs (+) indicate each individual model and the circles depict the multi-model means.*

Table 7. *Distribution of the simulated change in mean winter precipitation (%) amongst models using the CMIP3 SRES B1 and A2 scenarios and the CMIP5 RCP2.6 and 8.5 scenarios, for each U.S. region. The lowest, 25th percentile, median, 75th percentile and highest values are given for 2041–2070, with respect to the reference period of 1971–2000.*

Region	Scenario	Lowest	25th Percentile	Median	75th Percentile	Highest
Northeast	SRES B1	−6.3	1.5	6.0	10.0	15.4
	RCP2.6	0.2	4.3	7.9	16.1	31.6
	SRES A2	−6.4	5.0	10.1	13.5	20.3
	RCP8.5	2.2	6.7	15.8	19.2	31.8
Southeast	SRES B1	−15.9	−3.6	0.3	4.8	7.8
	RCP2.6	−4.0	0.4	2.4	8.5	26.4
	SRES A2	−20.6	−8.6	5.1	7.3	10.2
	RCP8.5	−22.6	1.4	7.2	16.8	18.2
Midwest	SRES B1	−7.7	0.2	5.1	8.1	12.2
	RCP2.6	−0.7	5.3	8.1	13.4	20.9
	SRES A2	−1.2	3.7	7.2	10.9	17.2
	RCP8.5	−9.9	6.5	16.4	19.8	34.3
Great Plains	SRES B1	−9.3	−1.8	2.7	7.3	8.9
	RCP2.6	−1.3	2.0	5.5	8.5	12.9
	SRES A2	−6.7	−1.8	5.1	6.9	11.0
	RCP8.5	−4.1	2.4	9.6	15.3	22.6
Southwest	SRES B1	−11.6	−5.2	−1.0	5.2	6.8
	RCP2.6	−11.1	−4.4	7.3	11.4	11.8
	SRES A2	−17.8	−2.9	3.9	5.5	17.9
	RCP8.5	−8.4	−5.1	3.4	14.7	41.1
Northwest	SRES B1	−1.7	0.3	4.9	7.8	24.0
	RCP2.6	−2.7	2.2	5.4	7.1	8.8
	SRES A2	1.0	1.7	4.2	10.0	26.6
	RCP8.5	−0.9	4.3	7.4	11.1	16.4
Alaska	SRES B1	5.0	8.7	16.2	18.4	19.7
	RCP2.6	2.4	4.4	12.4	23.1	31.0
	SRES A2	−0.4	9.1	17.8	22.0	30.7
	RCP8.5	8.1	17.1	21.5	38.0	50.0
Hawai‘i	SRES B1	−16.5	−5.6	−2.7	3.5	31.3
	RCP2.6	−18.7	−11.4	−1.1	3.8	19.3
	SRES A2	−16.1	−8.8	−1.6	3.9	61.9
	RCP8.5	−43.1	−20.7	−7.1	8.7	11.2
Contiguous U.S.	SRES B1	−3.2	−1.0	2.3	5.0	7.8
	RCP2.6	−2.4	3.1	5.4	7.4	15.1
	SRES A2	−5.9	−0.7	5.8	6.9	9.6
	RCP8.5	−7.1	4.0	9.0	12.7	26.4

Table 8. *Distribution of the simulated change in mean spring precipitation (%) amongst models using the CMIP3 SRES B1 and A2 scenarios and the CMIP5 RCP2.6 and 8.5 scenarios, for each U.S. region. The lowest, 25th percentile, median, 75th percentile and highest values are given for 2041–2070, with respect to the reference period of 1971–2000.*

Region	Scenario	Lowest	25th Percentile	Median	75th Percentile	Highest
Northeast	SRES B1	−0.7	1.6	6.6	8.2	11.1
	RCP2.6	0.3	4.7	7.7	11.1	15.7
	SRES A2	−6.1	2.5	6.0	9.8	12.8
	RCP8.5	1.3	7.3	11.2	18.2	25.0
Southeast	SRES B1	−14.5	−5.3	0.7	3.2	7.5
	RCP2.6	−4.0	1.3	3.5	8.5	13.8
	SRES A2	−16.2	−11.2	−0.3	4.0	7.1
	RCP8.5	−13.8	0.7	3.0	8.9	17.0
Midwest	SRES B1	−4.6	2.5	8.4	10.0	10.4
	RCP2.6	1.8	5.1	7.2	14.3	16.5
	SRES A2	−1.7	3.9	8.9	11.6	17.2
	RCP8.5	−0.3	9.1	14.0	18.1	39.1
Great Plains	SRES B1	−7.5	0.6	3.8	7.0	10.2
	RCP2.6	−4.0	3.1	6.1	10.0	15.5
	SRES A2	−10.4	−1.1	2.7	9.2	11.1
	RCP8.5	−12.5	4.5	8.5	11.5	21.8
Southwest	SRES B1	−18.3	−10.4	−5.9	−3.1	3.0
	RCP2.6	−8.9	−7.6	−0.6	4.1	11.5
	SRES A2	−37.0	−18.0	−9.9	−4.6	5.8
	RCP8.5	−20.0	−10.4	−2.9	2.8	7.2
Northwest	SRES B1	−0.9	0.6	4.5	8.3	10.0
	RCP2.6	−0.3	1.3	2.6	10.4	13.5
	SRES A2	−4.5	1.4	4.7	6.6	10.4
	RCP8.5	−2.7	0.6	3.7	7.4	21.4
Alaska	SRES B1	0.5	6.4	7.2	11.9	19.4
	RCP2.6	−2.6	5.0	10.7	14.4	26.2
	SRES A2	2.6	8.5	10.5	15.5	17.8
	RCP8.5	−1.4	11.1	15.7	24.4	36.2
Hawai‘i	SRES B1	−20.7	−9.7	−4.5	4.6	19.0
	RCP2.6	−39.5	−17.2	−3.7	2.5	34.6
	SRES A2	−22.1	−12.9	−2.8	4.9	20.2
	RCP8.5	−43.5	−19.3	−7.8	4.1	23.6
Contiguous U.S.	SRES B1	−6.7	−0.7	2.1	3.4	6.2
	RCP2.6	−0.2	2.0	3.7	7.3	12.4
	SRES A2	−8.1	−5.3	0.5	3.7	7.6
	RCP8.5	−7.9	2.2	5.8	7.8	20.0

Table 9. *Distribution of the simulated change in mean summer precipitation (%) amongst models using the CMIP3 SRES B1 and A2 scenarios and the CMIP5 RCP2.6 and 8.5 scenarios, for each U.S. region. The lowest, 25th percentile, median, 75th percentile and highest values are given for 2041–2070, with respect to the reference period of 1971–2000.*

Region	Scenario	Lowest	25th Percentile	Median	75th Percentile	Highest
Northeast	SRES B1	−3.7	−1.4	1.8	6.8	14.6
	RCP2.6	0.3	1.9	4.6	6.8	9.3
	SRES A2	−11.8	−5.8	1.9	4.9	20.1
	RCP8.5	−3.4	0.1	3.0	5.9	9.0
Southeast	SRES B1	−21.4	−5.5	0.4	8.3	13.5
	RCP2.6	−9.8	−1.1	2.3	6.3	18.3
	SRES A2	−38.7	−14.8	−0.8	9.1	15.3
	RCP8.5	−14.3	−12.9	1.9	7.1	17.9
Midwest	SRES B1	−11.1	−8.5	−0.3	5.4	12.4
	RCP2.6	−23.4	−2.5	−0.1	5.1	15.0
	SRES A2	−20.0	−12.8	−0.9	4.6	17.9
	RCP8.5	−20.1	−11.6	−5.0	5.1	15.4
Great Plains	SRES B1	−14.7	−8.6	0.4	3.8	6.7
	RCP2.6	−18.8	−4.1	−1.4	1.9	7.5
	SRES A2	−25.9	−19.8	−4.3	5.2	7.5
	RCP8.5	−21.1	−9.2	−5.3	2.9	7.3
Southwest	SRES B1	−17.3	−10.1	−5.6	9.9	16.2
	RCP2.6	−27.0	−9.8	3.2	6.7	17.2
	SRES A2	−41.0	−24.8	−8.6	−2.9	4.5
	RCP8.5	−22.3	−18.9	−7.0	2.9	12.5
Northwest	SRES B1	−28.5	−20.6	−7.3	1.4	8.6
	RCP2.6	−20.0	−11.3	−0.7	2.2	13.2
	SRES A2	−37.4	−29.5	−21.5	−5.1	−2.4
	RCP8.5	−27.4	−23.6	−8.1	−4.1	7.0
Alaska	SRES B1	3.2	5.6	8.5	13.5	17.4
	RCP2.6	−1.1	5.4	9.3	14.7	21.6
	SRES A2	3.7	5.2	12.6	14.9	19.6
	RCP8.5	4.3	9.1	16.4	23.3	42.7
Hawai‘i	SRES B1	−18.4	−16.4	−8.7	−0.3	52.2
	RCP2.6	−25.5	−11.4	−0.8	5.4	37.9
	SRES A2	−32.8	−21.8	−7.0	2.6	58.4
	RCP8.5	−35.9	−18.2	−4.6	12.7	70.4
Contiguous U.S.	SRES B1	−13.4	−7.0	−2.2	3.9	7.9
	RCP2.6	−18.5	−1.5	0.8	3.7	5.4
	SRES A2	−24.4	−17.1	−7.7	−0.9	5.9
	RCP8.5	−18.1	−10.8	−4.6	1.2	3.6

Table 10. *Distribution of the simulated change in mean fall precipitation (%) amongst models using the CMIP3 SRES B1 and A2 scenarios and the CMIP5 RCP2.6 and 8.5 scenarios, for each U.S. region. The lowest, 25th percentile, median, 75th percentile and highest values are given for 2041–2070, with respect to the reference period of 1971–2000.*

Region	Scenario	Lowest	25th Percentile	Median	75th Percentile	Highest
Northeast	SRES B1	−10.6	−3.6	−0.2	3.8	11.0
	RCP2.6	−4.3	−0.5	3.7	7.4	11.3
	SRES A2	−9.3	−2.0	1.6	6.4	13.5
	RCP8.5	−2.9	1.7	5.3	8.7	12.0
Southeast	SRES B1	−13.4	−2.4	1.1	5.9	12.1
	RCP2.6	−4.1	−1.0	2.5	5.5	13.5
	SRES A2	−10.7	−3.1	3.3	6.2	10.5
	RCP8.5	−3.6	1.4	6.0	8.4	20.6
Midwest	SRES B1	−17.2	−4.8	2.7	5.6	7.8
	RCP2.6	−4.3	0.1	3.0	8.9	13.0
	SRES A2	−7.8	−1.3	3.4	7.8	12.2
	RCP8.5	−2.3	3.3	6.7	10.7	17.5
Great Plains	SRES B1	−15.7	−2.2	−0.2	3.8	6.0
	RCP2.6	−6.9	−0.2	2.1	5.2	13.9
	SRES A2	−14.5	−3.6	0.3	5.1	10.6
	RCP8.5	−8.4	−0.4	2.2	5.9	9.9
Southwest	SRES B1	−21.6	−6.7	0.6	4.4	13.4
	RCP2.6	−15.6	−2.7	−1.7	5.7	15.5
	SRES A2	−22.3	−11.9	−2.5	2.1	14.7
	RCP8.5	−13.9	−7.1	−2.9	−2.3	4.1
Northwest	SRES B1	−7.5	−0.9	4.1	8.8	12.8
	RCP2.6	−11.2	−0.9	1.6	7.3	7.7
	SRES A2	−13.7	−0.1	4.0	10.4	22.4
	RCP8.5	−7.9	−5.8	1.6	6.4	10.8
Alaska	SRES B1	3.5	5.1	9.3	13.3	17.6
	RCP2.6	2.7	7.4	12.9	20.5	30.6
	SRES A2	6.0	8.6	13.3	18.4	20.5
	RCP8.5	9.5	17.7	22.0	27.6	41.9
Hawai‘i	SRES B1	−23.6	−6.7	−1.6	12.6	28.1
	RCP2.6	−16.4	−3.6	3.8	30.0	39.5
	SRES A2	−24.1	−8.7	−0.7	11.8	33.7
	RCP8.5	−17.3	−4.6	3.3	31.5	50.5
Contiguous U.S.	SRES B1	−13.7	−1.8	1.8	2.8	5.1
	RCP2.6	−2.4	−0.4	1.7	5.3	7.9
	SRES A2	−10.4	−1.0	1.4	3.7	8.4
	RCP8.5	−4.7	0.1	2.2	4.5	7.3

At the other end of the distribution, there is a general tendency for the CMIP5 RCP8.5 simulations to have the largest increases in the highest values, with the exception of Hawai‘i, the Northwest, and the Southeast. This is reflected in the value for the contiguous U.S. as well, with the CMIP5 RCP8.5 having the largest increase in the highest value for both winter and spring, but the fall having only modest increases in the largest values. Generally, the CMIP5 RCP8.5 simulations produce the largest increases in annual precipitation, and the CMIP3 SRES B1 scenarios produce the smallest increases.

Summer, on the other hand, shows a distinct difference from the other three seasons in the modeled changes. The central and western regions as well as Hawai‘i all show declines in the median summer precipitation across both the CMIP3 and CMIP5 simulations. Only Alaska shows a large increase in the median summer precipitation, with the other regions generally showing small increases or decreases. In many regions, the range between the highest and lowest values is quite large, approaching 45% in some regions and forcing scenarios. Many of these large differences are driven by very large decreases in the lowest values. For the contiguous United States, the median for each forcing scenario shows only modest declines, with the CMIP5 RCP2.6 having virtually no change.

Similar to the temperature results shown in Fig. 10, an analysis of precipitation change on decadal time scales was performed on the CMIP3 and CMIP5 models with respect to the most recent historical decade of 2001–2010. Figure 34 shows the simulated change in decadal mean values of annual precipitation for each future decadal time period with respect to 2001–2010 for the southwest U.S. region. For CMIP3, the A2, A1B, and B1 emissions scenarios are shown. For CMIP5, all four RCP scenarios are shown. Unlike for temperature, most of the model values of precipitation change are not statistically significant in all decades out to 2091–2099 and almost all are within the 10th to 90th percentile range of the historical annual precipitation anomalies. For the high A2 and RCP8.5 scenarios (top panels), the multi-model mean change is negative and statistically significant for a few decades in the latter half of the 20th century. But, even in these cases, most of the individual models indicate changes that are not statistically significant. There are minor differences between the CMIP3 and CMIP5 results.

Decadal results for each season are shown for CMIP3 A2 simulations (Fig. 35) and CMIP3 RCP8.5 simulations (Fig. 36). The results are similar to those for annual precipitation. Most of the model values of precipitation change are not statistically significant in all decades out to 2091–2099 and almost all are within the 10th to 90th percentile range of the historical annual precipitation anomalies. The multi-model mean precipitation changes are not statistically significant for any decade in fall and winter for both A2 and RCP8.5. For summer, there are statistically significant decreases from the 2041–2050 decade onward for A2, and in the 2071–2080 decade for RCP8.5. For spring, there are statistically significant decreases in the late 21st century for both A2 and RCP8.5. There are minor differences between the CMIP3 and CMIP5 results.

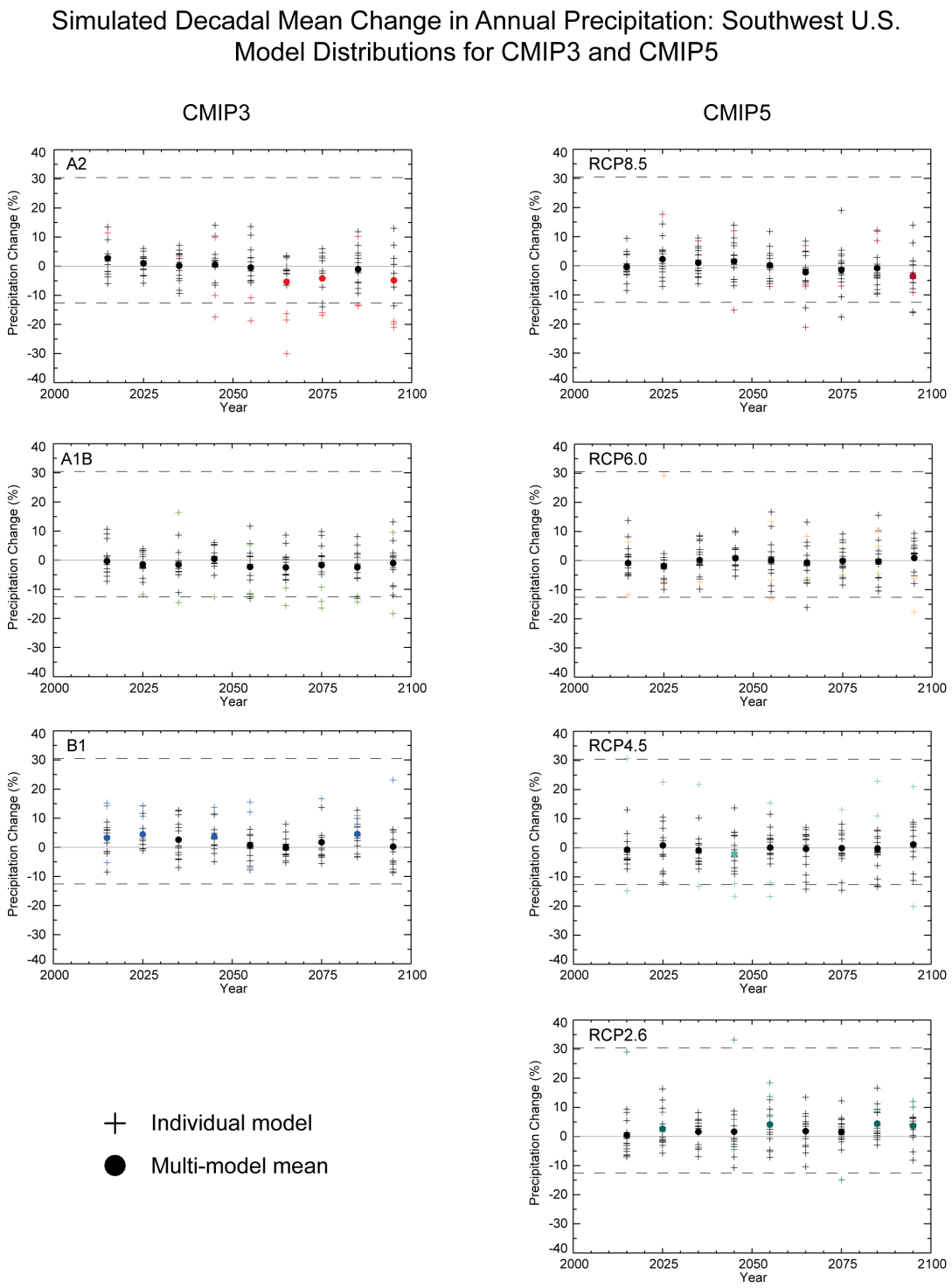

Figure 34. *Model distributions of simulated decadal mean change in annual precipitation (%) for the Southwest United States, for each future decadal time period (represented by their approximate midpoints, e.g., 2015 = 2011–2020), with respect to the reference period of 2001–2010. The upper panel shows values for the CMIP3 SRES B1 (blue), A1B (green), and A2 (red) scenarios. The lower panel shows values for the CMIP5 RCP2.6 (light teal), 4.5 (dark teal), 6.0 (yellow), and 8.5 (dark red) scenarios. Each individual model is represented by a plus sign (+), with circles depicting the multi-model means. These symbols are shown in color if the value is statistically significant at the 95% confidence level. Dashed lines indicate the 10th and 90th percentiles of observed precipitation anomaly values from 1981–2010.*

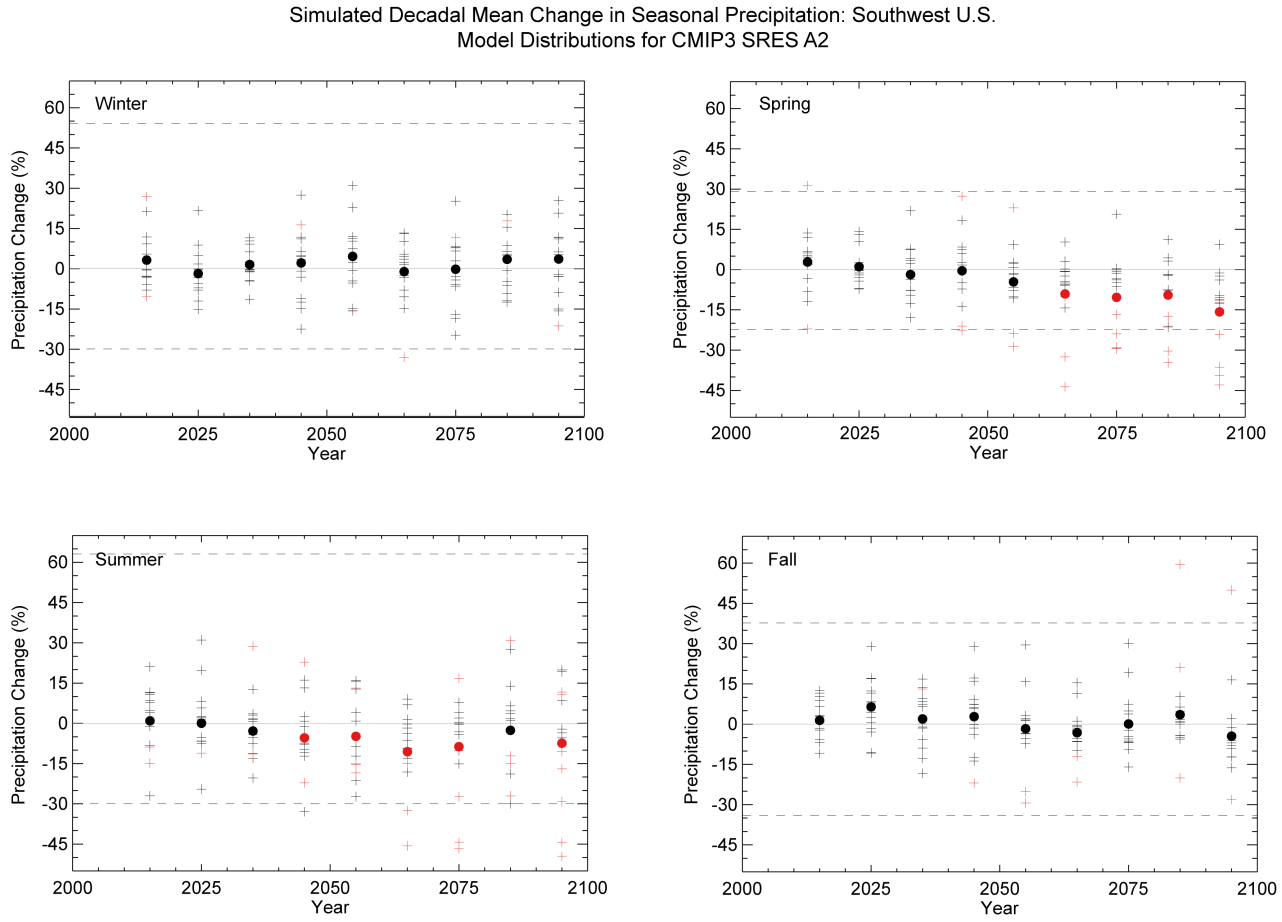

Figure 35. *Model distributions of simulated decadal mean change in seasonal precipitation (%) for the Southwest United States, for each future decadal time period (represented by their approximate midpoints, e.g., 2015 = 2011–2020), with respect to the reference period of 2001–2010. Values are given for each of the CMIP3 SRES A2 emissions scenario. Each individual model is represented by a plus sign (+), with circles depicting the multi-model means. These symbols are shown in color if the value is statistically significant at the 95% confidence level. Dashed lines indicate the 10th and 90th percentiles of observed precipitation anomaly values from 1981–2010.*

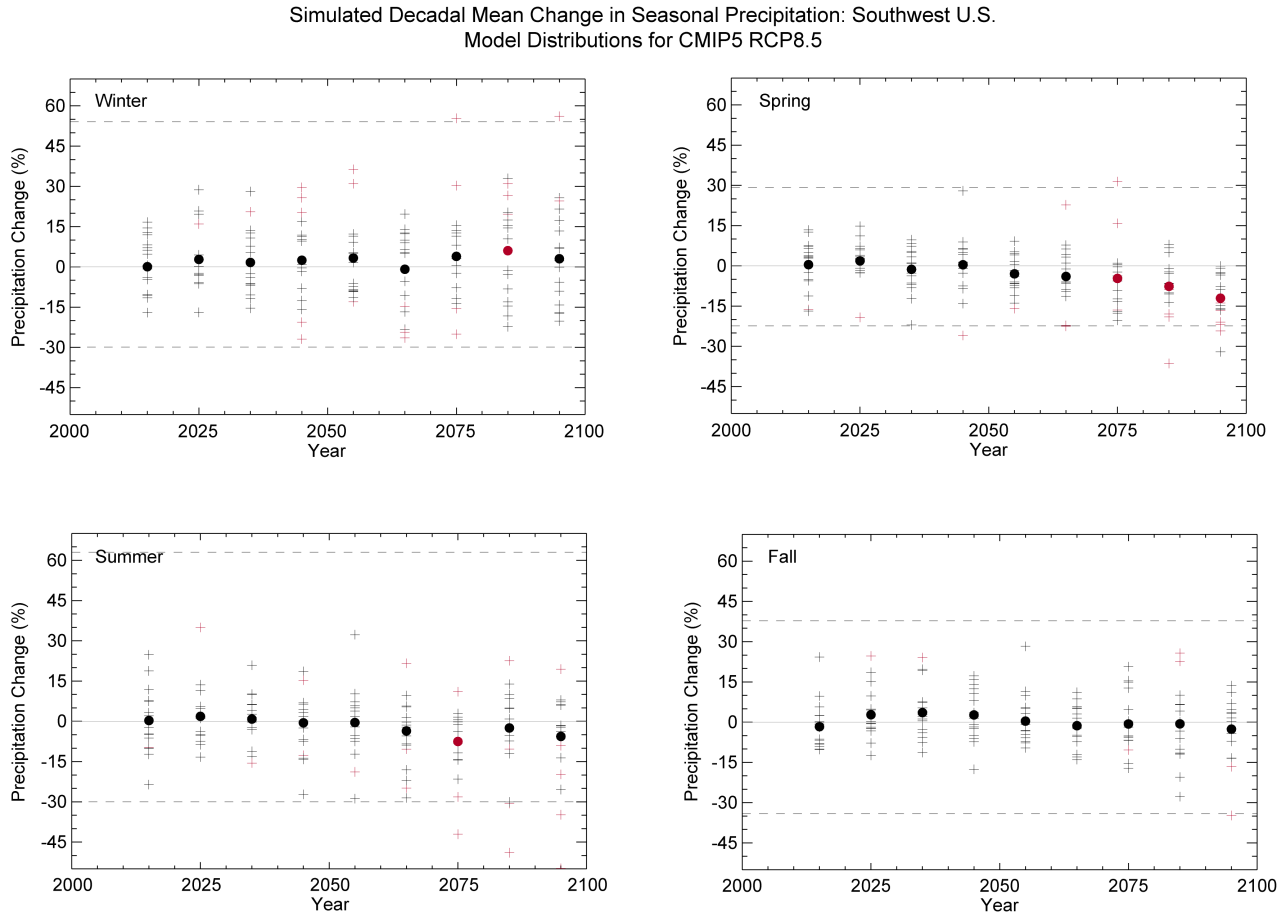

Figure 36. *Model distributions of simulated decadal mean change in seasonal precipitation (%) for the Southwest United States, for each future decadal time period (represented by their approximate midpoints, e.g., 2015 = 2011–2020), with respect to the reference period of 2001–2010. Values are given for each of the CMIP5 RCP scenario. Each individual model is represented by a plus sign (+), with circles depicting the multi-model means. These symbols are shown in color if the value is statistically significant at the 95% confidence level. Dashed lines indicate the 10th and 90th percentiles of observed precipitation anomaly values from 1981–2010.*

5.2.2. Extreme Precipitation

The simulated change in the annual maximum 1-day precipitation totals for 2046–2065 for RCP8.5 (Fig. 37a) indicates increases of 5% to 15% in most parts of the contiguous U.S., with slightly smaller increases in south Texas and slightly larger increases in parts of the intermountain west and northeast. Most models do not indicate these changes to be statistically significant across the majority of the country, i.e., these grid points satisfy category 1 (see Section 3). For Alaska (Fig. 37b), however, the models agree that the amount of 1-day precipitation will increase (all grid points satisfy category 3), with increases ranging from 10% to greater than 15%. Hawai‘i also sees increases in the annual maximum 1-day precipitation, but these changes are less than 10% and not statistically significant for most models (category 1). The dependence of regional changes on emissions scenarios (Fig. 38) is relatively small. For CMIP3 (Fig. 38, top panel), the increases are slightly greater for the A1B and A2 scenarios than for the B1 scenario. However the differences among the scenarios are small compared to the interquartile range of approximately 5% or more. For CMIP5 (Fig. 38, bottom panel), the range of changes among the four RCPs is slightly higher than for the three CMIP3 scenarios. In most regions, the RCP6.0 and RCP8.5 increases are larger than the RCP2.6 and RCP4.5 results. The differences between the CMIP3 and CMIP5 results are not substantive when considering the differences in forcing.

The simulated change in the annual maximum 5-day precipitation total for 2046–2065 for RCP8.5 (Fig. 39a) indicates increases of 5% to 15% in most parts of the contiguous United States, with slightly smaller increases in the western Gulf Coast. In most areas, the changes are not indicated to be statistically significant for the majority of models (grid points satisfy category 1). For Alaska and Hawai‘i (Fig. 39b), spatial patterns are similar to that for the annual maximum 1-day precipitation. The models are in agreement that 5-day precipitation amounts will increase across the majority of the state (category 3), and again reach values of greater than +15%. For Hawai‘i, the increases are once again small (being mostly in the 0%–5% range), with grid points satisfying category 1. The dependence of regional changes on emissions scenarios (Fig. 40) is relatively small. For CMIP3 (Fig. 40, top panel), the increases are slightly greater for the A1B and A2 scenarios than for the B1 scenario. However the differences among the scenarios are small compared to the interquartile range of approximately 5% or more. For CMIP5 (Fig. 40, bottom panel), the range of changes among the four RCPs is slightly higher than for the three CMIP3 scenarios. In most regions, the RCP8.5 increases are larger than for the other RCP scenarios. The differences between the CMIP3 and CMIP5 results are not substantive when considering the differences in forcing. These results are roughly similar to those for maximum 1-day precipitation (Figs. 37 and 38).

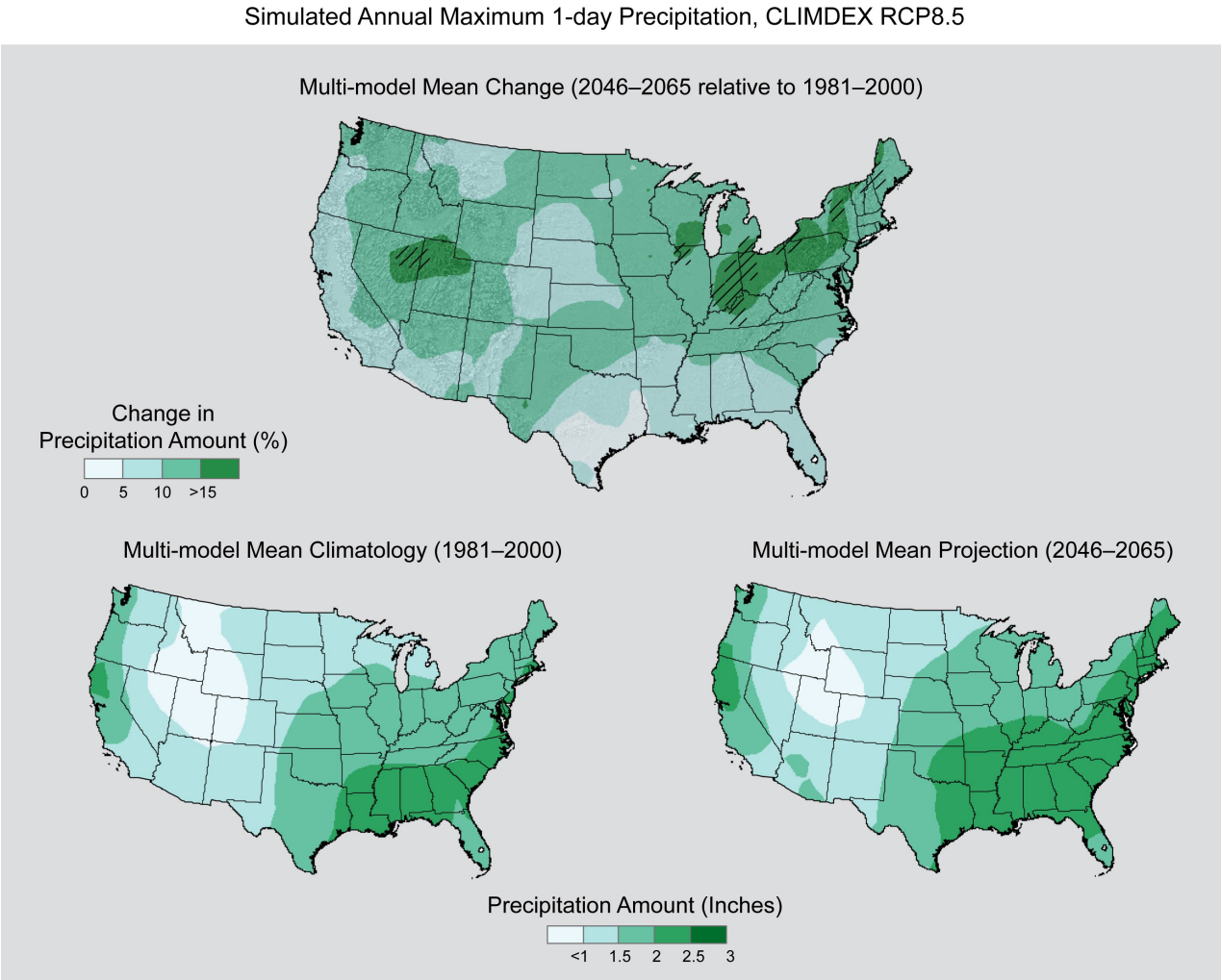

Figure 37a. *Simulated multi-model mean change in annual maximum 1-day precipitation (Rx1day) for the contiguous United States, for 2046–2065 with respect to the reference period of 1981–2000, using the CLIMDEX RCP8.5 scenario (top). Color only (category 1) indicates that less than 50% of the models show a statistically significant change. Color with hatching (category 3) indicates that more than 50% of the models show a statistically significant change, and more than 67% agree on the sign of the change (see Section 3). Multi-model mean climatology indicating the Rx1day for 1981–2000 (bottom left). Multi-model mean projection indicating the Rx1day for 2046–2065 (bottom right).*

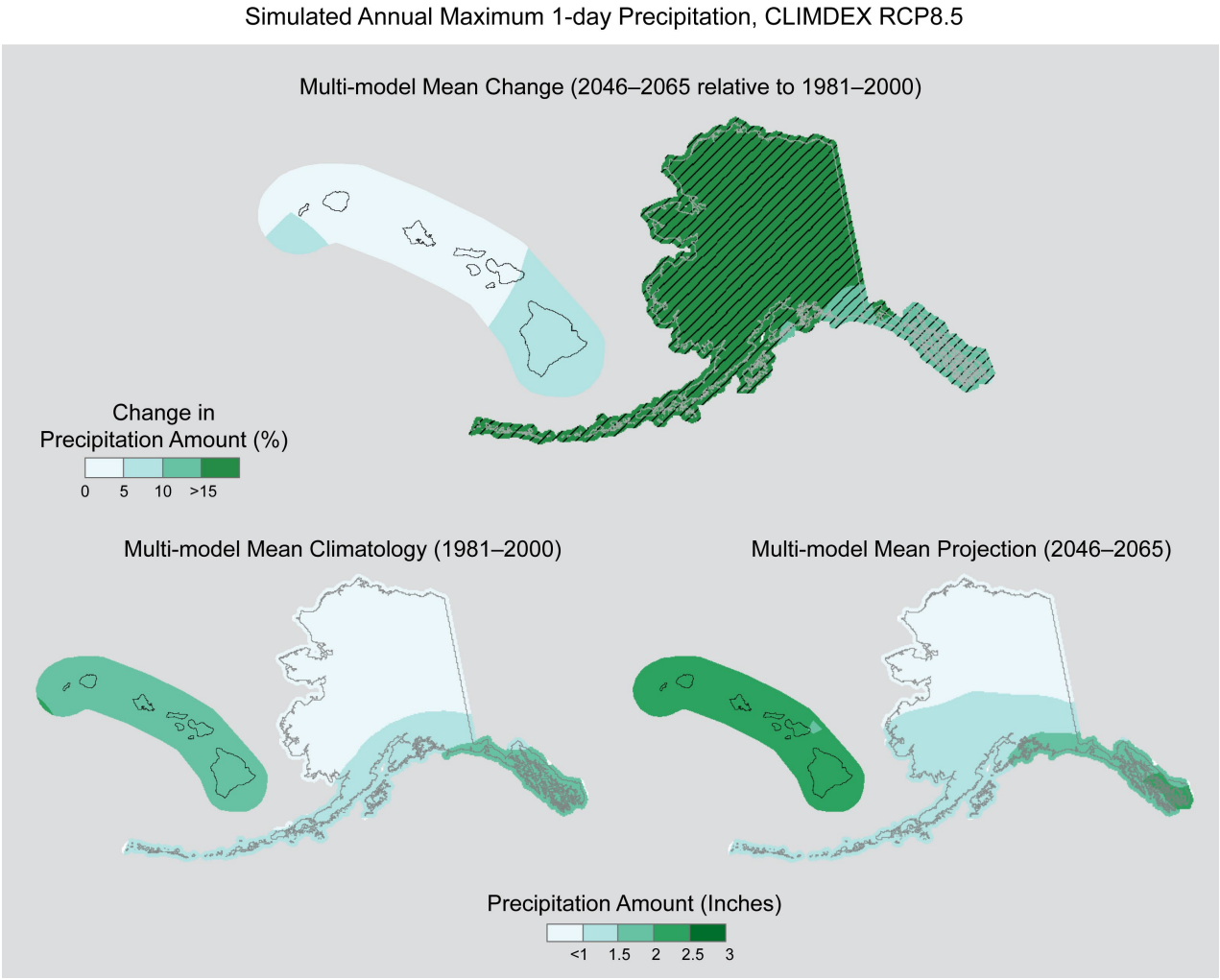

Figure 37b. *Simulated multi-model mean change in annual maximum 1-day precipitation (Rx1day) for Alaska and Hawai'i, for 2046–2065 with respect to the reference period of 1981–2000, using the CLIMDEX RCP8.5 scenario (top). Color only (category 1) indicates that less than 50% of the models show a statistically significant change. Color with hatching (category 3) indicates that more than 50% of the models show a statistically significant change, and more than 67% agree on the sign of the change (see Section 3). Multi-model mean climatology indicating the Rx1day for 1981–2000 (bottom left). Multi-model mean projection indicating the Rx1day for 2046–2065 (bottom right).*

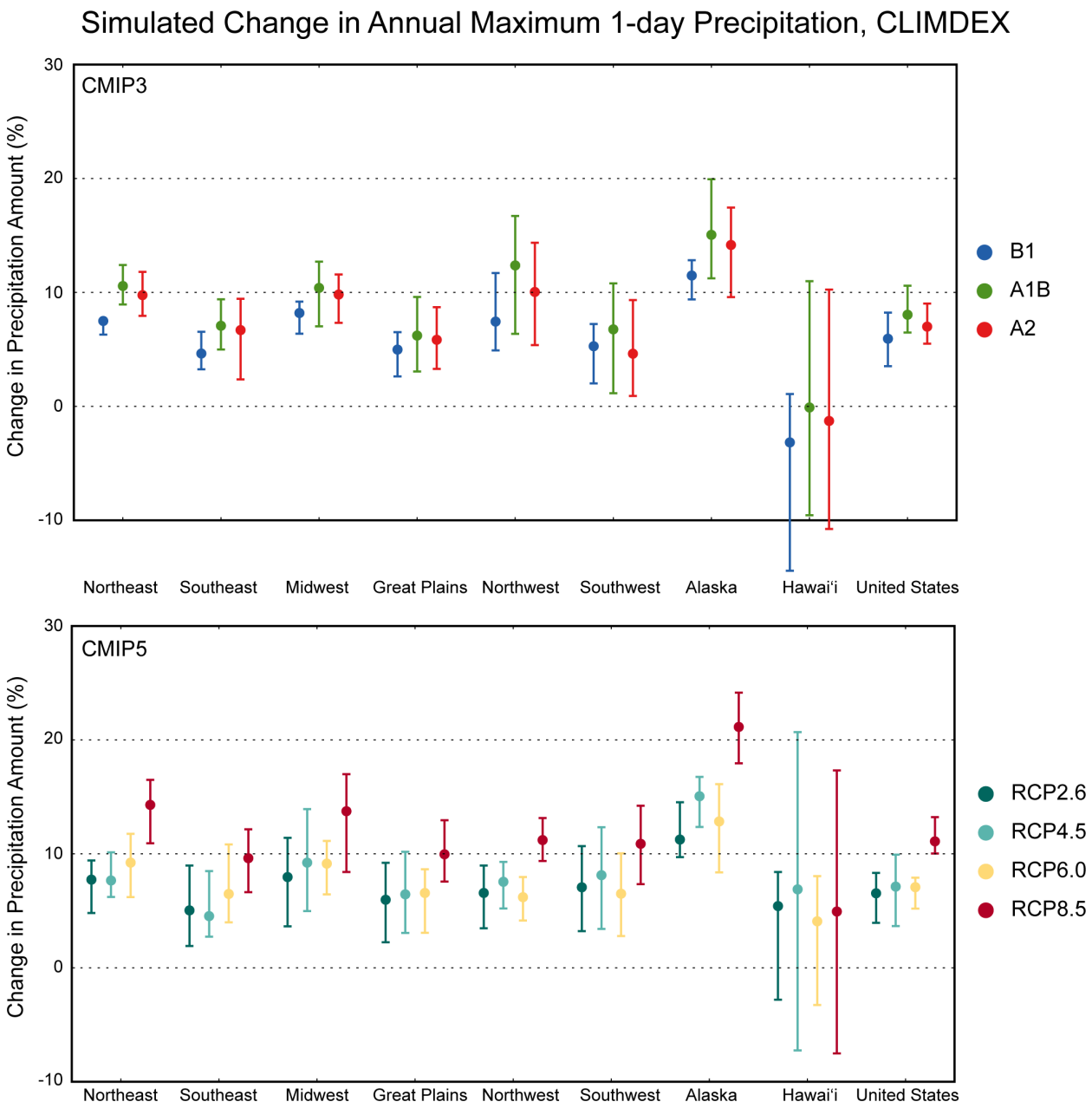

Figure 38. *Simulated change in annual maximum 1-day precipitation (Rx1day) for each region and the contiguous United States, for 2046–2065 with respect to the reference period of 1981–2000. The upper panel shows values for the CLIMDEX SRES B1 (blue), A1B (green), and A2 (red) scenarios. The lower panel shows values for the CLIMDEX RCP2.6 (dark teal), 4.5 (light teal), 6.0 (yellow), and 8.5 (dark red) scenarios. Bars indicate the interquartile ranges of model values and circles depict the multi-model means.*

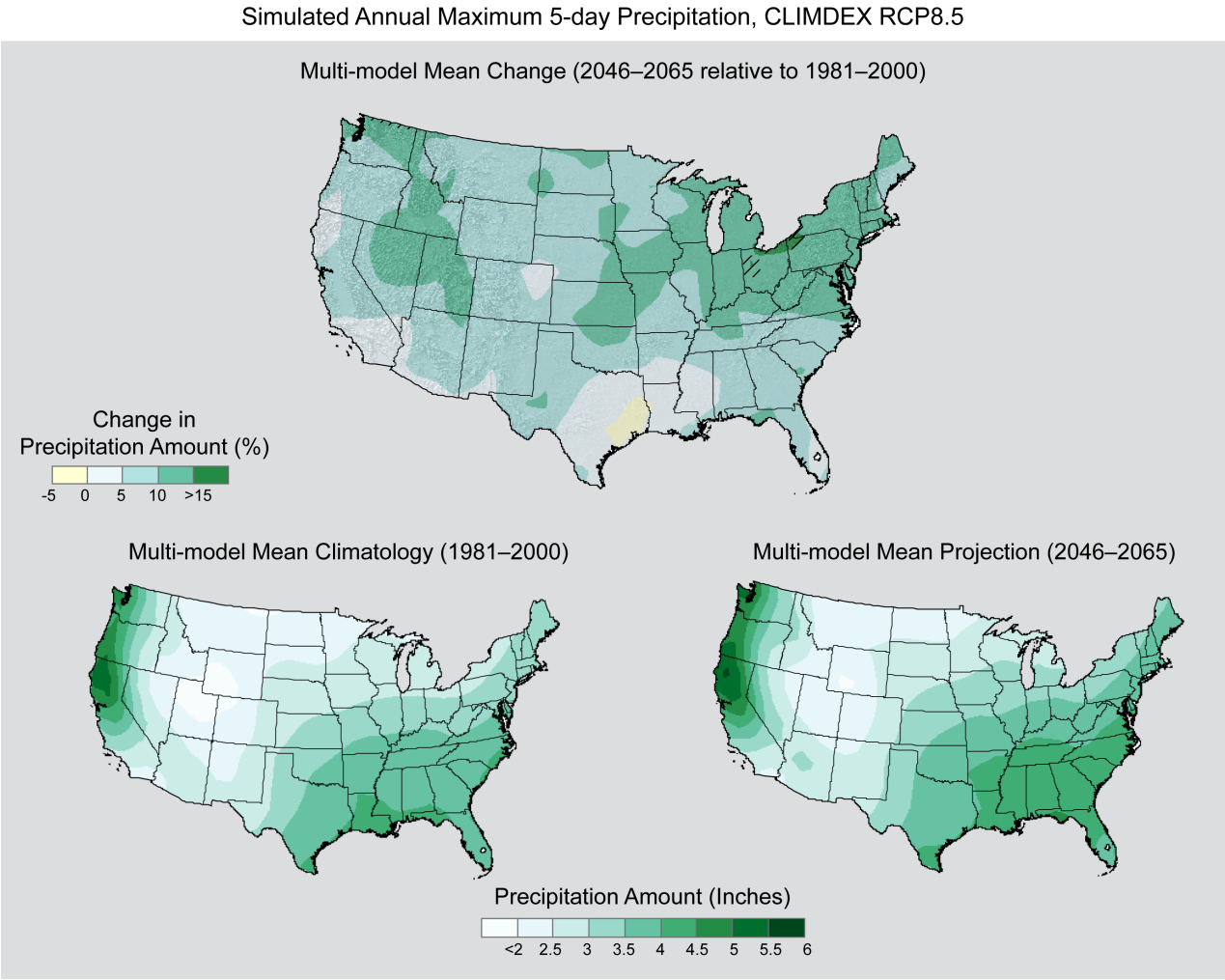

Figure 39a. *Simulated multi-model mean change in annual maximum 5-day precipitation (Rx5day) for the contiguous United States, for 2046–2065 with respect to the reference period of 1971–2000, using the CLIMDEX RCP8.5 scenario (top). Color only (category 1) indicates that less than 50% of the models show a statistically significant change. Color with hatching (category 3) indicates that more than 50% of the models show a statistically significant change, and more than 67% agree on the sign of the change (see Section 3). Multi-model mean climatology indicating the Rx5day for 1981–2000 (bottom left). Multi-model mean projection indicating the Rx5day for 2046–2065 (bottom right).*

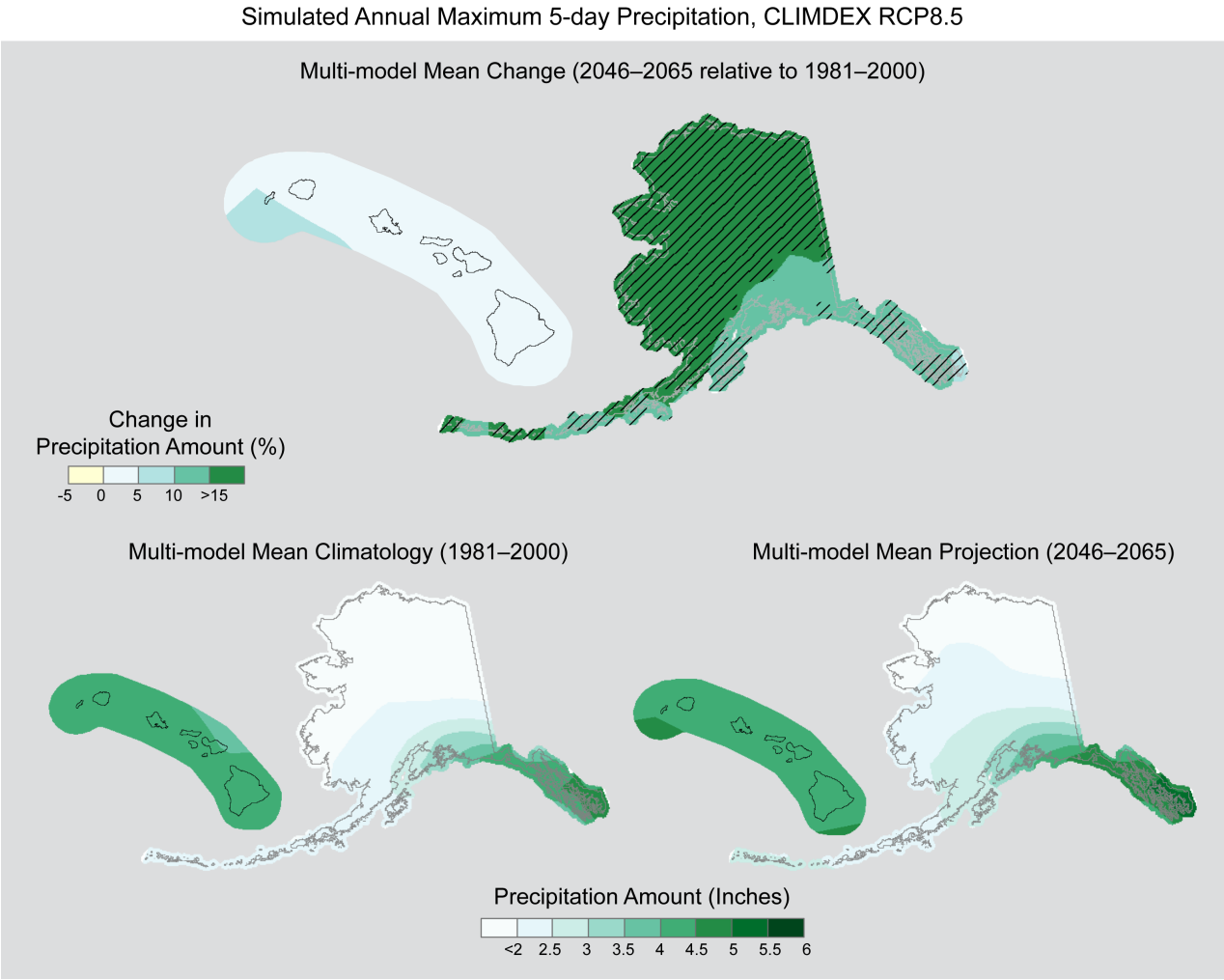

Figure 39b. *Simulated multi-model mean change in annual maximum 5-day precipitation (Rx5day) for Alaska and Hawai'i, for 2046–2065 with respect to the reference period of 1971–2000, using the CLIMDEX RCP8.5 scenario (top). Color only (category 1) indicates that less than 50% of the models show a statistically significant change. Color with hatching (category 3) indicates that more than 50% of the models show a statistically significant change, and more than 67% agree on the sign of the change (see Section 3). Multi-model mean climatology indicating the Rx5day for 1981–2000 (bottom left). Multi-model mean projection indicating the Rx5day for 2046–2065 (bottom right).*

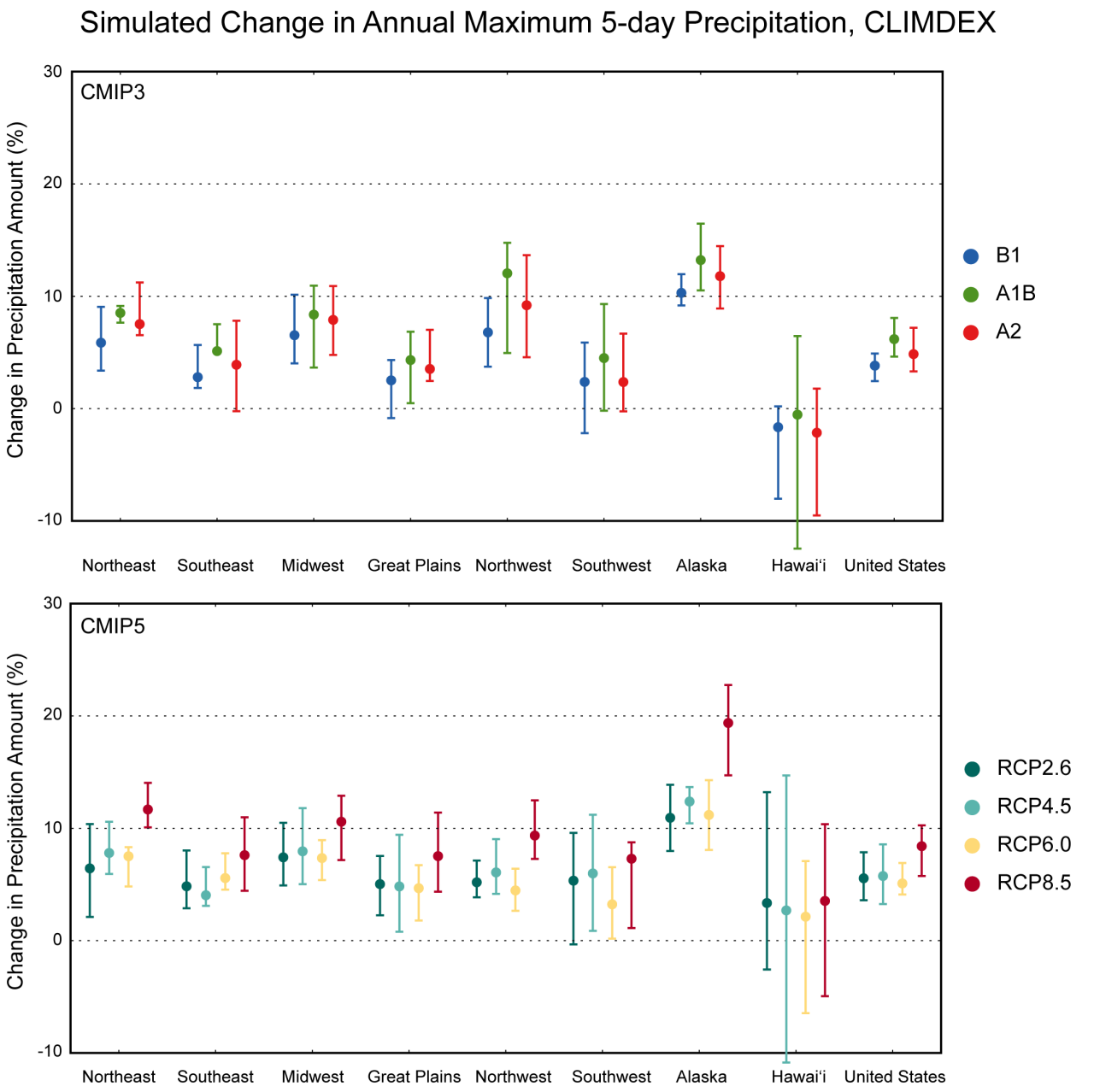

Figure 40. *Simulated change in annual maximum 5-day precipitation (Rx5day) for each region and the contiguous United States, for 2046–2065 with respect to the reference period of 1981–2000. The upper panel shows values for the CLIMDEX SRES B1 (blue), A1B (green), and A2 (red) scenarios. The lower panel shows values for the CLIMDEX RCP2.6 (dark teal), 4.5 (light teal), 6.0 (yellow), and 8.5 (dark red) scenarios. Bars indicate the interquartile ranges of model values and circles depict the multi-model means.*

Simulations for 2046–2065 for RCP8.5 indicate little change in the annual longest duration of consecutive dry days in most parts of the contiguous United States, with increases of 2 to 10 days in the extreme south and west (Fig. 41a). Alaska sees mainly decreases in the longest dry spell, whereas increases of up to 6 days are seen for Hawai‘i (Fig. 41b). However, these changes are not statistically significant for most models (all grid points satisfy category 1). The dependence of regional changes on emissions scenarios (Fig. 42) is relatively small in most regions, the exceptions being the Northwest and Southwest. For CMIP3 (Fig. 42, top panel), the increases in the Northwest and Southwest are approximately twice as large, or about 3 to 4 days, for the A1B and A2 scenarios than for the B1 scenario. However, even in these regions the differences among the scenarios are small compared to the interquartile range of approximately 5 to 10 days. There are multi-model mean decreases for Alaska, the only region with decreases (or shorter dry spells in the future). However, the decreases are small (about two days). For CMIP5 (Fig. 42, bottom panel), the range of changes among the four RCPs is similar to that for the three CMIP3 scenarios. The differences between the CMIP3 and CMIP5 results are not substantive, except for the Southwest where the CMIP5 increases are smaller than the CMIP3 increases.

Simulations for 2046–2065 for RCP8.5 indicate little change in all parts of the contiguous U.S. in the annual longest duration of consecutive wet days, with changes of less than one day almost everywhere (Fig. 43a). Most models indicate that these changes are not statistically significant anywhere (category 1). Values for Alaska (Fig. 43b) range from decreases of 1 day in south-central parts of the state to increases of greater than 1 day in northern and western coastal areas. Statistically significant increases are indicated (category 3) for the northernmost reaches of the state. Hawai‘i also sees increases in the length of the longest wet spell, however, these changes are small (between 0 and 1 day), and again satisfy category 1. The dependence of regional changes on scenario (Fig. 44) is very small in all regions. For CMIP3 (Fig. 44, top panel), the multi-model mean changes are mostly less than one day and much smaller than the interquartile range of 2 to 4 days. For CMIP5 (Fig. 44, bottom panel), the range of changes among the four RCPs is very small. The interquartile range for the CMIP5 scenarios is mostly 1 to 2 days. The differences between the CMIP3 and CMIP5 results are not substantive, except that the interquartile range for the CMIP5 results is considerably smaller (about half) than for the CMIP3 results.

The CLIMDEX R99pTOT index is the total annual precipitation falling on days with daily precipitation above the 99th percentile of daily precipitation amounts. As with the WSDI and the CSDI, the 99th percentile threshold for the present climate is applied to the future climate simulations as well. The simulated change in the R99pTOT for 2046–2065 for RCP8.5 (Fig. 45a) indicates increases of 20% to more than 50% over most parts of the contiguous United States. Small increases of less than 20% are indicated for areas along the Gulf Coast. The changes are not statistically significant in most areas, the exceptions being much of the Northeast and parts of the intermountain west and Northwest. Alaska sees the greatest changes (Fig. 45b), with statistically significant increases of more than 90% across the majority of the state. Increases for Hawai‘i are smaller and not statistically significant, ranging from 0% to 20%. The dependence of regional changes on scenario (Fig. 46) generally indicates somewhat greater increases for A1B and A2 compared to B1, but these scenario differences are smaller than the interquartile range of results. For CMIP3 (Fig. 46, top panel), the multi-model mean changes are largest for the Northwest and Alaska and smallest (near zero) for Hawai‘i. For CMIP5 (Fig. 46, bottom panel), the increases are generally the largest for RCP8.5. The interquartile range for the CMIP5 scenarios is 20% to more than 40%. The differences between the CMIP3 and CMIP5 results are not substantive.

Simulated Annual Longest Dry Spell, CLIMDEX RCP8.5

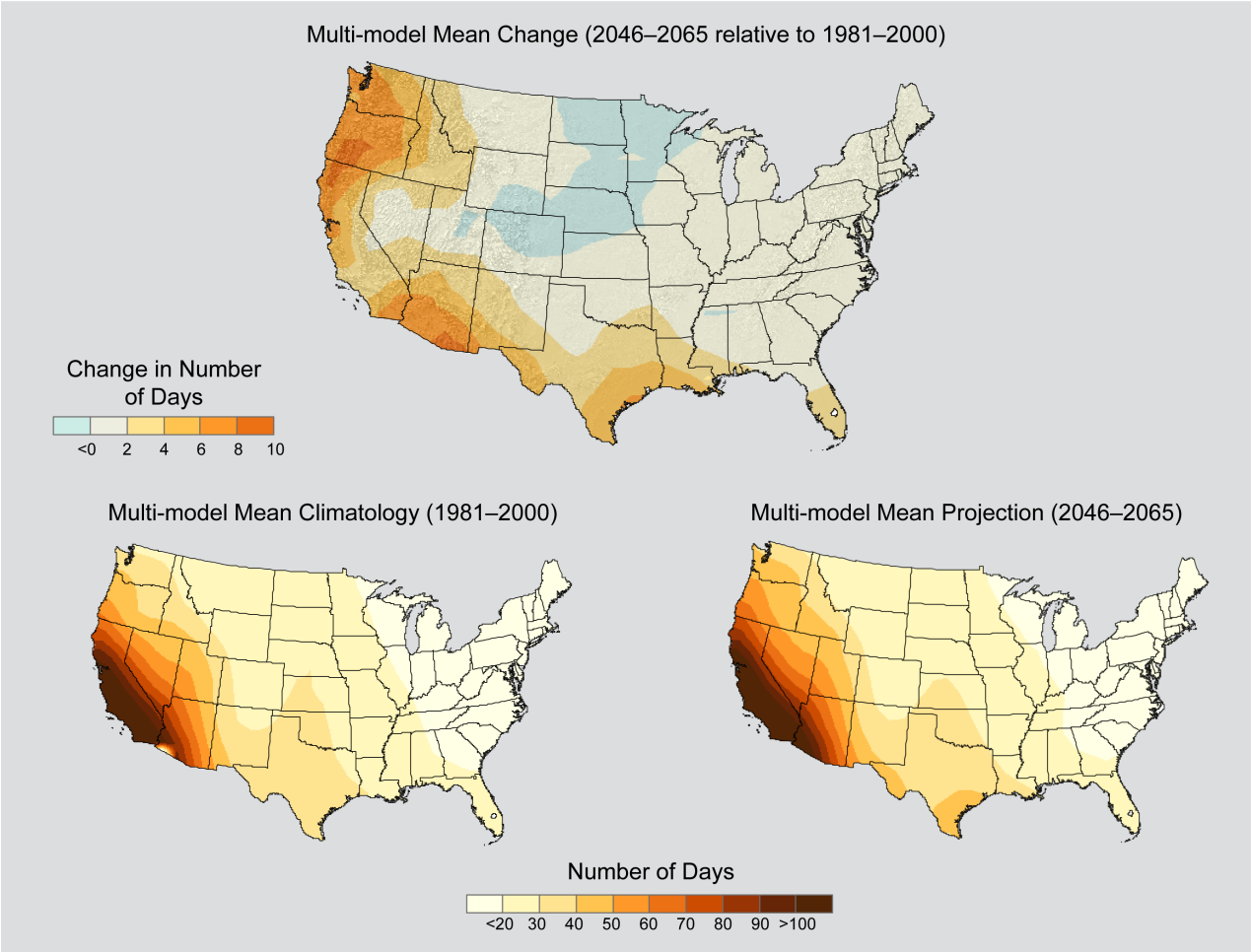

Figure 41a. *Simulated multi-model mean change in the annual maximum number of consecutive dry days (CDD) for the contiguous United States, for 2046–2065 with respect to the reference period of 1981–2000, using the CLIMDEX RCP8.5 scenario (top). Color only (category 1) indicates that less than 50% of the models show a statistically significant change (see Section 3). Multi-model mean climatology indicating the annual number of CDD for 1981–2000 (bottom left). Multi-model mean projection indicating the annual number of CDD for 2046–2065 (bottom right).*

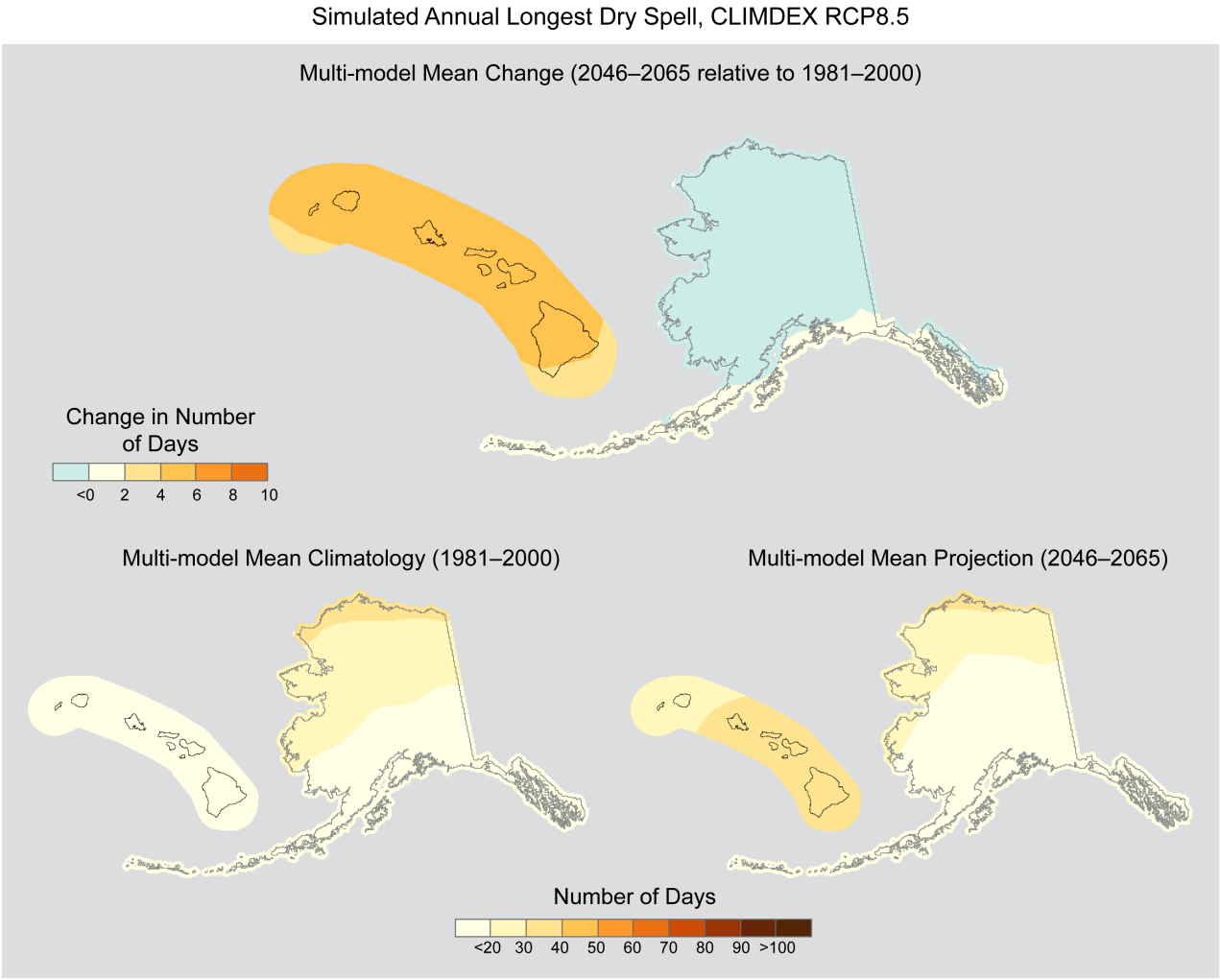

Figure 41b. *Simulated multi-model mean change in the annual maximum number of consecutive dry days (CDD) for Alaska and Hawai'i, for 2046–2065 with respect to the reference period of 1981–2000, using the CLIMDEX RCP8.5 scenario (top). Color only (category 1) indicates that less than 50% of the models show a statistically significant change (see Section 3). Multi-model mean climatology indicating the annual number of CDD for 1981–2000 (bottom left). Multi-model mean projection indicating the annual number of CDD for 2046–2065 (bottom right).*

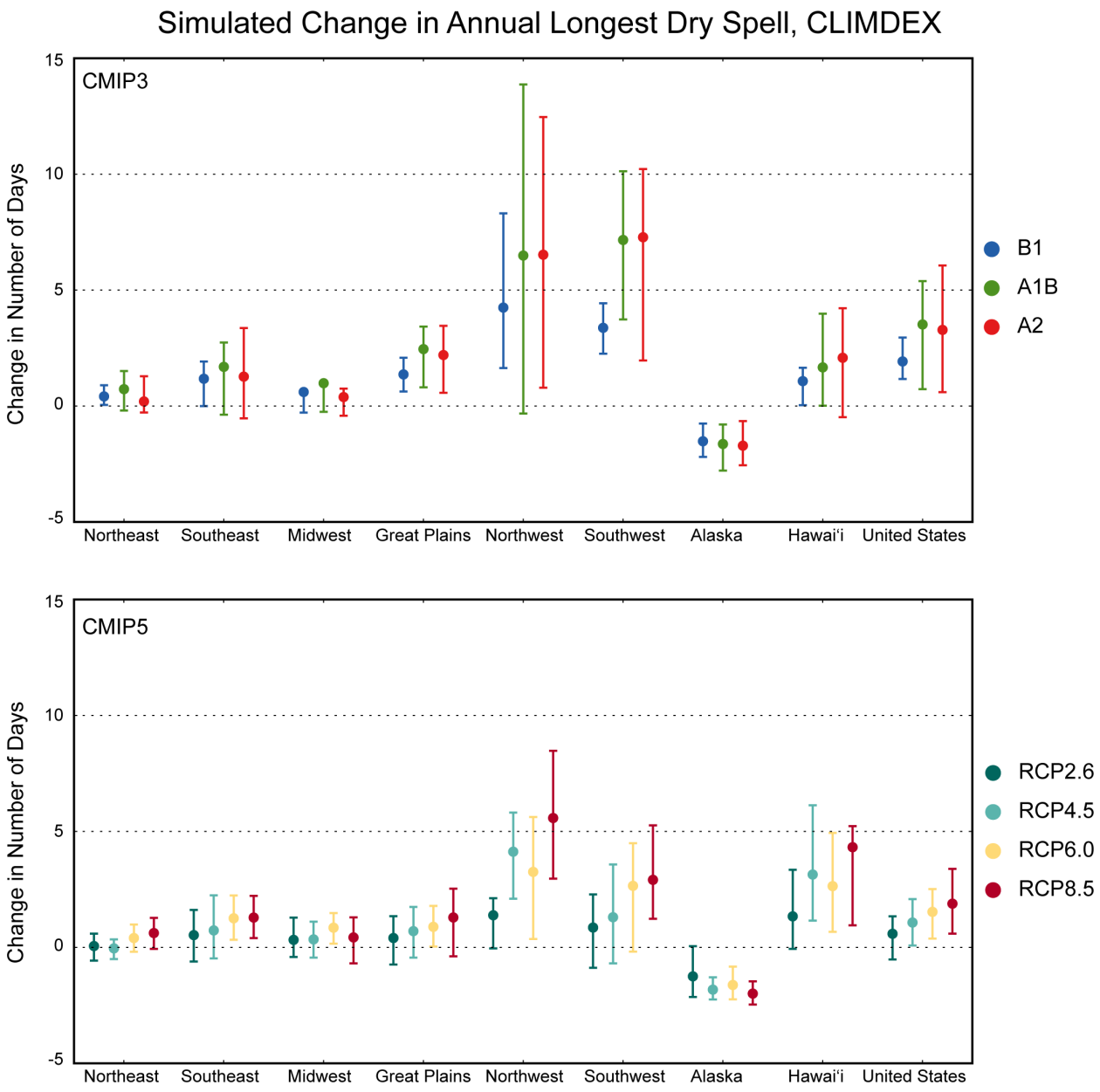

Figure 42. *Simulated change in the annual maximum number of consecutive dry days (CDD) for each region and the contiguous United States, for 2046–2065 with respect to the reference period of 1981–2000. The upper panel shows values for the CLIMDEX SRES B1 (blue), A1B (green), and A2 (red) scenarios. The lower panel shows values for the CLIMDEX RCP2.6 (dark teal), 4.5 (light teal), 6.0 (yellow), and 8.5 (dark red) scenarios. Bars indicate the interquartile ranges of model values and circles depict the multi-model means.*

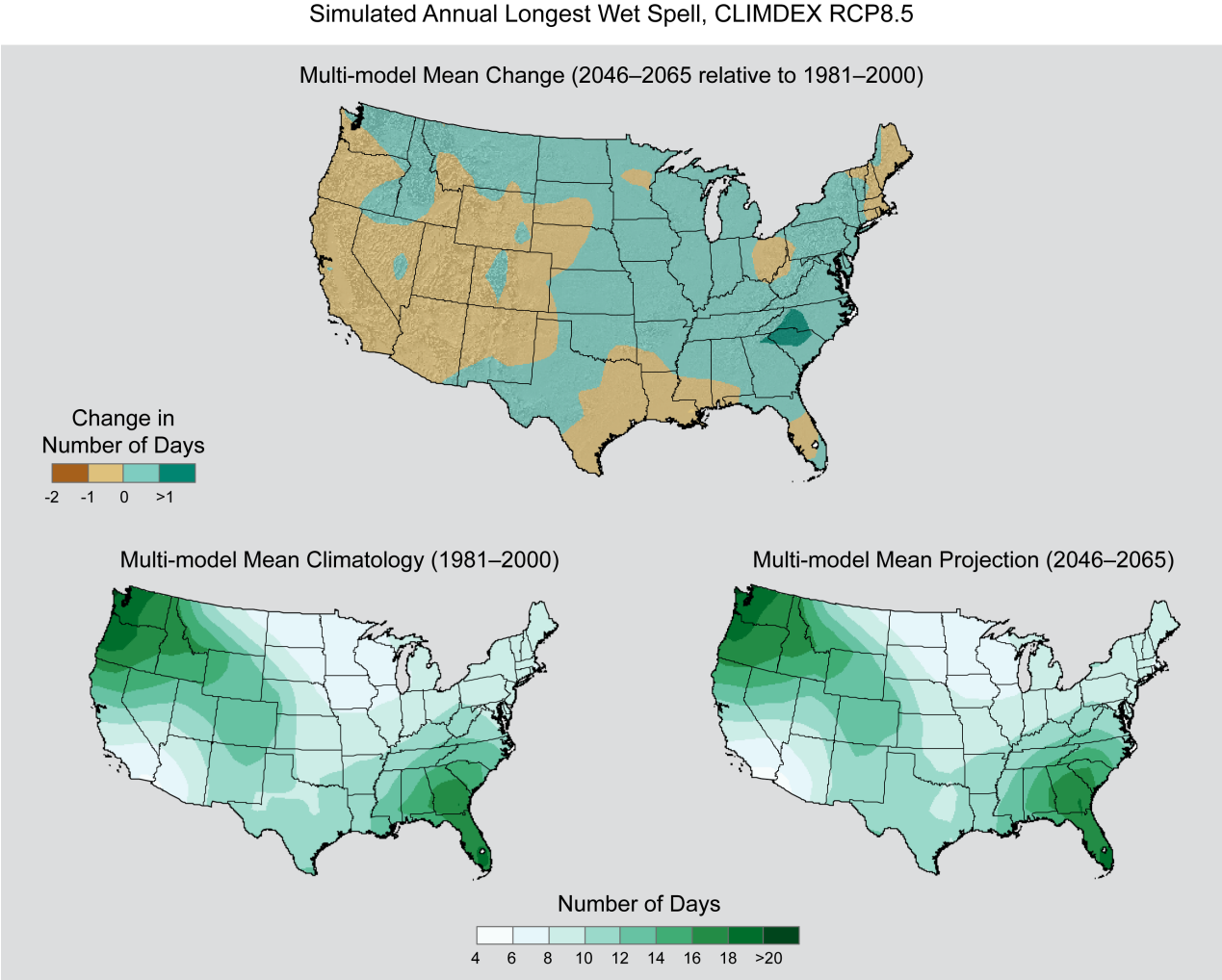

Figure 43a. *Simulated multi-model mean change in the annual maximum number of consecutive wet days (CWD) for the contiguous United States, for 2046–2065 with respect to the reference period of 1981–2000, using the CLIMDEX RCP8.5 scenario (top). Color only (category 1) indicates that less than 50% of the models show a statistically significant change (see Section 3). Multi-model mean climatology indicating the annual number of CWD for 1981–2000 (bottom left). Multi-model mean projection indicating the annual number of CWD for 2046–2065 (bottom right).*

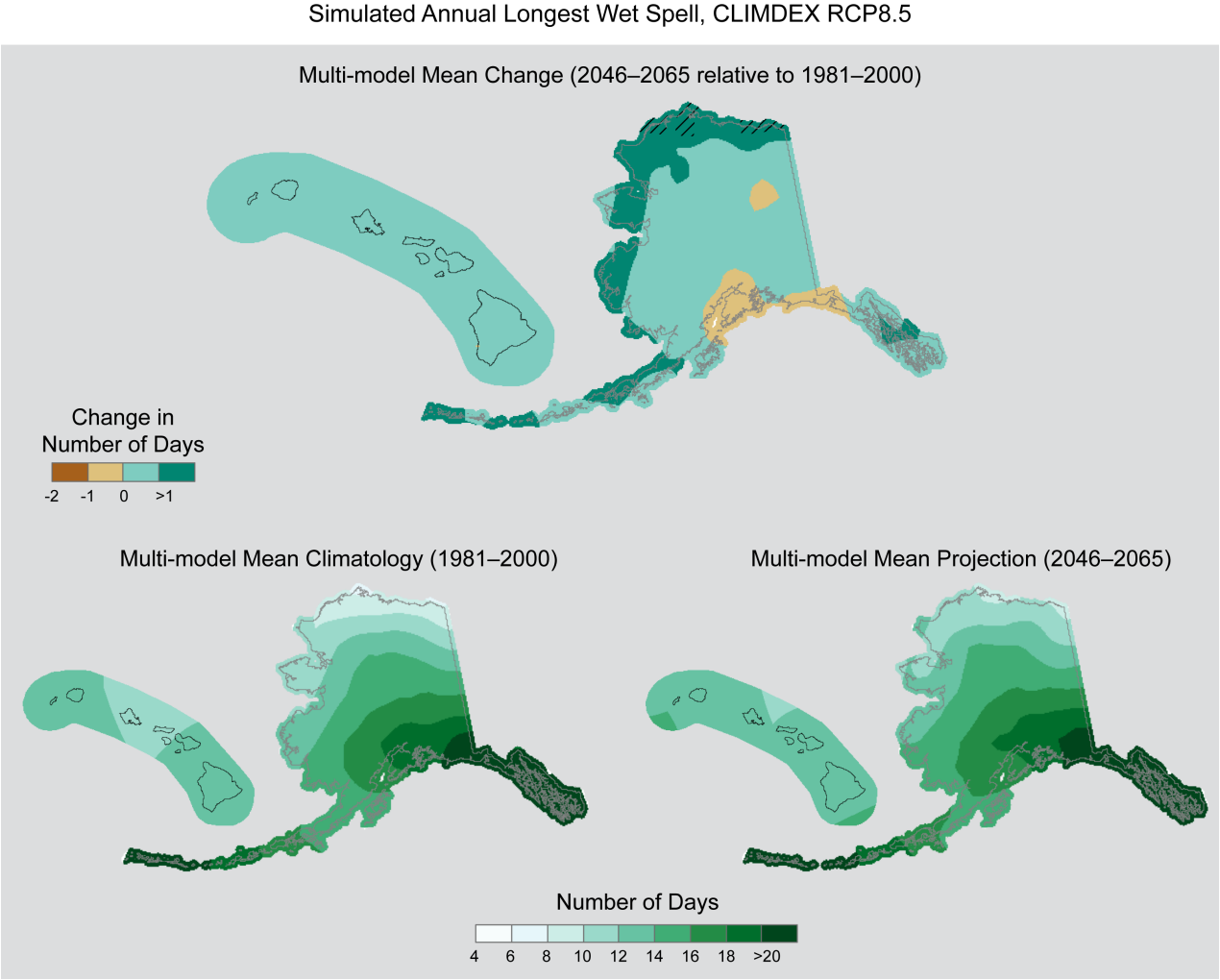

Figure 43b. *Simulated multi-model mean change in the annual maximum number of consecutive wet days (CWD) for Alaska and Hawai'i, for 2046–2065 with respect to the reference period of 1981–2000, using the CLIMDEX RCP8.5 scenario (top). Color only (category 1) indicates that less than 50% of the models show a statistically significant change (see Section 3). Multi-model mean climatology indicating the annual number of CWD for 1981–2000 (bottom left). Multi-model mean projection indicating the annual number of CWD for 2046–2065 (bottom right).*

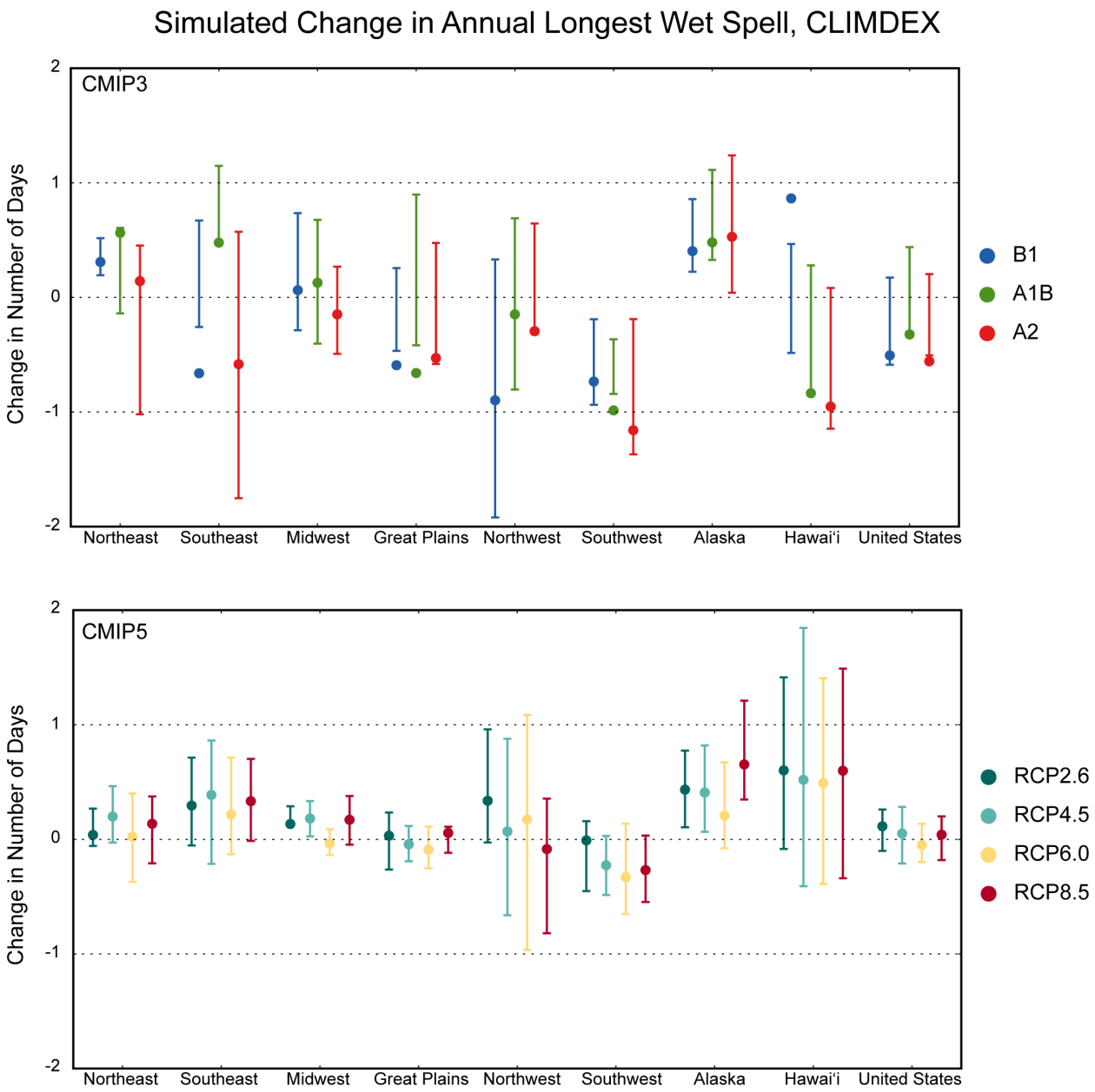

Figure 44. *Simulated change in the annual maximum number of consecutive wet days (CWD) for each region and the contiguous United States, for 2046–2065 with respect to the reference period of 1981–2000. The upper panel shows values for the CLIMDEX SRES B1 (blue), A1B (green), and A2 (red) scenarios. The lower panel shows values for the CLIMDEX RCP2.6 (dark teal), 4.5 (light teal), 6.0 (yellow), and 8.5 (dark red) scenarios. Bars indicate the interquartile ranges of model values and circles depict the multi-model means.*

Simulated Annual Total Precipitation for Days Above the 99th Percentile, CLIMDEX RCP8.5

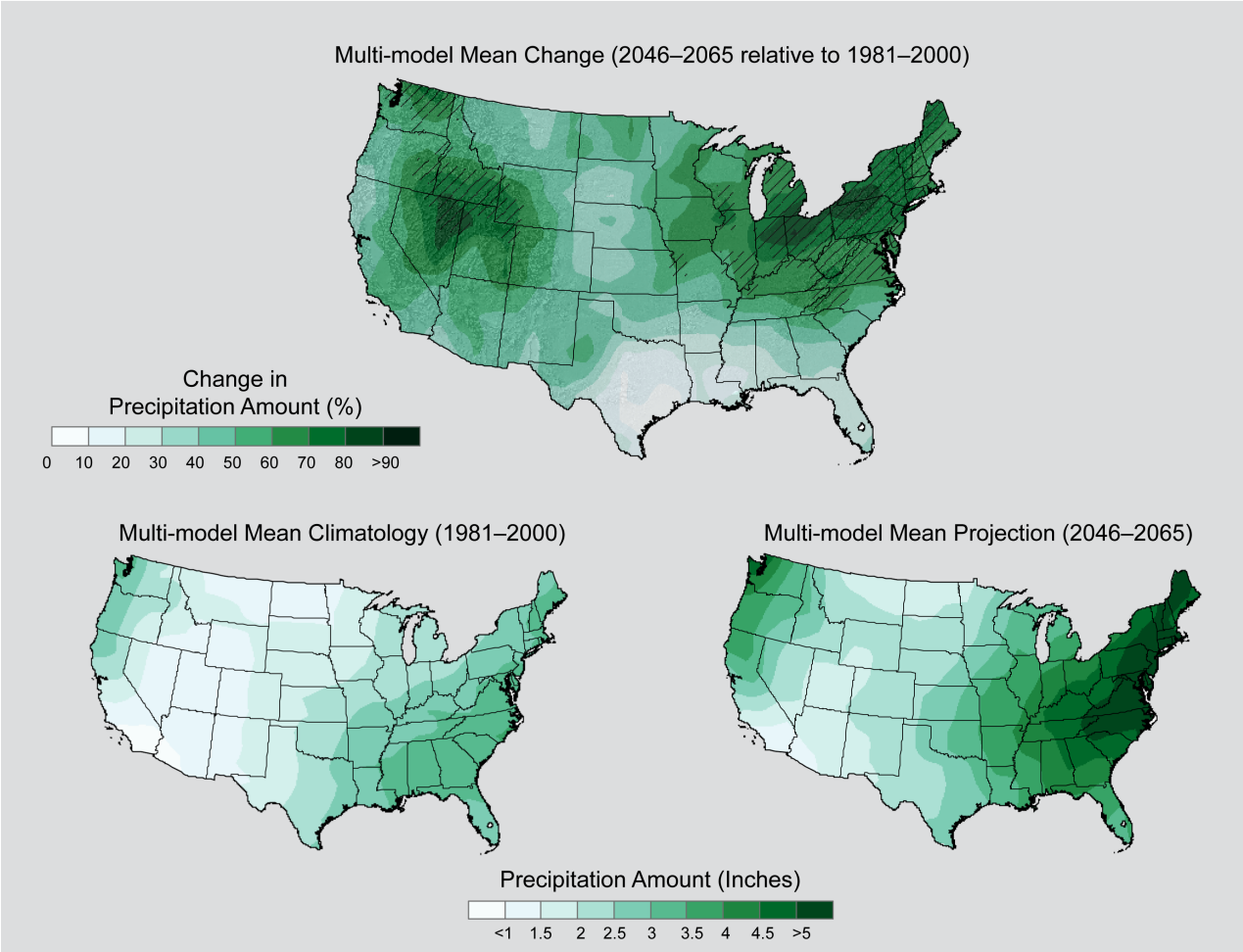

Figure 45a. *Simulated multi-model mean change in annual total precipitation for days above the 99th percentile (R99pTOT) for the contiguous United States, for 2046–2065 with respect to the reference period of 1981–2000, using the CLIMDEX RCP8.5 scenario (top). Color only (category 1) indicates that less than 50% of the models show a statistically significant change. Color with hatching (category 3) indicates that more than 50% of the models show a statistically significant change, and more than 67% agree on the sign of the change (see Section 3). Multi-model mean climatology indicating the R99pTOT for 1981–2000 (bottom left). Multi-model mean projection indicating the R99pTOT for 2046–2065 (bottom right).*

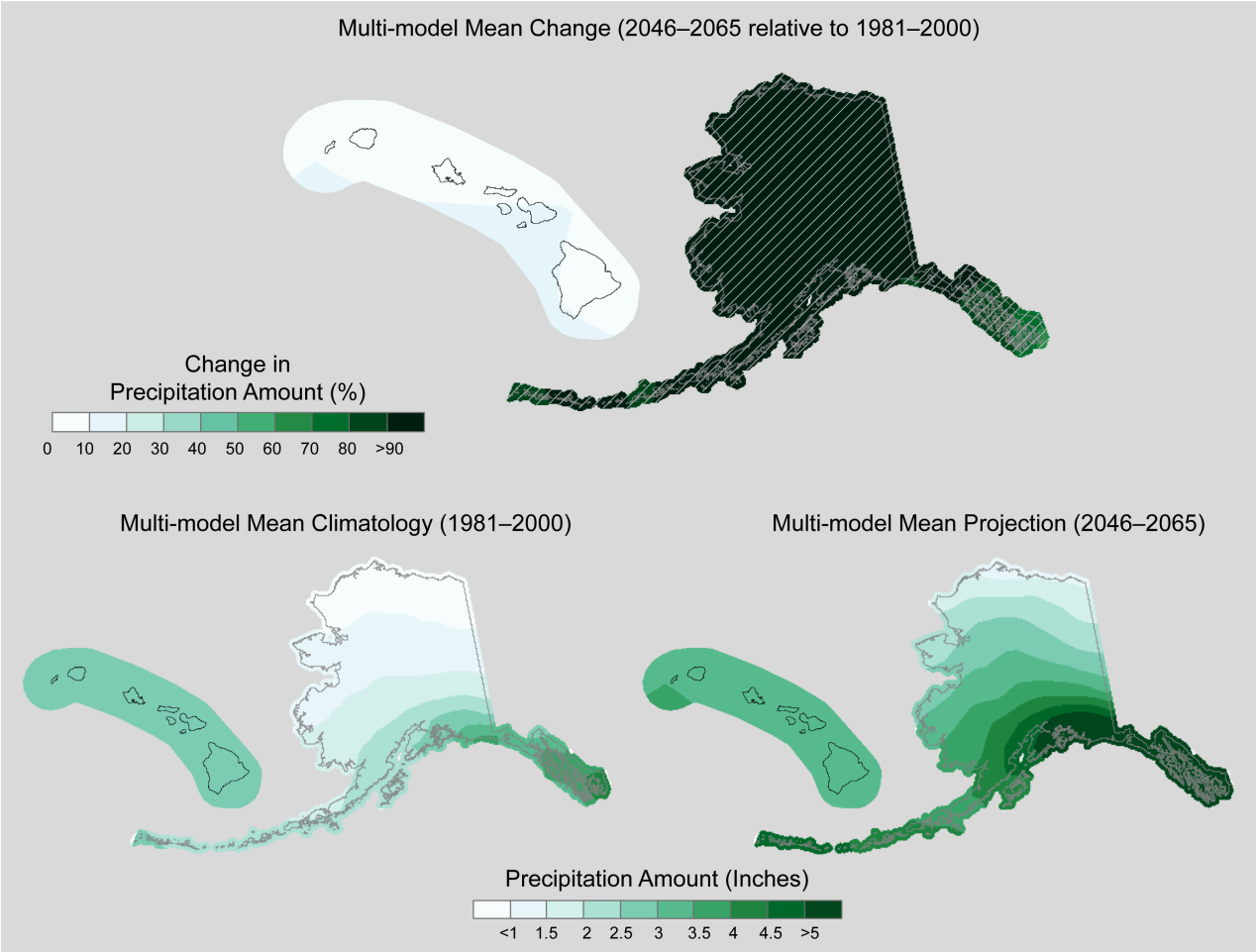

Figure 45b. *Simulated multi-model mean change in annual total precipitation for days above the 99th percentile (R99pTOT) for Alaska and Hawai'i, for 2046–2065 with respect to the reference period of 1981–2000, using the CLIMDEX RCP8.5 scenario (top). Color only (category 1) indicates that less than 50% of the models show a statistically significant change. Color with hatching (category 3) indicates that more than 50% of the models show a statistically significant change, and more than 67% agree on the sign of the change (see Section 3). Multi-model mean climatology indicating the R99pTOT for 1981–2000 (bottom left). Multi-model mean projection indicating the R99pTOT for 2046–2065 (bottom right).*

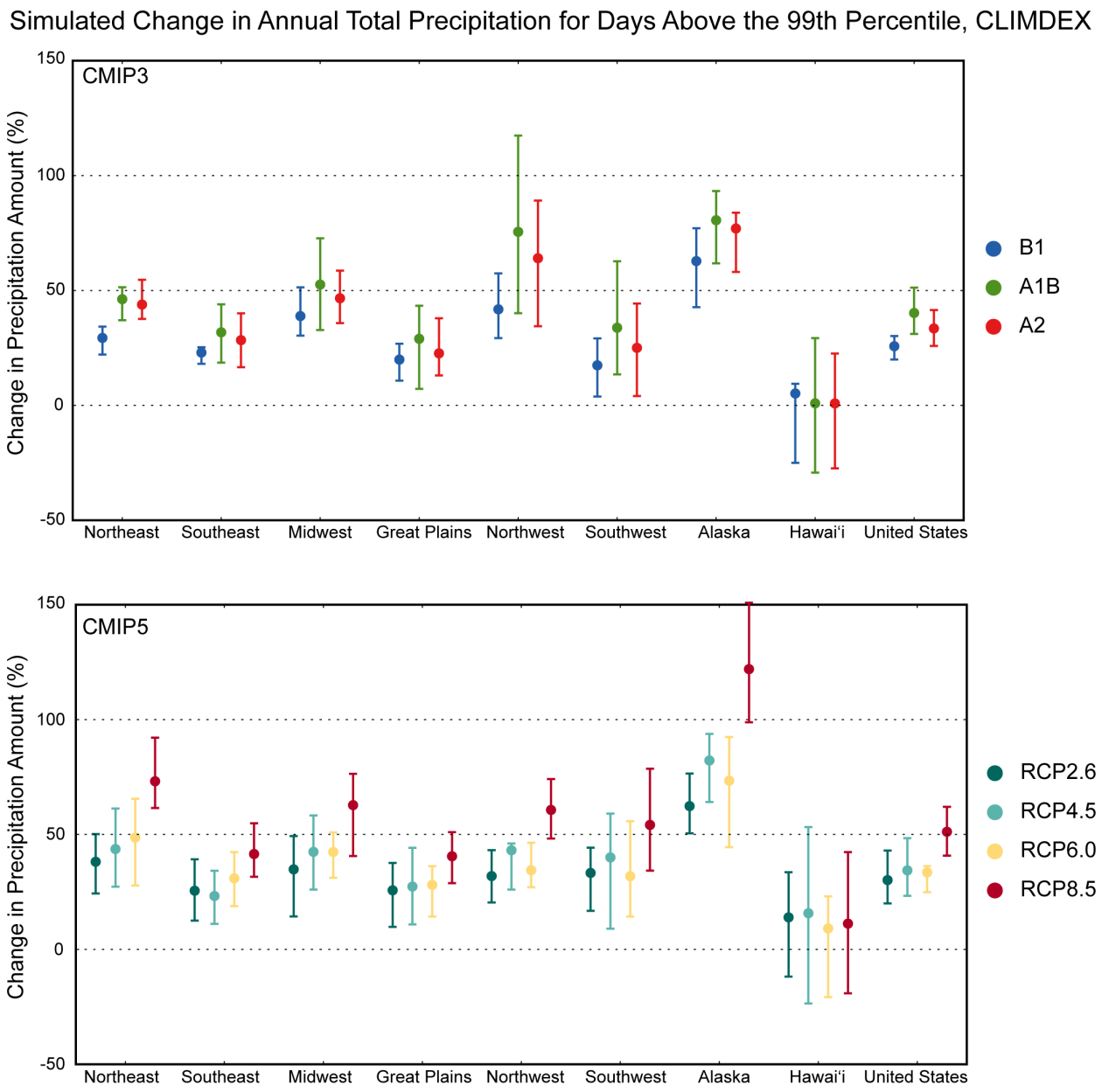

Figure 46. *Simulated change in annual total precipitation for days above the 99th percentile (R99pTOT) for each region and the contiguous United State, for 2046–2065 with respect to the reference period of 1981–2000. The upper panel shows values for the CLIMDEX SRES B1 (blue), A1B (green), and A2 (red) scenarios. The lower panel shows values for the CLIMDEX RCP2.6 (dark teal), 4.5 (light teal), 6.0 (yellow), and 8.5 (dark red) scenarios. Bars indicate the interquartile ranges of model values and circles depict the multi-model means.*

6. SUMMARY

The primary purpose of this document is to compare U.S. temperature and precipitation projections between the CMIP3 and CMIP5 suite of model simulations. This is in support of the National Climate Assessment. Analysis of a set of CMIP3 projections was presented in NOAA Technical Report NESDIS 142. Results are presented herein for seven different scenarios: the A2, A1B, and B1 emissions scenarios for CMIP3 and the RCP2.6, RCP4.5, RCP6.0, and RCP8.5 scenarios for CMIP5. Three future periods are analyzed: 2021–2050, 2041–2070, and 2070–2099, and results presented as changes with respect to a reference period of 1971–2000.

Overall, the similarities between the CMIP3 and CMIP5 models are much greater than any differences. The scenarios used in these two experiments are different. Also, there are more models in the CMIP5 suite. Thus, an exact comparison between the two experiments is not possible, and some of the mostly minor differences probably arise from these two factors.

The climate characteristics simulated by climate models for these scenarios have the following key features:

- Both the CMIP3 and CMIP5 model simulations indicate that spatial variations in temperature increase are relatively small, with the greatest temperature increases simulated in the interior and generally lesser values in coastal regions. The temperature increases across the entire contiguous U.S. are statistically significant (for all three future time periods and all scenarios).
- Temperature increases are simulated to be similar in magnitude for the high and low scenarios for the near future, whereas late in the 21st century the high scenarios indicate much greater warming. The range of temperature changes across scenarios is larger in the CMIP5 suite than in CMIP3.
- The range of simulated temperature changes across models is substantial, indicating substantial uncertainty in the magnitude of warming associated with each scenario. However, in each model simulation, the warming is unequivocal and large compared to historical variations. This is also true for all of the derived temperature variables described below. The results for CMIP3 and CMIP5 are similar.
- The number of days with minimum temperatures below 0°C is simulated to decrease by 10 to 20 days in the south to more than 30 days elsewhere by mid-century in the RCP8.5 scenario. There do not appear to be any substantive differences between the CMIP3 and CMIP5 results when considering differences in scenarios.
- The number of days with minimum temperatures above 20°C is simulated to increase by about 20 to 40 days in much of the northern United States, with larger increases of 40 or more days across the south by mid-century in the RCP8.5 scenario. There do not appear to be any substantive differences between the CMIP3 and CMIP5 results when considering differences in scenarios.
- Increases in the length of the freeze-free season are about 20 to 40 days over most of the United States, with smaller increases in the far south and west by mid-century in the RCP8.5 scenario. There do not appear to be any substantive differences between the CMIP3 and CMIP5 results when considering differences in scenarios.

- The annual highest daily maximum temperature is simulated to increase by about 5°F to 9°F over most of the U.S. by mid-century in the RCP8.5 scenario. The annual lowest value of the daily maximum temperature is simulated to increase by about 4°F to 10°F over most of the United States. The annual lowest daily minimum temperature is simulated to increase by about 4°F to more than 12°F over most of the United States. There do not appear to be any substantive differences between the CMIP3 and CMIP5 results when considering differences in scenarios.
- Warm (cold) spells are defined as periods of at least 6 days in length when the maximum (minimum) temperature is above (below) the 90th (10th) percentile threshold. Future changes in the length of these spells are based on present-day thresholds. Increases in the length of the annual longest warm spell are very large, ranging from about 60 days in the northeast to more than 100 days in the intermountain west by mid-century in the RCP8.5 scenario. Cold spells are projected to become very infrequent. There do not appear to be any substantive differences between the CMIP3 and CMIP5 results when considering differences in scenarios.
- Precipitation is simulated by both the CMIP3 and CMIP5 models to generally increase in the north and decrease in the southwest. The magnitude of increases and decreases are larger for the higher scenarios. The pattern of changes is similar in CMIP3 and CMIP5. The range of model-simulated precipitation changes is considerably larger than the multi-model mean change. Thus, there is great uncertainty associated with future precipitation changes in these scenarios.
- Contrasted with mean precipitation changes, extreme precipitation is generally projected to increase almost everywhere. The annual maximum 1-day and 5-day precipitation amounts increase by 5% to 15% in most areas by mid-century under the RCP8.5 scenario. The total annual precipitation falling on days with daily precipitation above the 99th percentile increases by 20% to more than 50% in most areas. There is little difference between the CMIP3 and CMIP5 results, except that in Hawai‘i the CMIP3 models project little change or decreases (the only U.S. area of decreases) while CMIP5 models project slight increases.
- Most of the modeled values of decadal precipitation change are not statistically significant with respect to 2001–2010, out to 2091–2099.

A comparison of model simulations of the 20th century with observations indicates the following:

- The observed changes in temperature are generally within the envelope of modeled changes on an annual basis. The CMIP3 and CMIP5 simulations of U.S. 20th century temperature are very similar to one another.
- The variability in observed precipitation change tends to be somewhat higher than that of the models, although decadal values are generally within the envelope of the model simulations.

APPENDIX: Model Robustness and Uncertainty

There are a number of methods for quantifying model robustness and uncertainty. They all aim to identify regions with large, significant or robust changes, regions with small changes, regions where models disagree, or a combination of those. We briefly describe and compare five methods from the IPCC Fifth Assessment Report (AR5; IPCC 2013) using the projected change in annual precipitation for 2070–2099, relative to 1971–2000, from CMIP5 RCP8.5 simulations. These methods are also depicted in Fig. A1.

Method #1: Regions where the change in the multi-model mean exceeds two standard deviations of internal variability, and where at least 90% of the models agree on the sign of change, are hatched and interpreted as "large change with high model agreement." Regions where the mutli-model mean change is less than one standard deviation of internal variability are stippled and interpreted as "small signal or low agreement of models" (Fig. A1a). The standard deviation of internal variability is calculated using the CMIP5 pre-industrial runs with model simulations longer than 150 years.

Method #2: This is an improvement to method #1 to further distinguish the case where there is high agreement among the models that the change is "small." Thus, it eliminates the ambiguous "small or low agreement" condition in method #1. In Fig. A1b, regions where the multi-model mean change is less than one standard deviation, and at least 80% of the individual models show a change smaller than one standard deviation of internal variability, are stippled.

Method #3: Knutti and Sedlacek (2013) define a dimensionless robustness index, R, which measures the signal-to-noise ratio. A value of R=1 implies perfect model agreement; low or negative values imply poor model agreement. In Fig. A1c, regions with R>0.8 are hatched and interpreted as "robust large change." Regions where at least 80% of the models individually show less than one standard deviation of internal variability are stippled and interpreted as "change unlikely to emerge from variability."

Method #4: Tebaldi et al. (2011) separate a lack of model agreement from a lack of signal. In Fig. A1d, regions are hatched and interpreted as "robust large change" when more than 50% of the models show significant change and at least 80% of those agree on the sign of change. Regions where more than 50% of the models show significant change, but less than 80% of those agree on the sign of change, are masked as white and interpreted as "unreliable." No stippling is defined in this method.

Method #5: Power et al. (2012) define a variable "D" as the precipitation change divided by the standard deviation. Regions where the probability of ensemble mean "D*" is very likely to be less than 0.2 (i.e., $Pr|D^*|<0.2$) are then identified. Note that 0.2 is an arbitrary choice. In Fig. A1e, the regions masked as white are interpreted as "significance in small change," and regions with hatching are interpreted as "significance in larger change."

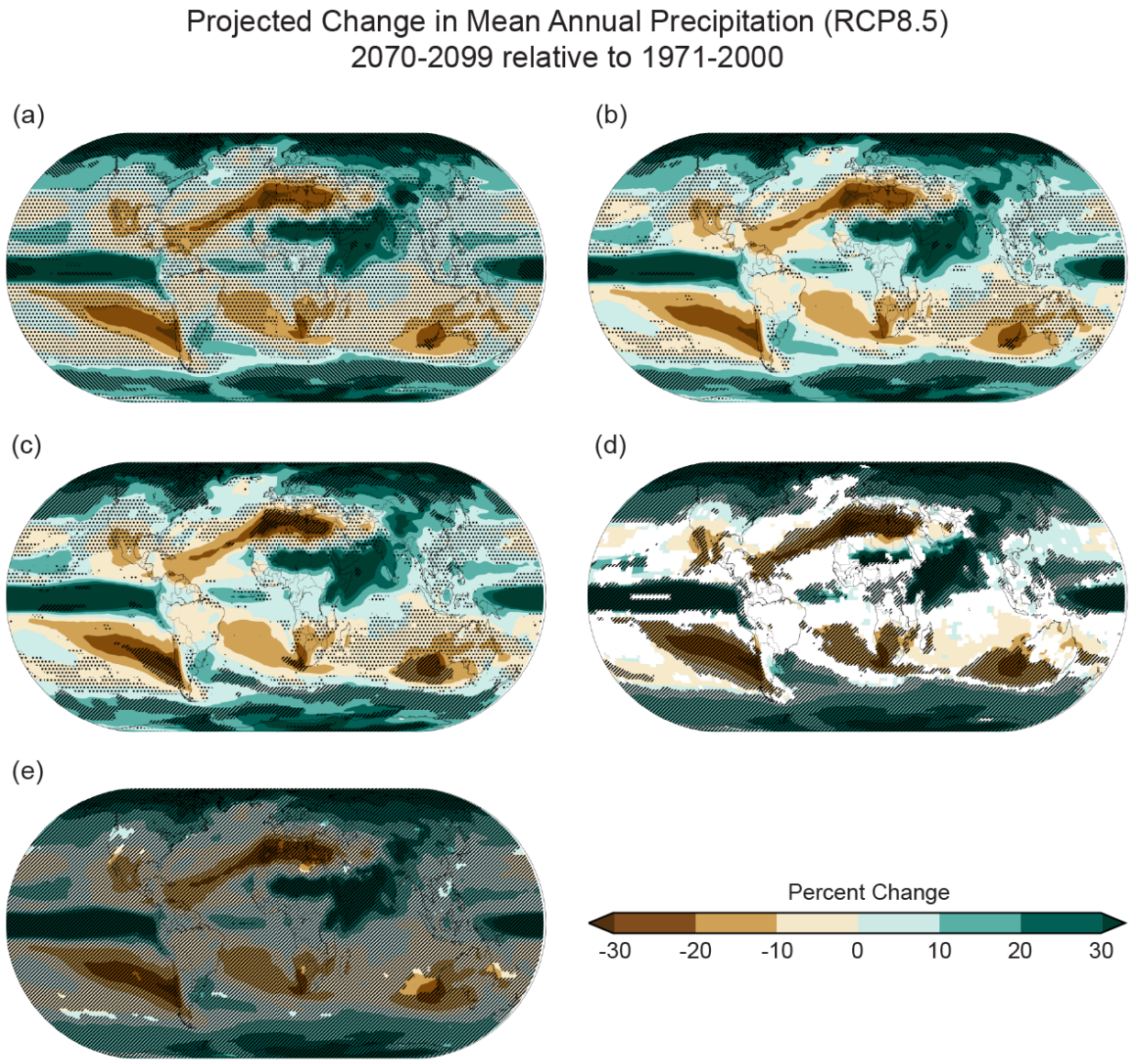

Figure A1. *Projected change in annual mean precipitation (%) for 2070–2099 with respect to the reference period of 1971–2000. These are multi-model means using CMIP5 RCP8.5 simulations. The choice of the variable and time frame is just for illustration of how different methods used in the IPCC Fifth Assessment Report (IPCC 2013) quantify model robustness and uncertainty. The coloring of the multi-model mean values for each map is identical and only hatching and stippling differs based on the method shown. Different methods for hatching and stippling are shown, determined (a) from relating the multi-model mean to internal variability, (b) as in (a) but hatching here indicates high model agreement for 'small change', (c) by the robustness measure by Knutti and Sedlacek (2013), (d) by the method proposed by Tebaldi et al. (2011), and (e) by the method by Power et al. (2012).*

Figures A1a–e compare the robustness and uncertainty estimates from the five methods described above. The results from methods #1–4 all indicate high model agreement in annual precipitation change with regards to:

1) Large increases in the high latitudes and the equatorial Pacific Ocean, and
2) Small changes or large uncertainty in many areas of the tropics (outside of the Pacific Ocean) and mid-latitudes, such as most of Australia and the western United States.

The results from methods #1–4 also exhibit some differences:

1) High model agreement regarding significant change in annual precipitation over the northeast and southwest United States is shown in Fig. A1d, but not in Figs. A1a–c, and
2) High model agreement regarding significant decreases in annual precipitation over the Mediterranean region is shown in Figs. A1c–d, but not in Figs. A1a–b. These differences are mainly due to the ways in which the significance of change is characterized, and the thresholds for level of agreement among methods #1–4.

Fig. A1e shows significance in annual precipitation change over most of the earth's surface. The result from method #5 differs from those of the other methods. The reason is that method #5 produces a statement about the mean of the distribution being significantly different from zero, assuming that the models are independent and randomly distributed around reality. Methods #1–4, on the other hand, use an "indistinguishable" interpretation, in which each model and reality are drawn from the same distribution. In that case, the hatching and stippling characterize the likelihood.

REFERENCES

CCCMA, 2014: Environment Canada - Climate Change - CCCMA - Data - ETCCDI Extremes Indices Archive. [Available online at http://www.cccma.ec.gc.ca/data/climdex/.]

Cook, B. I., R. L. Miller, and R. Seager, 2009: Amplification of the North American "Dust Bowl" drought through human-induced land degradation. *Proc. Natl. Acad. Sci.*, **106,** 4997-5001, doi:10.1073/pnas.0810200106.

Hayhoe, K., 2014: Development and Dissemination of a High-Resolution National Climate Change Dataset. [Available online at http://cida.usgs.gov/thredds/fileServer/dcp/files/Hayhoe_USGS_downscaled_database_final_report.pdf.]

IPCC, 2000: *Special Report on Emissions Scenarios. A Special Report of Working Group III of the Intergovernmental Panel on Climate Change.* [N. Nakicenovic, and R. Swart, Eds.], Cambridge University Press, 570 pp.

——, 2007: *Climate Change 2007: The Physical Science Basis. Contribution of Working Group I to the Fourth Assessment Report of the Intergovernmental Panel on Climate Change.* [S. Solomon, and Coauthors, Eds.], Cambridge University Press, 996 pp.

——, 2013: *Climate Change 2013: The Physical Science Basis. Contribution of Working Group I to the Fifth Assessment Report of the Intergovernmental Panel on Climate Change.* [T. F. Stocker, and Coauthors, Eds.], Cambridge University Press, 1535 pp.

Keener, V. W., K. Hamilton, S. K. Izuka, K. E. Kunkel, L. E. Stevens, and L. Sun, 2013: Regional Climate Trends and Scenarios for the U.S. National Climate Assessment: Part 8. Climate of the Pacific Islands. U.S. NOAA Technical Report NESDIS 142-8, 45 pp.

Knutti, R., and J. Sedlacek, 2013: Robustness and uncertainties in the new CMIP5 climate model projections. *Nat. Clim. Change*, **3,** 369-373, doi:10.1038/nclimate1716.

Kumar, S., J. Kinter, P. A. Dirmeyer, Z. T. Pan, and J. Adams, 2013: Multidecadal climate variability and the "warming hole" in North America: Results from CMIP5 twentieth- and twenty-first-century climate simulations. *J. Climate*, **26,** 3511-3527, doi:10.1175/JCLI-D-12-00535.1.

Kunkel, K. E., X.-Z. Liang, J. Zhu, and Y. Lin, 2006: Can CGCMs simulate the twentieth-century "warming hole" in the central United States? *J. Climate*, **19,** 4137-4153, doi:10.1175/JCLI3848.1.

Kunkel, K. E., and Coauthors, 2013a: Regional Climate Trends and Scenarios for the U.S. National Climate Assessment: Part 1. Climate of the Northeast U.S. NOAA Technical Report NESDIS 142-1, 80 pp.

Kunkel, K. E., and Coauthors, 2013b: Regional Climate Trends and Scenarios for the U.S. National Climate Assessment: Part 2. Climate of the Southeast U.S. NOAA Technical Report NESDIS 142-2, 95 pp.

Kunkel, K. E., and Coauthors, 2013c: Regional Climate Trends and Scenarios for the U.S. National Climate Assessment: Part 3. Climate of the Midwest U.S. NOAA Technical Report NESDIS 142-3, 96 pp.

Kunkel, K. E., and Coauthors, 2013d: Regional Climate Trends and Scenarios for the U.S. National Climate Assessment: Part 4. Climate of the U.S. Great Plains. NOAA Technical Report NESDIS 142-4, 83 pp.

Kunkel, K. E., and Coauthors, 2013e: Regional Climate Trends and Scenarios for the U.S. National Climate Assessment: Part 5. Climate of the Southwest U.S. NOAA Technical Report NESDIS 142-5, 79 pp.

Kunkel, K. E., and Coauthors, 2013f: Regional Climate Trends and Scenarios for the U.S. National Climate Assessment: Part 6. Climate of the Northwest U.S. NOAA Technical Report NESDIS 142-6, 76 pp.

Kunkel, K. E., L. E. Stevens, S. E. Stevens, L. Sun, E. Janssen, D. Wuebbles, and J. G. Dobson, 2013g: Regional Climate Trends and Scenarios for the U.S. National Climate Assessment: Part 9. Climate of the Contiguous United States. NOAA Technical Report NESDIS 142-9, 78 pp.

Melillo, J. M., Terese (T.C.) Richmond, and G. W. Yohe, Eds., 2014: *Climate Change Impacts in the United States: The Third National Climate Assessment*. U.S. Global Change Research Program, 842 pp.

Moss, R. H., and Coauthors, 2010: The next generation of scenarios for climate change research and assessment. *Nature*, **463,** 747-756, doi:10.1038/nature08823.

Overland, J. E., M. Wang, N. A. Bond, J. E. Walsh, V. M. Kattsov, and W. L. Chapman, 2011: Considerations in the selection of global climate models for regional climate projections: The Arctic as a case study. *J. Climate*, **24,** 1583-1597, doi:10.1175/2010JCLI3462.1.

Pan, Z. T., X. D. Liu, S. Kumar, Z. Q. Gao, and J. Kinter, 2013: Intermodel variability and mechanism attribution of central and southeastern U.S. anomalous cooling in the twentieth century as simulated by CMIP5 models. *J. Climate*, **26,** 6215-6237, doi:10.1175/JCLI-D-12-00559.1.

PCMDI, 2014: CMIP3 Climate Model Documentation, References, and Links. [Available online at http://www-pcmdi.llnl.gov/ipcc/model_documentation/ipcc_model_documentation.php.]

Power, S. B., F. Delage, R. Colman, and A. Moise, 2012: Consensus on twenty-first-century rainfall projections in climate models more widespread than previously thought. *J. Climate*, **25,** 3792-3809, doi:10.1175/JCLI-D-11-00354.1.

Sillmann, J., V. V. Kharin, F. W. Zwiers, X. Zhang, and D. Bronaugh, 2013a: Climate extremes indices in the CMIP5 multimodel ensemble: Part 1. Model evaluation in the present climate. *J. Geophys. Res.*, **118,** 1716-1733, doi:10.1002/jgrd.50203.

——, 2013b: Climate extremes indices in the CMIP5 multimodel ensemble: Part 2. Future climate projections. *J. Geophys. Res.*, **118,** 2473-2493, doi:10.1002/jgrd.50188.

Stewart, B. C., K. E. Kunkel, L. E. Stevens, L. Sun, and J. E. Walsh, 2013: Regional Climate Trends and Scenarios for the U.S. National Climate Assessment: Part 7. Climate of Alaska. NOAA Technical Report NESDIS 142-7, 61 pp.

Tebaldi, C., J. M. Arblaster, and R. Knutti, 2011: Mapping model agreement on future climate projections. *Geophys. Res. Lett.*, **38,** L23701, doi:10.1029/2011GL049863.

van Vuuren, D. P., and Coauthors, 2011: The representative concentration pathways: An overview. *Climatic Change*, **109,** 5-31, doi:10.1007/s10584-011-0148-z.

Vose, R. S., and Coauthors, 2014: Improved historical temperature and precipitation time series for U.S. climate divisions. *J. Appl. Meteorol. Clim.*, **53,** 1232-1251, doi:10.1175/JAMC-D-13-0248.1.

ACKNOWLEDGEMENTS

We acknowledge the World Climate Research Programme's (WCRP) Working Group on Coupled Modelling (WGCM) for their roles in making available the WCRP CMIP3 and CMIP5 multi-model datasets. We thank the climate modeling groups (listed in Tables 1–4) for producing and making available their model output. For CMIP, the U.S. Department of Energy's Program for Climate Model Diagnosis and Intercomparison (PCMDI) provides coordinating support and led development of software infrastructure in partnership with the Global Organization for Earth System Science Portals (GO-ESSP).

We acknowledge the World Meteorological Organization (WMO) Expert Team on Climate Change Detection and Indices (ETCCDI) for providing CLIMDEX data, which were obtained from the Environment Canada's Canadian Centre for Climate Modelling and Analysis (ECCCMA).

We would also like to thank Jessicca Griffin of the Cooperative Institute for Climate and Satellites – North Carolina (CICS-NC) and Deb Misch of Jamison Professional Services, Inc. for providing graphical support, Tom Maycock of CICS-NC for providing editorial support, and James McMahon of LMI for providing logistical support throughout the review and publication process.